

Spatial Scale of Agglomeration and Dispersion: Number, Spacing, and the Spatial Extent of Cities

Takashi Akamatsu, Tomoya Mori, Minoru Osawa, and Yuki Takayama*

August 30, 2024

Abstract

Cities have become fewer, bigger, and flatter in many countries. Better transport access has fostered concentration of economic activities toward fewer, bigger cities, while each city has become more decentralized. We show that two types of dispersion forces against spatial agglomeration explain the dual evolution of cities. Dispersion forces within a city, such as those arising from the consumption of limited land, affect only the city's residents. A decrease in transport costs reduces the relative benefits of agglomeration in a congested central location, making the population distribution in each city flatter and more spread out to achieve a balance between the costs and benefits of agglomeration. Dispersion forces that spill over beyond a city, such as market crowding, make locations near the city unattractive. Lower transport costs promote competition for a wider area around each city, leaving fewer cities with larger distances between them. A model's comparative static results, and thus its policy implications, depend on the type of dispersion forces it incorporates.

JEL: C62, R12, R13

Keywords: agglomeration patterns; spatial scale of dispersion force, many regions, economic geography

*Akamatsu: Tohoku University, Aoba, Aramaki-aza Aoba-ku, Sendai, Miyagi 980-8579, Japan, akamatsu@plan.civil.tohoku.ac.jp. akamatsu@plan.civil.tohoku.ac.jp. Mori: Kyoto University, Yoshida-Honmachi, Sakyo-ku, Kyoto, Kyoto 606-8501 Japan, mori@kier.kyoto-u.ac.jp. Osawa: Kyoto University, Yoshida-Honmachi, Sakyo-ku, Kyoto, Kyoto 606-8501 Japan, osawa.minoru.4z@kyoto-u.ac.jp. Takayama: Tokyo Institute of Technology, 2-12-1 W6-9 Ookayama, Meguro, Tokyo 152-8850, Japan, takayama.y.af@m.titech.ac.jp. We are indebted to Kristian Behrens, Gilles Duranton, Yasusada Murata, Jonathan Newton, Michael Pflüger, Diego Puga, Esteban Rossi-Hansberg, Akihisa Shibata, and Jacques-François Thisse for their constructive comments. We are grateful to all seminar and conference participants at various institutions. This research has been supported by JSPS KAKENHI 17H00987, 18H01556, 19K15108, 21K04299, 22K04353, 22H01610, and 22H01617. This research was conducted as part of the project, "Agglomeration-based Framework for Empirical and Policy Analyses of Regional Economies," undertaken at the Research Institute of Economy, Trade and Industry. We acknowledge financial support from the Kajima Foundations and the Murata Science Foundation.

1 Introduction

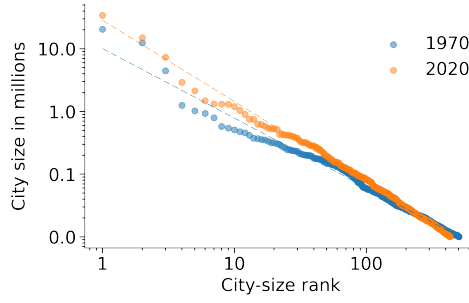
Cities lie at the heart of the modern economy, with the urban areas in post-industrial countries typically comprising many cities. The canonical approach for explaining the existence of cities has been the analysis of trade-offs between agglomeration and dispersion forces, mediated by transport costs between locations.¹ On the role of transport costs, the evolution of Japanese cities between 1970 and 2020 offer a striking demonstration. After 1960, Japanese high-speed railway and highway networks were constructed almost from scratch across the country,² suggesting that the decline in transport costs has been the major driver of the evolution of cities. During this period, the population has concentrated more in fewer bigger cities than in smaller cities. At the same time, within each city, population and employment have become more dispersed. The population rank-size plot in 2020 features a steeper slope compared to that of 1970 (Figure 1A). The population share of the top 100 cities increased by 19%, while the population share of the remaining cities decreased by 17%. On the other hand, cities have become flatter and flatter. On average, cities experienced a 35% decrease in maximum population density, a 24% decrease in average population density (Figure 1B), and an 86% increase in areal size (Figure 1C). Such a two-faced urban evolution has been observed also in other countries, including China, France, and the US in the past 20 years,³ suggesting the possibility of a general explanation beyond country-specific contexts.

This study argues that the combination of *local* and *global* dispersion forces concerning economic agglomeration can explain the observed dual evolution of cities. The former, “local” dispersion forces are effective *within* each location. For example, competition over a limited land plot produces a congestion force through the land market that discourages firms or consumers to enter that location. Such an effect reduces the population density in the city center, and flattens the geographic distribution of the city’s population. The latter, “global” dispersion forces extend beyond each location. A representative example is the market crowding effect due to trade linkages *between* locations. Urban population concentration enlarges the city’s home market and attract retailers. However, suburban areas near the city are less attractive due to their smaller markets and intense competition from the city. As a result, multiple economic agglomerations emerge while maintaining a certain distance from each other. The distance between agglomerations increases as transport costs decrease. We employ a stylized spatial model to demonstrate that the two types of dispersion forces have contrastive implications for the spatial patterns of economic activities and their comparative statics.

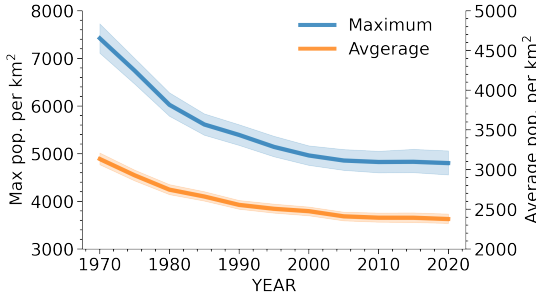
¹See Fujita et al. (1999a); Baldwin et al. (2003); Duranton and Puga (2004); Fujita and Thisse (2013).

²Between 1970 and 2020, the total highway (high-speed railway) length increased from 1,119 km (515 km) to 9,050 km (3,106 km), which is more than a eight (six) times increase. See Appendix B.

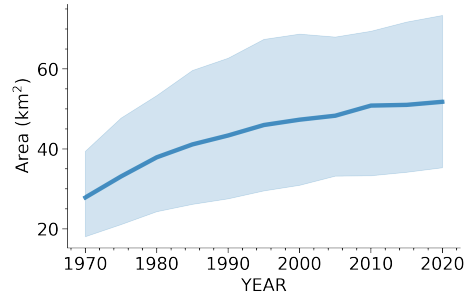
³See Appendix B. Also, Combes et al. (2020) obtained similar results for France for a much longer duration of time by constructing original panel data for French cities during the 1760–2020 period.



(A) Population rank-size plot



(B) Maximum and average density



(C) Area

Figure 1: Global concentration and local dispersion in Japan from 1970 to 2020.

Note: We define a *city* as a set of contiguous 1km-by-1km grid cells with a population density of at least 1000/km² each that add up to a total population of at least 10,000. See Appendix B for details. In (B) and (C), the average across all cities in each year is shown with 90% confidence intervals.

Basic intuitions can be explained without formal analysis. Consider a many-location economy where there are mobile agents (consumers or firms) who choose their locations. Suppose that there is an agglomeration force so that mobile agents prefer proximity to others. All mobile agents agglomerate in one location without dispersion forces. Once dispersion forces are introduced, they may deviate from the agglomeration.

If we introduce only a local dispersion force, a monocentric spatial distribution as in Figure 2A emerges. Suppose that there are only negative congestion externalities effective *within* each location (local dispersion forces). Then, agents can avoid congestion by relocating to the locations *adjacent* to the central location while enjoying the proximity to other agents. Such relocations will continue to a point where the merit of the proximity to others and local negative externalities are balanced out, resulting in a monocentric distribution of agents in equilibrium.

If instead we introduce a global dispersion force, polycentric spatial distributions as in Figure 2B can emerge. Again, consider a state where all agents concentrate in one location due to some agglomeration forces. Suppose we add a global dispersion force such as the market crowding effect through trade. All locations face negative effects due to market crowding but to different degrees. The closer a location is to the population center, the tougher the negative effects (the so-called “agglomeration shadow”). If the level of negative effects at the center is too high, mobile agents may consider relocation.

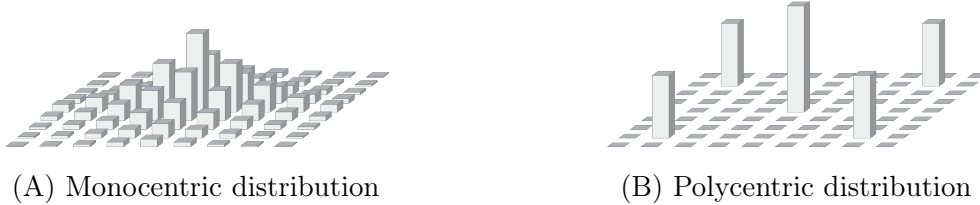


Figure 2: Spatial patterns in a square geography with symmetric local fundamentals.

They will move to locations *remote from* the existing agglomeration, while they also tend to agglomerate at the new location due to the presumed agglomeration forces. Thus, the economy ends up with a polycentric structure in equilibrium.

When transport costs fall, global and local dispersion forces impact the spatial distribution of agents in distinct ways. Specifically, better transport access fosters (discourages) population concentration under global (local) dispersion forces. On the one hand, decreasing transport costs enables firms and consumers to reach more distant markets, allowing firms and consumers to agglomerate in a smaller number of locations. Some agglomerations may lag behind as their proximity to other centers hampers its economic prosperity due to their agglomeration shadow. As a result, fewer and bigger agglomerations can survive, which we may call *global concentration*. On the other hand, lower transport costs reduce the need for agents to be located closer to each other, which in turn raises the relative importance of congestion forces within each location. Consequently, each agglomeration experiences *local dispersion* (or *flattening*) as they become geographically more spread. If there are both local and global dispersion forces, then global concentration and local dispersion occur simultaneously, as observed in Japan and other countries. That said, distinguishing local and global dispersion forces allows us to categorize spatial models into three prototypical classes with different implications: models with only global, only local, and local and global dispersion forces (Table 1 on Page 21).

We also contribute to the literature on quantitative spatial models (as surveyed by, e.g., Redding and Rossi-Hansberg, 2017) by elucidating the impact of endogenous economic forces on their implications. We show that counterfactual results in a quantitative spatial model can fundamentally differ depending on the model’s dispersion force. In particular, policy suggestions for transport investments can be in opposite directions. We observe that, if the model only has global dispersion forces (e.g., Krugman, 1991), agglomeration toward a smaller number of locations will occur when transport costs decline. For this class of models, initial regional advantages are amplified when transport access improves. The converse is true if the model has only local dispersion forces (e.g., Allen and Arkolakis, 2014). In this class of models, initial advantages diminish when transport access improves. In other words, enhanced transport links between core and periphery regions may disadvantage the periphery in models with global dispersion forces but ben-

efit it in models with local dispersion forces. Thus, to avoid unintended consequences of transport investments, it is crucial to identify what are the key dispersion forces behind the spatial problem at hand, so that an appropriate model can be constructed for counterfactual projections.

The remainder of this paper is organized as follows: Section 2 introduces the basic framework. Section 3 considers a many-region geography and characterizes endogenous spatial configuration in spatial models. Section 4 discuss the effect of exogenous regional heterogeneities on the comparative statics under transport improvements. Section 5 concludes the paper with discussions on the implications of our results. Appendix A provides the proofs. Appendices B–F are provided as Online Appendix.

2 Basic framework

Section 2.1 introduces our theoretical setup, which covers various models in the literature. Section 2.2 provides a recap on the theory of *endogenous agglomeration* with a simple two-region model. Section 2.3 introduces the notion of the spatial scale of dispersion forces and discusses its implications on spatial patterns and their comparative statics.

2.1 Economic geography models: A general setup

Consider an economy comprised of N *regions*, where a “region” indicates an arbitrary discrete spatial unit such as a grid cell, a county, or municipality. Let $\mathcal{N} \equiv \{1, 2, \dots, N\}$ be the set of regions. There is a continuum of mobile *agents*, such as consumers or firms, who seek to maximize their utility by choosing their locations. Let $x_i \geq 0$ be the mass of agents in region i , so that $\mathbf{x} \equiv (x_i)_{i \in \mathcal{N}}$ is the spatial distribution of agents. The total mass of agents is normalized to unity: $\sum_{i \in \mathcal{N}} x_i = 1$. We assume that the *payoff* (i.e., the indirect utility) of agents in region i is given as a function of the spatial distribution \mathbf{x} , and denote it by $v_i(\mathbf{x})$ and let $\mathbf{v}(\mathbf{x}) \equiv (v_i(\mathbf{x}))_{i \in \mathcal{N}}$. Agents can freely relocate across the regions to improve their payoffs. A spatial distribution \mathbf{x} is called a *spatial equilibrium* when no agent can improve their payoff unilaterally by relocation.⁴

An *economic geography model* is a model that determines spatial distributions of agents as spatial equilibria. The indispensable feature of an economic geography model is the presence of spatial frictions, such as transport costs for shipments of goods between regions. We suppose that the payoff function \mathbf{v} depends on a *proximity matrix* $[\phi_{ij}]_{i \in \mathcal{N}, j \in \mathcal{N}}$ that summarizes interregional transport accessibility. Each entry $\phi_{ij} \in (0, 1]$ is an inverse measure of transport costs (i.e., the freeness of transport) between regions i and j where

⁴Formally, \mathbf{x} is a spatial equilibrium if $v^* = v_i(\mathbf{x}) \forall i \in \mathcal{N}$ with $x_i > 0$, while $v^* \geq v_i(\mathbf{x}) \forall i \in \mathcal{N}$ with $x_i = 0$, where $v^* = \max_{i \in \mathcal{N}} \{v_i(\mathbf{x})\}$. If $x_i > 0 \forall i \in \mathcal{N}$, this reduces to $v^* = v_i(\mathbf{x}) \forall i \in \mathcal{N}$. This is the standard notion of Nash equilibria in *population games* (Sandholm, 2010).

larger values indicate better accessibility with $\phi_{ij} = 1$ indicating no transport costs between regions i and j .

The payoff function \mathbf{v} can represent positive and negative economic forces regarding the spatial concentration of agents. Multiple equilibria can occur due to the positive externalities. When multiple equilibria exist, some of them may not be plausible because they are *unstable*. That is, a small migration shock may encourage further migration of agents so that snowball effects can kick the spatial distribution out of those equilibria. We focus on *locally stable* equilibria that are robust to small migration shocks under moderate assumptions on agents' relocation decisions. For example, we assume that agents tend to migrate toward regions with higher payoffs than their current residents.⁵

2.2 Endogenous agglomeration: A simple example

With economic geography models, the theory of endogenous agglomeration asks how ex-ante symmetric regions can become asymmetric by economic forces that drive agents to agglomerate. For the rest of Section 2, we suppose $N = 2$ for simplicity. If there are two regions with identical characteristics and equal transport access from one another, the proximity matrix is

$$\begin{bmatrix} \phi_{11} & \phi_{12} \\ \phi_{21} & \phi_{11} \end{bmatrix} = \begin{bmatrix} 1 & \phi \\ \phi & 1 \end{bmatrix}, \quad (1)$$

where ϕ is the freeness of transport between the two regions. The symmetric distribution of agents, $\bar{\mathbf{x}} \equiv (\frac{1}{2}, \frac{1}{2})$, is a spatial equilibrium. If $\bar{\mathbf{x}}$ is unstable, agglomeration will emerge as there should be stable asymmetric equilibria ($x_1 > x_2$ or $x_1 < x_2$). The fundamental feature of economic geography models is that changes in transport costs (ϕ for the two-region case) can trigger agglomeration from the symmetry (Krugman, 1991).

As a simple example, we consider a version of the seminal model by Beckmann (1976), who considered the trade-off between congestion costs and agents' desire to be close to each other.⁶ For a general number of regions, let

$$v_i(\mathbf{x}) = x_i^{-\beta} \left(\sum_{j \in \mathcal{N}} e^{-\tau \ell_{ij}} x_j \right)^\alpha \quad (2)$$

where $x_i^{-\beta}$ with $\beta > 0$ represents negative externalities of congestion and $(\sum_{j \in \mathcal{N}} e^{-\tau \ell_{ij}} x_j)^\alpha$ with $\alpha > 0$ is positive externalities of agglomeration; $\ell_{ij} > 0$ is the distance between i and j and $\tau > 0$. The general setup in Section 2.1 covers the model if we set $[\phi_{ij}] = [e^{-\tau \ell_{ij}}]$.

⁵See Appendix A.1 for formal discussions. We use equilibrium refinement by linear stability under evolutionary dynamics (Sandholm, 2010, Ch. 8). We presume a class of dynamics that includes the replicator dynamic (Taylor and Jonker, 1978) often employed in the literature (e.g., Fujita et al., 1999a).

⁶We consider a discrete-space and multiplicative version of the model instead of the original formulation in a continuous one-dimensional space.

For the symmetric two-region case, we have $\phi = e^{-\tau\ell_{12}} = e^{-\tau\ell_{21}} \in (0, 1)$ in (1). In the context of the model, ϕ represents the magnitude of distance-decaying positive externalities from one location to the other. A higher ϕ can be interpreted as a better interregional access. The stability of $\bar{\mathbf{x}} = (\frac{1}{2}, \frac{1}{2})$ can be determined by considering a hypothetical migrant between the two regions. Specifically, the payoff gain for the marginal migrant from region 2 to 1 can be measured by the elasticity of the payoff difference

$$\omega = \frac{\partial(v_1(\bar{\mathbf{x}}) - v_2(\bar{\mathbf{x}}))}{\partial x_1} \frac{\bar{x}}{\bar{v}} = \left(\frac{\partial v_1(\bar{\mathbf{x}})}{\partial x_1} - \frac{\partial v_2(\bar{\mathbf{x}})}{\partial x_1} \right) \frac{\bar{x}}{\bar{v}}, \quad (3)$$

where $\bar{v} = v_1(\bar{\mathbf{x}}) = v_2(\bar{\mathbf{x}})$ is the payoff level at $\bar{\mathbf{x}}$. We consider gain as the elasticity instead of the differential (i.e., we multiply by $\frac{\bar{x}}{\bar{v}}$) just to simplify the resulting formulae.⁷

If $\omega < 0$, a marginal increase in the mass of agents in region 1 induces a relative payoff decrease therein compared to the other region. Migrants are strictly worse off, and reverse migration should occur, meaning $\bar{\mathbf{x}}$ is stable. If $\omega > 0$ instead, such a marginal migration induces a relative payoff increase in region 1 compared to region 2. Agents are strictly better off when they migrate to the other region, indicating $\bar{\mathbf{x}}$ is unstable.⁸

If we start from a stable symmetry $\bar{\mathbf{x}}$, endogenous agglomeration occurs when ω turns negative to positive by the changes in the parameters of the economy. For the two-region Beckmann model, log-differentiating $\mathbf{v}(\mathbf{x})$ and (3) gives

$$\omega = \frac{\bar{x}}{\bar{v}} \left(v_1(\mathbf{x}) \left(-\frac{\beta}{x_1} + \frac{\alpha}{x_1 + \phi x_2} \right) - v_2(\mathbf{x}) \frac{\alpha \phi}{\phi x_1 + x_2} \right) \Big|_{\mathbf{x}=\bar{\mathbf{x}}} = -\beta + \alpha \frac{1 - \phi}{1 + \phi}. \quad (4)$$

If $\beta \geq \alpha$, $\bar{\mathbf{x}}$ is stable as $\omega < 0$ for all $\phi \in (0, 1)$, meaning that a strong congestion force can suppress endogenous agglomeration. If instead congestion force is moderate ($0 < \beta < \alpha$), $\bar{\mathbf{x}}$ is stable for $\phi \in (\phi^*, 1)$ and unstable for $\phi \in (0, \phi^*)$, where $\phi^* \equiv \frac{\alpha - \beta}{\alpha + \beta}$ is the solution to $\omega = 0$. Endogenous agglomeration occurs when $\phi \in (0, \phi^*)$. For this range of ϕ , interregional transport is sufficiently costly and the benefit of agglomeration overcomes negative congestion externalities.

Generally, for an economic geography model, negative (positive) terms in ω represent the model's dispersion (agglomeration) forces. In the Beckmann model, the first negative constant $-\beta$ in (4) corresponds to the congestion force $x_i^{-\beta}$, whereas the positive term $\alpha \frac{1 - \phi}{1 + \phi} > 0$ represents the agglomeration force. Intuitively, ϕ appears only in the latter, as the dispersion force in the model does not depend on interregional transport access.

⁷Considering gain as the elasticity simplifies formulae when the payoff function takes a multiplicative form as in (2), which is often the case for economic geography models in the literature.

⁸The marginal case, $\omega = 0$, is less important as it typically corresponds to very specific values of ϕ . Technically, $\omega = 0$ means that $\bar{\mathbf{x}}$ is a “nonhyperbolic” equilibrium, and we need a higher-order stability analysis to determine the stability of $\bar{\mathbf{x}}$ (Hirsch et al., 2012).

2.3 Local and global economic forces

As in the Beckmann example, endogenous forces in economic geography models may or may not depend on transport costs between regions. The congestion force in the Beckmann model is *local* in the sense that the population in each region determines the level of congestion in the region, irrespective of interregional transport costs or population in the other regions. The agglomeration force, in contrast, is *global* in the sense that the whole population distribution affects the magnitude of positive externalities in a region through costly interregional transport.

To distill such dependence of endogenous forces on the interregional transport cost structure, it is useful to study the payoff elasticity matrix at the symmetric equilibrium, $\mathbf{V} \equiv \frac{\bar{x}}{v} \nabla \mathbf{v}(\bar{\mathbf{x}}) = \frac{\bar{x}}{v} [\frac{\partial v_i}{\partial x_j}(\bar{\mathbf{x}})]_{i \in \mathcal{N}, j \in \mathcal{N}}$. For the Beckmann model, we have

$$\mathbf{V} = -\beta \mathbf{I} + \alpha \mathbf{D} \quad (5)$$

where \mathbf{I} is the identity matrix and \mathbf{D} is the *row-normalized proximity matrix*, which is

$$\mathbf{D} = \frac{1}{1 + \phi} \begin{bmatrix} 1 & \phi \\ \phi & 1 \end{bmatrix}. \quad (6)$$

for the two-region case.

We observe that the gain ω is an eigenvalue of \mathbf{V} . To see this, we note that $\mathbf{z} = (1, -1)$ is an eigenvector of \mathbf{D} , as we confirm $\mathbf{D}\mathbf{z} = \chi\mathbf{z}$ with

$$\chi = \frac{1 - \phi}{1 + \phi} \in (0, 1). \quad (7)$$

The eigenvector \mathbf{z} represents the migration pattern from the uniform distribution $\bar{\mathbf{x}}$ in the two-region economy as it corresponds to a population increase in one region and a decrease in the other.⁹ The eigenvalue χ is interpreted as an index of the marginally increased proximity due to marginal deviation of the form $\mathbf{x} = \bar{\mathbf{x}} + \epsilon\mathbf{z} = (\bar{x} + \epsilon, \bar{x} - \epsilon)$. Naturally, χ decreases in ϕ because deviation from the symmetry provides less proximity gain when transport becomes less costly (when ϕ increases). Given the representation of \mathbf{V} by \mathbf{D} as in (5), we see $\omega = -\beta + \alpha\chi$ is an eigenvalue of \mathbf{V} as $\mathbf{V}\mathbf{z} = (-\beta\mathbf{I} + \alpha\mathbf{D})\mathbf{z} = (-\beta + \alpha\chi)\mathbf{z}$.

In \mathbf{V} , the proximity structure of the symmetric two-region geography is summarized by \mathbf{D} . The representation of \mathbf{V} by \mathbf{D} then succinctly summarizes how endogenous agglomeration and dispersion forces act on the geography. In the Beckmann model, the first component of \mathbf{V} , $-\beta\mathbf{I}$, come from congestion force $x_i^{-\beta}$ and does not include \mathbf{D} . The second component, $\alpha\mathbf{D}$, from agglomeration force $(\sum_j \phi_{ij}x_j)^\alpha$ and depends on \mathbf{D} .

A similar representation of the payoff elasticity matrix \mathbf{V} by the row-normalized prox-

⁹The other eigenvector is $\mathbf{1} = (1, 1)$ with the associated eigenvalue 1, which represents the symmetric population increase in both regions and thus is irrelevant because we fix the total population.

imity matrix \mathbf{D} is possible for various models and allows us to compare models in a unified manner. In particular, we can distinguish between *local* and *global* forces by checking whether a force appears in \mathbf{V} as a term involving \mathbf{D} . As discussed, we say the *spatial scale* of an economic force is *local* if it appears as a constant term (the coefficient of \mathbf{I}) in \mathbf{V} , and it is *global* if it appears in other terms that involve \mathbf{D} .

It is noted that whether a particular economic force appears as a local or global force depends on specific modeling choices. For example, “congestion” can be a global force when the model considers traffic congestion over the interregional transport network. Likewise, “market crowding” may be a local force if markets are assumed to be closed within each region and there is no interregional trade.

2.4 Global dispersion force: A toy example

The Beckmann model provides the simplest example of a local dispersion force. As a toy example of a global dispersion force, consider the “inverted” Beckmann model, for which the payoff function is

$$v_i(\mathbf{x}) = x_i^\beta \left(\sum_{j \in \mathcal{N}} \phi_{ij} x_j \right)^{-\alpha} \quad (8)$$

with $\alpha, \beta > 0$. In this model, x_i^β is a local agglomeration force, and $(\sum_{j \in \mathcal{N}} \phi_{ij} x_j)^{-\alpha}$ is a *global* dispersion force. This dispersion force may be interpreted as congestion of local facilities that are accessible from other regions, where the level of competition is higher when there are more agents in close proximity of the region. Thus, agents avoid proximity to others in different locations.

For this model, we readily see

$$\mathbf{V} = \beta \mathbf{I} - \alpha \mathbf{D} \quad \text{and} \quad \omega = \beta - \alpha \chi. \quad (9)$$

The dispersion force is the first-order negative term of \mathbf{D} in \mathbf{V} . That is, if $\beta \geq \alpha$, $\bar{\mathbf{x}}$ is always unstable as $\omega > 0$ for all $\phi \in (0, 1)$ as we recall $\chi \in (0, 1)$. If the agglomeration force is sufficiently strong, full concentration in one of the regions is the stable equilibrium. If instead agglomeration force is moderate ($0 < \beta < \alpha$), $\bar{\mathbf{x}}$ is stable for $\phi \in (0, \phi^*)$ and unstable for $\phi \in (\phi^*, 1)$, where $\phi^* \equiv \frac{\beta - \alpha}{\alpha + \beta}$ is the solution to $\omega = 0$. Thus, the uniform distribution is unstable when $\phi \in (\phi^*, 1)$ and endogenous agglomeration must occur in this range of ϕ .

We observe that the two models have contrastive implications regarding *when* the symmetry becomes unstable. In the Beckmann model, dispersion occurs as transport costs decrease (as ϕ increases). The local dispersion force in this model is independent of ϕ . As the agglomeration force weakens with the increase of ϕ , this dispersion force

becomes relatively important for agents. The uniform distribution becomes stable when ϕ is large as it minimizes congestion externalities. On the other hand, in the “inverted” Beckmann model, agglomeration occurs as ϕ increases. The global dispersion force weakens as the negative spillover effects in each region becomes more similar as ϕ increases. The benefit of agglomeration becomes more important for agents as ϕ increases, resulting in agglomeration.¹⁰

2.5 Contrastive implications of local and global dispersion forces

The two-region examples suggest that the spatial scale of dispersion forces embedded in a model have significant impacts on the model’s implications. The key question is how the contrast between local and global dispersion forces appears in many-region settings.

As we will see, even when there are many regions, the impact of better transport access can be in opposite directions between local and global dispersion forces. The timing of agglomeration is the same as the two-region setting: dispersion occurs when transport costs are high (low) under a global (local) dispersion force. Section 4 will see that, when regions are heterogeneous in exogenous advantages, agglomeration toward advantageous locations proceeds as transport access improves if a model has only global dispersion force, and the converse is true for a model with only local dispersion force. If we focus on the population distribution, a better transport connection between the core and periphery regions will leave the periphery behind the core under the former, while it will benefit the periphery under the latter.

Furthermore, the spatial scale of dispersion forces is a crucial determinant for endogenous spatial patterns in many-region settings. The salient feature of a many-region economy is that it allows for diverse forms of spatial agglomeration. This contrasts with the two-region setting where the only form of agglomeration is the level of regional asymmetry (the bigger region’s population). In many-region settings, the type of dispersion forces determines the form of agglomeration. As discussed in Section 1, a global dispersion force induces the formation of multiple distinct economic agglomerations, whereas a local one induces the flattening of each economic agglomeration. Section 3 shows that polycentric spatial patterns as in Figure 2B occurs only under a global dispersion force. If instead the model has only local dispersion force, monocentric spatial patterns as in Figure 2A are the only possible form of agglomeration.

As we will see in the following, the representation of \mathbf{V} by \mathbf{D} for the model is common across the two-region and many-region settings for each model because we can simply

¹⁰In the two-region economy, the models by Krugman (1991) and Helpman (1998) are known to exhibit a similar contrast. In the Krugman (Helpman) model, \bar{x} is stable when ϕ is low (high), and spatial agglomeration occurs when ϕ is high (low). Their predictions are thus opposites of each other, and “Krugman’s scenario is reversed” in the Helpman model (Fujita and Thisse, 2013, Ch.8). This contrast comes from the difference in the spatial scale of their dispersion forces.

replace \mathbf{D} by its many-region version. Section 3 will introduce a unified taxonomy of economic geography models in the literature based on the spatial scale of dispersion forces by focusing on the structure of \mathbf{V} with respect to \mathbf{D} .

3 Endogenous agglomeration in the racetrack economy

Section 3.1 introduces a symmetric many-region geography to generalize the above discussion based on the symmetric two-region economy. Section 3.2 discusses endogenous agglomeration in the many-region economy under local dispersion forces to show that monocentric spatial patterns emerge under local dispersion forces. Section 3.3 discusses that polycentric spatial patterns emerge under global dispersion forces. Section 3.4 considers a general taxonomy of economic geography models by the composition of their dispersion forces. **Proposition 1** summarizes endogenous spatial patterns in each model class. Numerical examples also illustrate general implications on agglomeration behavior in the course of changing transport costs.

3.1 The symmetric racetrack economy

In the symmetric two-region economy, $\bar{\mathbf{x}} = (\frac{1}{2}, \frac{1}{2})$ is the obvious candidate of the starting point of analysis. In asymmetric N -region geography, however, the baseline equilibrium is already nontrivial because the symmetric spatial distribution $\bar{\mathbf{x}} \equiv (\bar{x}, \bar{x}, \dots, \bar{x})$ with $\bar{x} = \frac{1}{N}$ may not be an equilibrium. To employ $\bar{\mathbf{x}}$ as the common initial state for all economic geography models, we presume a symmetric geography. Specifically, we consider an N -region *symmetric racetrack economy* à la [Krugman \(1993\)](#) in which regions are equidistantly placed over a circle and transport is possible only along the circumference (Figure 3).

Assumption RE. *The proximity matrix $[\phi_{ij}]_{i \in \mathcal{N}, j \in \mathcal{N}}$ is given by $\phi_{ij} = \phi^{\ell_{ij}}$, where $\phi \in (0, 1)$ is the freeness of transport between two consecutive regions and $\ell_{ij} \equiv \min\{|i - j|, N - |i - j|\}$ is the distance between regions i and j over the circumference. N is a multiple of four.*

For example, if $N = 4$, the proximity matrix is

$$\begin{bmatrix} \phi_{11} & \phi_{12} & \phi_{13} & \phi_{14} \\ \phi_{21} & \phi_{22} & \phi_{23} & \phi_{24} \\ \phi_{31} & \phi_{32} & \phi_{33} & \phi_{34} \\ \phi_{41} & \phi_{42} & \phi_{43} & \phi_{44} \end{bmatrix} = \begin{bmatrix} 1 & \phi & \phi^2 & \phi \\ \phi & 1 & \phi & \phi^2 \\ \phi^2 & \phi & 1 & \phi \\ \phi & \phi^2 & \phi & 1 \end{bmatrix}. \quad (10)$$

Assumption RE removes the advantages from each region's unique position within transportation networks as it ensures that every region has the same level of accessibility to the other regions. We assume that N is a multiple of four only for simplicity (see Remark A.2

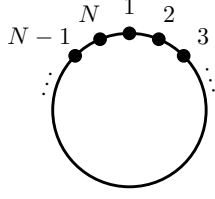


Figure 3: N -region racetrack economy.

in Appendix A for discussion). As seen, the level of interregional transport costs in this economy is summarized by a single parameter ϕ .

Furthermore, to focus on endogenous forces concerning population distribution, we suppose regional asymmetries such as amenity or productivity differences are absent.

Assumption S. *All regions are symmetric regarding their fundamentals.*

See Appendix A.1 for the precise version as a mathematical condition on \mathbf{v} .

Under Assumptions RE and S, the symmetric spatial distribution $\bar{\mathbf{x}}$ is always a spatial equilibrium. The spatial distribution remains flat if $\bar{\mathbf{x}}$ is stable, and agglomeration occurs when $\bar{\mathbf{x}}$ becomes unstable. We consider gradual changes in ϕ . We will see that, as in the two-region economy, the payoff elasticity matrix $\mathbf{V} = \frac{\bar{\mathbf{x}}}{\bar{v}} \left[\frac{\partial v_i(\bar{\mathbf{x}})}{\partial x_j} \right]_{i \in \mathcal{N}, j \in \mathcal{N}}$ at $\bar{\mathbf{x}}$ plays a key role in understanding endogenous agglomeration in this economy.

Before considering models in the literature, it is useful to study the following toy model to understand the basic characteristics of the racetrack geography:

$$v_i(\mathbf{x}) = \sum_{j \in \mathcal{N}} \phi_{ij} x_j. \quad (11)$$

The model is a special case of the Beckmann model (Section 2.2) without the congestion force ($\beta = 0$) and $\alpha = 1$. Because there is only an agglomeration force, $\bar{\mathbf{x}}$ cannot be stable and the agglomeration of all agents in a single region is always stable. If agents are to migrate from the symmetric equilibrium $\bar{\mathbf{x}}$, a monocentric spatial configuration should emerge in this toy model. How do we analytically confirm this idea?

The migration of a small fraction of agents from $\bar{\mathbf{x}}$ leads to a new spatial distribution \mathbf{x} . Let $z_i = x_i - \bar{x}$ denote the marginal increase (decrease) of the population in region i . What is the most desirable deviation $\mathbf{z} = (z_i)_{i \in \mathcal{N}}$ for agents? Let $\bar{v} = v_i(\bar{\mathbf{x}})$ be the payoff level at $\bar{\mathbf{x}}$, and $\delta v_i(\mathbf{z}) \equiv v_i(\bar{\mathbf{x}} + \mathbf{z}) - \bar{v}$ be marginal payoff difference under the population variation \mathbf{z} . Then, the aggregate payoff gain under variation \mathbf{z} can be measured by

$$\omega(\mathbf{z}) = \frac{\bar{\mathbf{x}}}{\bar{v}} \sum_{i \in \mathcal{N}} \delta v_i(\mathbf{z}) z_i, \quad (12)$$

as there are z_i agents migrated to (if $z_i > 0$) or from (if $z_i < 0$) region i , and their payoff

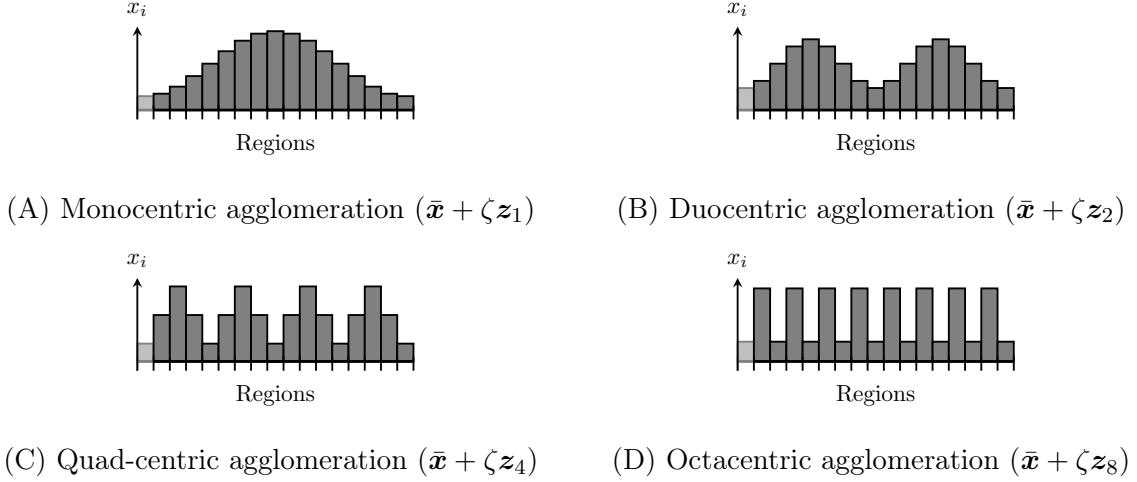


Figure 4: Spatial patterns induced by the eigenvectors $\{z_k\}$ of \mathbf{D} .

Note: The perturbed spatial distribution $\bar{x} + \zeta z_k$ with small ζ for the cases when k is a power of 2 are presented.

gain is $\delta v_i(\mathbf{z})$.¹¹

The most plausible deviation \mathbf{z} from \bar{x} should then maximize the aggregate payoff gain $\omega(\mathbf{z})$. A concise formula for $\omega(\mathbf{z})$ is given by the payoff elasticity matrix \mathbf{V} at \bar{x} :¹²

$$\omega(\mathbf{z}) = \mathbf{z}^\top \mathbf{V} \mathbf{z} \quad (13)$$

where \top denotes transpose. For the toy model (11), $\bar{v} = \bar{x} \sum_{j \in \mathcal{N}} \phi_{ij} = \bar{x} d$ where d is the common row sum of $[\phi_{ij}]$, and $\mathbf{V} = \frac{\bar{x}}{\bar{v}} [\phi_{ij}] = \frac{1}{d} [\phi_{ij}] = \mathbf{D}$. That is,

$$\omega(\mathbf{z}) = \mathbf{z}^\top \mathbf{D} \mathbf{z}. \quad (14)$$

The formula (14) shows that the most plausible deviation at \bar{x} in the toy model corresponds to the eigenvector of \mathbf{D} associated with its maximal eigenvalue. In fact, for the k th eigenvector of \mathbf{D} ,

$$\omega(\mathbf{z}_k) = \mathbf{z}_k^\top \mathbf{D} \mathbf{z}_k = \mathbf{z}_k^\top (\chi_k \mathbf{z}_k) = \chi_k \|\mathbf{z}_k\|^2 = \chi_k \quad (15)$$

where χ_k is the associated eigenvalue and we normalize $\|\mathbf{z}_k\| = 1$ for simplicity.

To understand what spatial configuration is preferred by agents, we need the eigenvectors $\{z_k\}$ and their associated eigenvalues $\{\chi_k\}$ of \mathbf{D} under Assumption RE. Akamatsu et al. (2012) provided analytical expressions for $\{z_k\}$ and $\{\chi_k\}$ (see Lemma A.1 in Appendix A). For completeness, we discuss general intuitions below. The eigenvectors $\{z_k\}$

¹¹In fact, the gain for a migrant from region j to i is $\frac{\bar{x}}{\bar{v}} (\delta v_i(\mathbf{z}) - \delta v_j(\mathbf{z}))$ and adding up this gain for all agents gives (12).

¹²By expanding $\mathbf{v}(\mathbf{x}) = \mathbf{v}(\bar{x} + \mathbf{z})$ about \bar{x} , $\delta v_i(\mathbf{z}) = v_i(\bar{x} + \mathbf{z}) - \bar{v} \approx \left(v_i(\bar{x}) + \sum_{j \in \mathcal{N}} \frac{\partial v_i(\bar{x})}{\partial x_j} z_j \right) - \bar{v} = \sum_{j \in \mathcal{N}} \frac{\partial v_i(\bar{x})}{\partial x_j} z_j$, so that $\frac{\bar{x}}{\bar{v}} \delta \mathbf{v}(\mathbf{x}) \approx \mathbf{V} \mathbf{z}$. Then, we see $\omega(\mathbf{z}) = \frac{\bar{x}}{\bar{v}} \mathbf{z}^\top (\delta \mathbf{v}(\mathbf{x})) = \mathbf{z}^\top \mathbf{V} \mathbf{z}$.

correspond to all symmetric population deviations \mathbf{z} under Assumption RE. Each \mathbf{z}_k is a cosine curve with k equally spaced peaks (Figure 4). The largest number of symmetric peaks is $k = \frac{N}{2}$ when agents concentrate in every other region. That is, there are essentially $\frac{N}{2}$ possible form of agglomeration.

In the toy model (11), we have $\omega(\mathbf{z}_k) = \chi_k$. This means that each eigenvalue χ_k can be interpreted as an index of the marginal increase of the average proximity among agents when the k -centric pattern $\bar{\mathbf{x}} + \zeta \mathbf{z}_k$ emerges from $\bar{\mathbf{x}}$. There are three key properties of $\{\chi_k\}$. First, every χ_k is positive and takes a value between 0 and 1. This is because any deviation from $\bar{\mathbf{x}}$ induces some agglomeration so that the average proximity among agents increases. Second, every χ_k decreases in ϕ because the proximity gain by migration decreases when transport costs decrease (ϕ increases). In particular, $\phi \rightarrow 0$ implies $\chi_k \rightarrow 1$ and $\phi \rightarrow 1$ implies $\chi_k \rightarrow 0$ for all k . Third and foremost, χ_k decreases in k , the number of peaks in \mathbf{z}_k , at given ϕ . In fact, under Assumption RE,

$$\max_k \{\chi_k\} = \chi_1 \quad \text{and} \quad \min_k \{\chi_k\} = \chi_{\frac{N}{2}} \quad (16)$$

at any level of $\phi \in (0, 1)$, where we recall that $\frac{N}{2}$ is the maximum possible number of symmetric peaks. Intuitively, the average proximity from one agent to others is the largest in a monocentric pattern (Figure 4A) compared with polycentric patterns (Figures 4B to 4D), with $k = \frac{N}{2}$ being the most ‘‘dispersed’’ form of a symmetric polycentric pattern.

From (14), (15) and (16), we see that the monocentric deviation \mathbf{z}_1 as in Figure 4A yields the maximum payoff gain in the toy model (as $\max_{\mathbf{z}} \omega(\mathbf{z}) = \omega(\mathbf{z}_1) = \chi_1$), confirming our initial guess. The model (11) has only an agglomeration force and there is no incentive for agents to deviate from a single agglomeration. In fact, $\omega(\mathbf{z})$ is positive for any deviation \mathbf{z} in the toy model and $\bar{\mathbf{x}}$ is always unstable. With dispersion forces, $\bar{\mathbf{x}}$ can be stable if $\omega(\mathbf{z})$ is negative for all possible deviations \mathbf{z} . If $\omega(\mathbf{z}_k)$ turns from negative to positive for some \mathbf{z}_k , then the k -centric deviation is attractive for agents than staying put, and $\bar{\mathbf{x}}$ becomes unstable. Below, we will see the spatial scale of dispersion forces determines the number of peaks that emerge when $\bar{\mathbf{x}}$ becomes unstable. In particular, we will see that the deviation from $\bar{\mathbf{x}}$ takes place towards either $k = 1$ or $k = \frac{N}{2}$ peaks, depending on the dispersion force(s) in the model.

3.2 Local dispersion force

The most simple dispersion force to include is a *local dispersion force* that depends only on the local population x_i in each region, as considered in the Beckmann model (Section 2.2). For the Beckmann model, we have $\mathbf{V} = -\beta \mathbf{I} + \alpha \mathbf{D}$, which is the same as the two-region case except that we use the many-region version for \mathbf{D} . Because \mathbf{D} and \mathbf{V} share the same

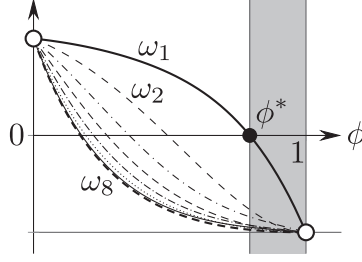


Figure 5: Curves of ω_k for the Beckmann model with a local dispersion force ($N = 16$).

set of eigenvectors, analogous to (15), we compute

$$\omega_k \equiv \omega(\mathbf{z}_k) = \mathbf{z}_k^\top \mathbf{V} \mathbf{z}_k = \mathbf{z}_k^\top (-\beta \mathbf{I} + \alpha \mathbf{D}) \mathbf{z}_k = -\beta + \alpha \chi_k. \quad (17)$$

Then, we see

$$\max_{\mathbf{z}} \omega(\mathbf{z}) = \max_k \{\omega_k\} = \max_k \{-\beta + \alpha \chi_k\} = -\beta + \max_k \{\alpha \chi_k\} = -\beta + \alpha \chi_1. \quad (18)$$

For mobile agents in the Beckmann model, \mathbf{z}_1 is the most beneficial migration pattern at any given ϕ . If $\omega_1 = \omega(\mathbf{z}_1) = -\beta + \alpha \chi_1 < 0$, then $\bar{\mathbf{x}}$ is stable. If $\bar{\mathbf{x}}$ should become unstable, a monocentric agglomeration as in Figure 4A emerges because ω_1 is the first to become positive among ω_k (Figure 5). As in the toy model, monocentric distributions are the most beneficial outcome because agents prefer proximity to others, albeit they must locally disperse to alleviate congestion.

As (17) shows, when \mathbf{V} is simply represented by \mathbf{D} , we can translate the relation between \mathbf{V} and \mathbf{D} to the relation between ω_k and χ_k . This approach covers richer models than the Beckmann model. We consider a quantitative model by Redding and Sturm (2008) as another example. We will see that the model has essentially the same implication as the Beckmann model regarding endogenous spatial patterns.

With agents consuming differentiated goods and housing, the payoff function of agents in the Redding–Sturm model is given by the following function of \mathbf{x} :

$$v_i(\mathbf{x}) = \left(\frac{x_i}{a_i} \right)^{-(1-\mu)} \left(\frac{w_i(\mathbf{x})}{P_i(\mathbf{x})} \right)^\mu \quad \forall i \in \mathcal{N}, \quad (19)$$

where a_i is the endowment of housing stock in region i , $\mu \in (0, 1)$ is the expenditure share of differentiated goods, and $1 - \mu \in (0, 1)$ is the expenditure share of housing. The Dixit–Stiglitz price index $P_i(\mathbf{x})$ is given by

$$P_i(\mathbf{x}) \equiv \left(\sum_{j \in \mathcal{N}} x_j (w_j(\mathbf{x}) \tau_{ji})^{1-\sigma} \right)^{\frac{1}{1-\sigma}} \quad (20)$$

where $\sigma > 1$ the elasticity of substitution between horizontally differentiated varieties, and $\tau_{ij} \geq 1$ the iceberg transport cost between regions. For one unit to arrive at destination j , τ_{ij} units must be shipped from origin i . Agents' wage $\mathbf{w}(\mathbf{x}) = (w_i(\mathbf{x}))_{i \in \mathcal{N}}$ is the unique solution for a system of nonlinear equations that summarizes the market equilibrium conditions given \mathbf{x} , such as goods and labor market clearing and the zero-profit condition of monopolistically competitive firms. Specifically, given \mathbf{x} , \mathbf{w} is the solution for

$$w_i = \sum_{j \in \mathcal{N}} \frac{(w_i \tau_{ij})^{1-\sigma}}{\sum_{k \in \mathcal{N}} x_k (w_k \tau_{kj})^{1-\sigma}} w_j x_j \quad \forall i \in \mathcal{N}. \quad (21)$$

The proximity matrix for this model is $[\phi_{ij}] = [\tau_{ij}^{1-\sigma}]$.

Imposing Assumption RE and Assumption S, the payoff elasticity matrix at the symmetric distribution $\bar{\mathbf{x}}$ is given as follows (see Appendix D for derivations):

$$\mathbf{V} = G^b(\mathbf{D})^{-1} G^\sharp(\mathbf{D}), \quad (22)$$

where we set

$$G^\sharp(\chi) \equiv -(1 - \mu) + \left(\frac{\mu}{\sigma} + \frac{\mu}{\sigma - 1} - (1 - \mu) \frac{\sigma - 1}{\sigma} \right) \chi, \quad (23)$$

$$G^b(\chi) \equiv 1 + \frac{\sigma - 1}{\sigma} \chi > 0 \quad (24)$$

and, for a polynomial $P(\chi) = c_0 + c_1 \chi + c_2 \chi^2 + \dots$, we define $P(\mathbf{D}) = c_0 \mathbf{I} + c_1 \mathbf{D} + c_2 \mathbf{D}^2 + \dots$. We can then conclude that¹³

$$\omega_k = \omega(\mathbf{z}_k) = \frac{G^\sharp(\chi_k)}{G^b(\chi_k)}. \quad (25)$$

If $\omega_k < 0$ for all k , then $\bar{\mathbf{x}}$ is stable. Only $G^\sharp(\cdot)$ matters for the sign of ω_k as $G^b(\cdot) > 0$. Focusing on G^\sharp in (23), we observe it can become positive only when $\frac{1}{\sigma} > 1 - \mu$, which means that dispersion force is sufficiently weaker than agglomeration force.¹⁴ Under this condition, we have $\frac{\mu}{\sigma} + \frac{\mu}{\sigma - 1} - (1 - \mu) \frac{\sigma - 1}{\sigma} > 0$ in (23).

We see a structure of \mathbf{V} common for the Redding–Sturm model and the Beckmann model. The tradeoff between agglomeration and dispersion forces appears in \mathbf{V} as

$$G^\sharp(\mathbf{D}) = -c_0 \mathbf{I} + c_1 \mathbf{D} \quad (26)$$

in both models, where $c_0 > 0$ and $c_1 > 0$ represent the magnitudes of dispersion and

¹³Because \mathbf{D} is a *circulant matrix*, $G^\sharp(\mathbf{D})$, $G^b(\mathbf{D})$, and $\mathbf{V} = G^b(\mathbf{D})^{-1} G^\sharp(\mathbf{D})$ are all circulant, and the k th eigenvalue–eigenvector pair of \mathbf{V} is obtained using that of \mathbf{D} (see Appendix A.1).

¹⁴This is a version of the so-called *no-black-hole condition* (Fujita et al., 1999a, p.59) and ensures that endogenous agglomeration can occur when ϕ changes.

agglomeration forces, respectively. The uniform distribution $\bar{\mathbf{x}}$ is stable when transport costs are low (ϕ is high), and the endogenous spatial configuration becomes monocentric in both the Beckmann model and the Redding–Sturm model.

Such commonality between the two models is no coincidence. The dispersion force in the Redding–Sturm model arises from competition in the housing market in each region that is accessible for local residents only. Consequently, the dispersion force does not depend on interregional proximity structure \mathbf{D} but only on the mass of agents *within* each region. In G^\sharp , it appears as negative constant term as in the Beckmann model, indicating it is a *local* dispersion force.

The agglomeration forces in the Redding–Sturm model is reflected to the coefficient $c_1 = \frac{\mu}{\sigma-1} + \frac{\mu}{\sigma} - (1-\mu)\frac{\sigma-1}{\sigma}$ of the first-order term of \mathbf{D} in (23). It has more complicated structure than the Beckmann model as it arises from the cost-of-living effects for the differentiated varieties and also a market size effect on agents’ income, as well as general equilibrium effects.¹⁵ Nonetheless, by focusing on the essential structure of \mathbf{V} as in (26), we can abstract from the microfoundations behind c_0 or c_1 to see that a monocentric pattern should emerge from $\bar{\mathbf{x}}$ in the Redding–Sturm model, and in that sense the model is in the same bracket as the Beckmann model.

3.3 Global dispersion force

This section explores the implications of global dispersion forces. As discussed in Section 2.3, we define *global dispersion forces* as negative effects of agglomeration that depend on the proximity structure between regions. The key difference between local and global dispersion forces is whether the force acts *within* or *between* locations. Section 2.3 considered the “inverted” Beckmann model as a toy example for a global dispersion force. A more natural one arises from competition over dispersed demand. We will see that such an economic force appears as a second-order term of \mathbf{D} in \mathbf{V} .

For example, consider the following toy model with interregional trade. There are fixed demands dispersed over regions and trade flows are given by gravity equations. Let μ_m be the expenditure in region m , which is fixed. Suppose each agent in region i receives an equal gravity-type share of $(\mu_m)_{m \in \mathcal{N}}$. Specifically, the share an agent in region i receives from region m is

$$q_{mi} = \frac{\phi_{im}}{\sum_{l \in \mathcal{N}} \phi_{lm} x_l}, \quad (27)$$

¹⁵A region with a better access to suppliers of differentiated good (firms) has a lower price index and favored by mobile consumers if the nominal wage is the same across regions ($\frac{\mu}{\sigma-1}$). Also, a region that have better access to consumers will face more demand, raising agents’ income ($\frac{\mu}{\sigma}$). The market clearing conditions then mediate all the effects including the dispersion force, adding the third term $-(1-\mu)\frac{\sigma-1}{\sigma}$. For detailed discussions on how endogenous forces in economic geography models are reflected in these coefficients, see also Remark D.1 in Appendix D.2.1 and Remark D.4 in Appendix D.2.2.

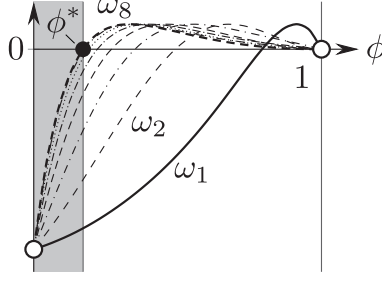


Figure 6: Curves of ω_k for the toy trade model with a global dispersion force ($N = 16$).

so that $\sum_{i \in \mathcal{N}} q_{mi} x_i = 1$. Then, the income of an agent in region i is

$$y_i = \sum_{m \in \mathcal{N}} q_{mi} \mu_m = \sum_{m \in \mathcal{N}} \frac{\phi_{im}}{\sum_{l \in \mathcal{N}} \phi_{lm} x_l} \mu_m. \quad (28)$$

For each k , we observe that: The closer regions i and k are, the larger expenditure from region m to i is. Also, more intense the competition over region m 's expenditure is (the larger $\sum_{l \in \mathcal{N}} \phi_{lm} x_l$ is), the smaller the expenditure from region m to i is.

Assume the same agglomeration force as the Beckmann model and suppose the payoff function is

$$v_i(\mathbf{x}) = \left(\sum_j \phi_{ij} x_j \right)^\alpha y_i. \quad (29)$$

Suppose $\mu_m = \mu$ for all m to satisfy Assumption S. Then, we have

$$\mathbf{V} = \alpha \mathbf{D} - \mathbf{D}^2. \quad (30)$$

The negative second-order term $-\mathbf{D}^2$ is the global dispersion force in the model. It represents competition effects embedded in the gravity equation. In this model, agents compete over geographically dispersed demands $\{\mu_m\}$. For an agent in region i , an increase in the number of competitors in region $j \neq i$ over the expenditure in region m ($\neq j \neq i$) implies less income from region m . The magnitude of such an effect depends on both ϕ_{im} and ϕ_{jm} , and thus appears as a second-order term of \mathbf{D} . In fact, in general,

$$\frac{\partial}{\partial x_j} q_{mi} = -\frac{\phi_{im}}{\sum_{l \in \mathcal{N}} \phi_{lm} x_l} \frac{\phi_{jm}}{\sum_{l \in \mathcal{N}} \phi_{lm} x_l} = -q_{im} q_{jm} < 0. \quad (31)$$

For each region m , this effect is stronger when the trade share q_{jm} of region- j competitors' over the demand in region m is larger (when ϕ_{jm} is small and region j is close to region m), but smaller when competition in region m is tough (when $\sum_{l \in \mathcal{N}} \phi_{lm} x_l$ is high).

From (30), we see

$$\omega_k = \alpha\chi_k - \chi_k^2 = \chi_k(\alpha - \chi_k). \quad (32)$$

The uniform distribution $\bar{\mathbf{x}}$ is stable if $\max_k \omega_k < 0$, that is, if $\alpha < \chi_k$ for all k , or when transport costs are high because χ_k s are decreasing in ϕ . Because $\min_k \chi_k = \chi_{\frac{N}{2}}$, $\bar{\mathbf{x}}$ is stable if $\alpha < \chi_{\frac{N}{2}}$. If $\bar{\mathbf{x}}$ becomes unstable, it is because $\omega_{\frac{N}{2}}$ turns to positive (Figure 6), so that the deviation toward $\mathbf{z}_{\frac{N}{2}}$ -direction becomes attractive for agents. That is, a $\frac{N}{2}$ -centric spatial pattern as in Figure 4D emerges.

As a less trivial example, the Krugman (1991) model is a model with a global dispersion force. In a many-region version of the model, its payoff function is

$$v_i(\mathbf{x}) = w_i(\mathbf{x})P_i(\mathbf{x})^{-\mu} \quad \forall i \in \mathcal{N}. \quad (33)$$

As in the Redding–Sturm model, $w_i(\mathbf{x})$ is the wage of mobile workers, $P_i(\mathbf{x})$ is the Dixit–Stiglitz price index as in (20), $\mu \in (0, 1)$ is the expenditure share of manufactured goods, $\sigma > 1$ the elasticity of substitution between horizontally differentiated varieties, and $\tau_{ij} \geq 1$ the iceberg transport cost. Wage $\mathbf{w}(\mathbf{x}) = (w_i(\mathbf{x}))_{i \in \mathcal{N}}$ is the unique solution for

$$w_i = \mu \sum_{j \in \mathcal{N}} \frac{(w_j \tau_{ij})^{1-\sigma}}{\sum_{k \in \mathcal{N}} x_k (w_k \tau_{kj})^{1-\sigma}} (w_i x_i + l_i) \quad \forall i \in \mathcal{N}, \quad (34)$$

where $l_i > 0$ is the total income of immobile consumers in region i . The proximity matrix is $[\phi_{ij}] = [\tau_{ij}^{1-\sigma}]$. The important differences from the Redding–Sturm model are that agents do not consume local housing and there are immobile consumers dispersed across the regions, which is similar to the toy model discussed above. The former difference removes the local dispersion force in the Redding–Sturm model, whereas the latter introduces a global dispersion force.

Analogous to the Redding–Sturm model, for the Krugman model under Assumption S (i.e., $l_i = l$ for all i), we have $\mathbf{V} = G^b(\mathbf{D})^{-1}G^\sharp(\mathbf{D})$ with

$$G^\sharp(\chi) = \left(\frac{\mu}{\sigma-1} + \frac{\mu}{\sigma} \right) \chi - \left(\frac{\mu^2}{\sigma-1} + \frac{1}{\sigma} \right) \chi^2, \quad (35)$$

$$G^b(\chi) = 1 - \frac{\mu}{\sigma} \chi - \frac{\sigma-1}{\sigma} \chi^2, \quad (36)$$

so that $\omega_k = \frac{G^\sharp(\chi_k)}{G^b(\chi_k)}$ (see Appendix D.2.1 for the derivation). Only $G^\sharp(\cdot)$ is relevant for the stability of $\bar{\mathbf{x}}$ as $G^b(\cdot) > 0$ if $\chi \in (0, 1)$. We can thus identify a structure of \mathbf{V} common for the Krugman model and the toy trade model as follows:

$$G^\sharp(\mathbf{D}) = c_1 \mathbf{D} - c_2 \mathbf{D}^2 \quad (37)$$

with $c_1 > 0$ and $c_2 > 0$ summarizing each model’s dispersion force and agglomeration force, respectively. As a consequence, endogenous agglomeration from $\bar{\mathbf{x}}$ in the Krugman model leads to $\frac{N}{2}$ -centric pattern as in the toy trade model.

The dispersion force in the Krugman model is the so-called *market-crowding effect* between firms (Baldwin et al., 2003, Ch. 2). If firms in a region are close to other firms (in the same region or in other regions), mobile workers are discouraged from entering such a region because those firms face fierce market competition and can only pay low nominal wages. This competition mechanism is the same as in the toy trade model discussed above. While agents tend to agglomerate locally because of positive externalities, when there are multiple agglomerations, the locations of such agglomerations must be geographically as dispersed as possible to alleviate negative effects of competition. This results in the formation of $\frac{N}{2}$ agglomerations in our symmetric N -region economy.

3.4 The three model classes

In the examples presented above, we see the payoff elasticity matrix \mathbf{V} at $\bar{\mathbf{x}}$ satisfies

$$\mathbf{V} \simeq c_0 \mathbf{I} + c_1 \mathbf{D} + c_2 \mathbf{D}^2 \quad (38)$$

where the notation $\mathbf{V} \simeq \mathbf{X}$ indicates $\mathbf{V} = \bar{\mathbf{V}} \mathbf{X}$ with a matrix $\bar{\mathbf{V}}$ that is irrelevant for the stability of $\bar{\mathbf{x}}$. Specifically, by (38) we indicate that

$$\text{sgn}[\omega_k] = \text{sgn}[c_0 + c_1 \chi_k + c_2 \chi_k^2] \quad (39)$$

so that $c_0 \mathbf{I} + c_1 \mathbf{D} + c_2 \mathbf{D}^2$ is the component of \mathbf{V} that governs the stability of $\bar{\mathbf{x}}$. In fact, many extant models result in such a quadratic form.¹⁶

The coefficients $\{c_0, c_1, c_2\}$ in (38) are given by the model parameters. In (38), c_0 summarizes all the forces that work *within* each location (or *local* forces). The latter two coefficients $\{c_1, c_2\}$ correspond to *global* forces. The direct effects from one region to another, such as the agglomeration externalities in the Beckmann model (Section 2.2), are summarized by c_1 . Similarly, c_2 summarizes the indirect or “second-order” effects from region j to region k , and then from region k to region i , which typically arise from competition effects embedded in the gravity formula (Section 3.3).

Each coefficient represents the *net* effect at the corresponding order of \mathbf{D} . For example, there may be both positive and negative local externalities (e.g., local agglomeration economies and local congestion). If a model considers both these forces, then c_0 for the model becomes their composite. If $c_0 > 0$, it means the parameter values are such that

¹⁶For example, (38) covers models of endogenous city center formation (e.g., Beckmann, 1976), “new economic geography” models with a single monopolistically competitive industry (e.g., Krugman, 1991; Helpman, 1998; Redding and Sturm, 2008), and the “universal gravity” framework (Allen et al., 2019) including Allen and Arkolakis (2014).

Dispersion force	Global	Local	Examples
Class I	✓		Harris and Wilson (1978) Krugman (1991) Puga (1999) (§3) Forslid and Ottaviano (2003) Pflüger (2004)
Class II		✓	Beckmann (1976) Helpman (1998) Murata and Thisse (2005) Redding and Sturm (2008) Allen and Arkolakis (2014) Redding and Rossi-Hansberg (2017) (§3).
Class III	✓	✓	Tabuchi (1998) Puga (1999) (§4) Pflüger and Südekum (2008) Takayama and Akamatsu (2011)

Table 1: Spatial scale of dispersion forces at work and model classes

local agglomeration force dominates the local dispersion force. Converse is true if $c_0 < 0$.

By distinguishing local and global dispersion forces, we can define three prototypical model classes: models with only global, only local, and both global and local dispersion forces. Focusing on \mathbf{V} of the form (38), the three model classes are characterized as follows (see Appendix A.1 for the formal definitions of the three model classes). Table 1 lists examples in the literature.

The *Class I* models have only global dispersion forces. Possible forms of \mathbf{V} include

$$\mathbf{V} \simeq c_1 \mathbf{D} - c_2 \mathbf{D}^2, \quad \mathbf{V} \simeq c_0 \mathbf{I} - c_2 \mathbf{D}^2, \quad \text{or} \quad \mathbf{V} \simeq c_0 \mathbf{I} - c_1 \mathbf{D}, \quad (40)$$

where $c_k > 0$ are model-dependent constants.(we assume $c_k > 0$ hereafter). Global dispersion forces appear as negative terms of \mathbf{D} . The symmetry $\bar{\mathbf{x}}$ is stable when transport costs are high.

The *Class II* models have only local dispersion forces as their effective dispersion forces. Typical form of \mathbf{V} are

$$\mathbf{V} \simeq -c_0 \mathbf{I} + c_1 \mathbf{D}, \quad \text{and} \quad \mathbf{V} \simeq -c_0 \mathbf{I} + c_1 \mathbf{D} - c_2 \mathbf{D}^2, \quad (41)$$

where $-c_0 < 0$ represents the local dispersion force. The symmetry is stable when transport costs are low. While there may be a global dispersion force ($-c_2 \mathbf{D}^2$), c_2 is so small for any set of parameter values that $\bar{\mathbf{x}}$ cannot become stable when transport costs are high (e.g., Helpman, 1998). In this sense, global dispersion forces are essentially non-existent in Class II models.

Finally, *Class III* models are the synthesis of Classes I and II, and have both local

and global dispersion forces:

$$\mathbf{V} \simeq -c_0 \mathbf{I} + c_1 \mathbf{D} - c_2 \mathbf{D}^2. \quad (42)$$

In this model class, c_2 is sufficiently large so that $\bar{\mathbf{x}}$ is stable when transport costs are high. The uniform distribution $\bar{\mathbf{x}}$ is stable either when transport costs are high or low.

The three model classes behave differently when $\bar{\mathbf{x}}$ becomes unstable. By focusing on the most plausible deviation for agents as in Sections 3.2 and 3.3, we can formally characterize the endogenous spatial patterns that emerge in Class I, II, or III models (see Appendix A.1 for the proof as well as the formal definitions of the model classes).

Proposition 1. *Suppose Assumptions RE and S. Consider an economic geography model. Suppose endogenous agglomeration occurs in the model.*

- (a) *If the model is of Class I, then the uniform distribution $\bar{\mathbf{x}}$ is stable when transport costs are high. Specifically, with some $\phi^* \in (0, 1)$, $\bar{\mathbf{x}}$ is stable for all $\phi \in (0, \phi^*)$ and unstable for all $\phi \in (\phi^*, 1)$. A polycentric pattern with $\frac{N}{2}$ peaks emerges when $\bar{\mathbf{x}}$ becomes unstable at ϕ^* .*
- (b) *If the model is of Class II, then $\bar{\mathbf{x}}$ is stable when transport costs are low. Specifically, with some $\phi^{**} \in (0, 1)$, $\bar{\mathbf{x}}$ is stable for all $\phi \in (\phi^{**}, 1)$ and unstable for all $\phi \in (0, \phi^{**})$. A monocentric pattern emerges when $\bar{\mathbf{x}}$ becomes unstable at ϕ^{**} .*
- (c) *If the model is of Class III, then $\bar{\mathbf{x}}$ is stable when transport costs are either high or low. Specifically, there are $\phi^*, \phi^{**} \in (0, 1)$ with $\phi^* < \phi^{**}$ such that $\bar{\mathbf{x}}$ is stable for all $\phi \in (0, \phi^*) \cup (\phi^{**}, 1)$. A polycentric pattern with $\frac{N}{2}$ peaks emerges at ϕ^* , whereas a monocentric pattern emerges at ϕ^{**} .*

Note that (a) and (b) generalize the two-region case (Section 2.3) in that the uniform distribution is stable for the high (low) levels of transport costs. The new dimension is the spatial distribution. Class I models produce a $\frac{N}{2}$ -centric distribution, which may be interpreted as the formation of $\frac{N}{2}$ small cities (Figure 4D), each of which is confined in a single region (or, there is no local dispersion). Class II models produce a monocentric distribution, which can be interpreted as the formation of a large economic agglomeration extending over multiple regions (Figure 4A). Class III is a synthesis of Classes I and II. In contrast to Class I models, in a polycentric pattern in Class III models, each agglomeration can be bell-shaped and extend over multiple regions (or, local dispersion can occur). The contrast between Classes I and II in terms of endogenous spatial patterns is hidden in the two-region setup.

3.5 Evolution of spatial patterns

Proposition 1 shows endogenous agglomeration patterns are qualitatively different be-

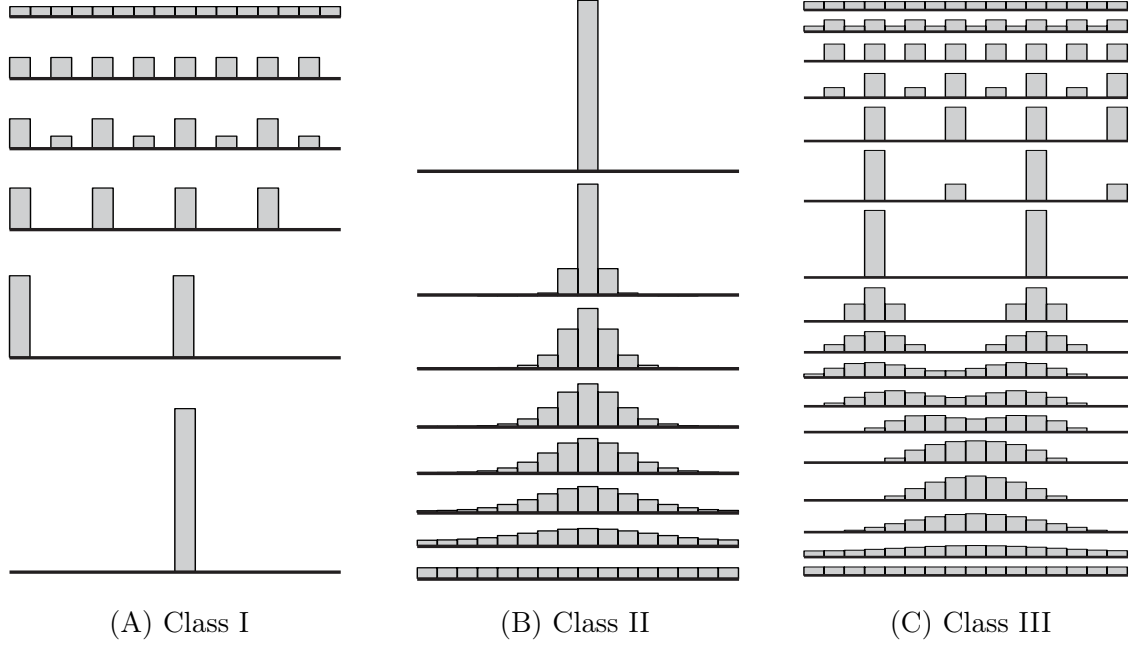


Figure 7: Stable spatial patterns at different transport cost levels as transport costs go down from top to bottom (ϕ increases from around zero to around one).

tween the three model classes. This result is based on the local stability analysis of the uniform distribution \bar{x} . The whole path of spatial equilibria along the transport cost axis (“global behavior”) is also of interest. To study such behavior, we can assume a specific payoff function instead of a general class of economic geography models. However, such analyses suffer from intrinsic model dependence. We here instead provide numerical examples to illustrate representative agglomeration behavior common for each model class when transport costs decrease.¹⁷

Figure 7 depicts the typical global behaviors of the three model classes on the $N = 16$ racetrack economy. Starting from \bar{x} , we follow a path of stable spatial distribution from $\phi = 0$ (high transport costs) to $\phi = 1$ (low transport costs).¹⁸ The lower in each figure, the higher ϕ . For interpretability, the spatial distributions in the racetrack economy are visualized on a line segment; the leftmost region is neighboring to the rightmost one. Figure 7A considers a many-region version of Krugman (1991)’s model as a representative example of Class I. When ϕ is small, the uniformity \bar{x} is the stable spatial configuration. A polycentric distribution with $\frac{16}{2} = 8$ agglomerations endogenously emerges when ϕ reaches the critical value [Proposition 1 (a)]. An increase in ϕ induces a decrease in the number of agglomerations, an increase in the spacing between them, and an increase in the size of each agglomeration. The number of agglomerations evolves as

¹⁷See Remark A.3 in Appendix A for a discussion on general and model-specific results in the literature.

¹⁸For each model, we consider the representative equilibrium path that starts from \bar{x} , but there can be many other equilibrium paths for, in particular, Class I and III models because the exact location of agglomerations can be different for these class of models. For an example of thorough numerical analyses, see, e.g., Ikeda et al. (2012b) on the Krugman (1991) model.

16 \rightarrow 8 \rightarrow 4 \rightarrow 2 \rightarrow 1. In this class of models, once established agglomeration can decline when it is absorbed in *agglomeration shadow* (Arthur, 1994; Fujita and Krugman, 1995) of other bigger agglomerations. For the fifth region from the left in Figure 7A, transport improvements increase its population initially but it loses population in the later stages. Class I models suggest that, under a global dispersion force, the number of agglomerations decreases and spacing between them increases when interregional transport costs decreases. Further, the growths of bigger agglomerations are at the expense of smaller agglomerations.

In Class II models, only monocentric distributions emerge endogenously. Figure 7B considers Helpman (1998)'s model. The symmetry \bar{x} is unstable when ϕ is small and agents concentrate around a single peak. When the transport cost decreases, it causes the flattening of the single agglomeration as the peak population density is reduced. At the critical level of ϕ , the spatial distribution becomes uniform [Proposition 1 (b)].

Class III is a synthesis of Classes I and II. Figure 7C considers a Class III model proposed by Pflüger and Südekum (2008). The uniform distribution is stable when ϕ is small. As ϕ increases, octa-centric agglomerations emerge at some point as in Class I models. Multiple bell-shaped agglomerations are generated at moderate levels of transport cost. Further decrease in transport costs causes a decrease in the number of agglomerations (as in Class I models) and the flattening of each agglomeration (as in Class II models). When ϕ is close to one, the spatial distribution becomes monocentric, similar to the Class II model in Figure 7B. The overall behavior of the Class III model is qualitatively consistent with the two-faced evolution of Japanese cities (global concentration and local flattening) discussed in Section 1.

Appendix C provides numerical simulations for the $N = 8$ case with bifurcation diagrams. Also, Appendix E provides numerical simulations for the case we drop Assumption RE by considering a long narrow economy and a square economy. The discussed contrasts between model classes regarding the number, size, and spatial extent of cities generalize beyond the symmetric racetrack economy.

4 Regional heterogeneities

The previous sections abstract from geographical asymmetries to focus on endogenous economic forces that remains under the symmetry of geography. Exogenous asymmetries undoubtedly play important roles in shaping real-world economic geography. This section considers how the spatial scale of dispersion forces matters when the underlying geography is asymmetric. We will see that when interregional access improves, the regions with higher (lower) exogenous local advantage experience population increase if the model has only a global (local) dispersion force.

4.1 Evaluating the impacts of local characteristics

As an example of local factors in economic geography models, consider the model by [Allen and Arkolakis \(2014\)](#). The model is a perfectly competitive economic geography model with agglomeration and dispersion forces. The payoff function of the model is

$$v_i(\mathbf{x}) = \underbrace{\left(u_i x_i^\beta\right)}_{\substack{\text{Local amenity} \\ \text{(dispersion force)}}} \left(\sum_{k \in \mathcal{N}} w_k^{1-\sigma} (A_k x_k^\alpha)^{\sigma-1} \phi_{ki}\right)^{1/(\sigma-1)} w_i \quad (43)$$

with wage $\mathbf{w} = (w_i)_{i \in \mathcal{N}}$ given as the unique solution for the market equilibrium conditions

$$w_i x_i = \sum_{j \in \mathcal{N}} \frac{w_i^{1-\sigma} \underbrace{(b_i x_i^\alpha)^{\sigma-1}}_{\substack{\text{Local productivity spillover (agglomeration force)}}} \phi_{ij}}{\sum_{k \in \mathcal{N}} w_k^{1-\sigma} (b_k x_k^\alpha)^{\sigma-1} \phi_{kj}} w_j x_j \quad \forall i \in \mathcal{N} \quad (44)$$

where $\alpha > 0$, $\beta < 0$, $\sigma > 1$. Here, $\mathbf{u} = (u_i)_{i \in \mathcal{N}}$ and $\mathbf{b} = (b_i)_{i \in \mathcal{N}}$ are the region-specific exogenous parameters for local amenity and productivity. Suppose equilibrium is unique, and the current population distribution \mathbf{x} is observed. Then, the value of exogenous parameters that realize \mathbf{x} as the spatial equilibrium, $\hat{\mathbf{u}} = \mathbf{u}(\mathbf{x})$ and $\hat{\mathbf{b}} = \mathbf{b}(\mathbf{x})$, are uniquely obtained by solving (44) and the payoff equalization $v^* = v_i(\mathbf{x}) \forall i$ together. Counterfactual analyses can then be done, for example, by considering how the equilibrium spatial distribution changes when interregional transport costs change under the premise that $\hat{\mathbf{u}}$ and $\hat{\mathbf{b}}$ are fixed. How such local parameters affect counterfactual equilibria?

Throughout Section 4, we retain Assumption [RE](#) and focus on the role of local regional characteristics. Let $\mathbf{a} = (a_i)_{i \in \mathcal{N}}$ with $a_i > 0$ be exogenous characteristics of region i , which may or may not affect the payoffs in other regions. For example, a_i may be the level of exogenous amenities in region i ¹⁹ or region i 's exogenous productivity. In the latter case, trade flows and the resulting payoffs in other regions can depend on a_i . Under Assumption [RE](#), all regions are symmetric if $\mathbf{a} = \bar{\mathbf{a}} \equiv (\bar{a}, \bar{a}, \dots, \bar{a})$ for some $\bar{a} > 0$ and $(\bar{\mathbf{x}}, \bar{\mathbf{a}})$ is an equilibrium. Consider an infinitesimal variation in the local characteristic so that $\mathbf{a} \neq \bar{\mathbf{a}}$ with the average fixed at \bar{a} . Suppose there is a new equilibrium under \mathbf{a} , say $\mathbf{x}(\mathbf{a})$, which is close to $\bar{\mathbf{x}}$. We assume that $\bar{\mathbf{x}}$ is stable, as otherwise considering the perturbed version $\mathbf{x}(\mathbf{a})$ is nonsensical.

How to measure the overall impact of such variation in \mathbf{a} in shaping the new equilibrium? We can consider the covariance between region i 's relative (dis)advantage $a_i - \bar{a}$

¹⁹In our framework, all endogenous mechanisms related to agents' spatial distribution \mathbf{x} , including exogenous amenities (e.g., [Diamond, 2016](#)), are embedded in the payoff function \mathbf{v} . We can see \mathbf{a} as the exogenous region-specific parameters that must be introduced in quantitative analysis.

and the relative deviation of its population from the uniformity, $x_i(\mathbf{a}) - \bar{x}$:

$$\rho \equiv \sum_{i \in \mathcal{N}} (a_i - \bar{a}) (x_i(\mathbf{a}) - \bar{x}). \quad (45)$$

For example, \mathbf{a} does not affect \mathbf{x} in the model at all if $\rho = 0$. When \mathbf{a} corresponds to regional advantages in the model, it is natural that $(x_i(\mathbf{a}) - \bar{x})(a_i - \bar{a}) > 0$ for all $i \in \mathcal{N}$ so that ρ is positive. To focus on a class of local characteristics that acts positively for the payoff for agents, we assume $\rho > 0$ for \mathbf{a} under consideration.

A natural question upon considering ρ is whether it increases or decreases when transport costs change when we fix \mathbf{a} . The response of ρ can be seen as the aggregate of responses of the individual regions in the counterfactual exercises with quantitative spatial models (QSMs). Does improved transportation access strengthen (weaken) the role of asymmetries in local characteristics? As discussed above, calibration of a QSM under a given proximity structure \mathbf{D} requires \mathbf{a} to be set to a specific value that realizes the observed data (such as agents' spatial distribution \mathbf{x}) as the equilibrium of the model. Typical counterfactual questions then ask the effects of changes in interregional transport costs (the proximity structure \mathbf{D}) under the assumption that \mathbf{a} does not change.

Let $\tilde{\mathbf{x}}(\mathbf{a})$ be the counterfactual equilibrium after transport costs change under an economic geography model, and $\tilde{\rho}$ be the corresponding correlation computed by (45). Then, the response of ρ under the model is simply

$$\Delta\rho \equiv \tilde{\rho} - \rho = \sum_{i \in \mathcal{N}} (a_i - \bar{a}) (\tilde{x}_i(\mathbf{a}) - x_i(\mathbf{a})) \quad (46)$$

because $a_i - \bar{a}$ are common for ρ and $\tilde{\rho}$. If $\Delta\rho$ is positive, advantageous (disadvantageous) regions attract (lose) population under the counterfactual transport costs change. The converse is true if $\Delta\rho$ is negative. Thus, the response of ρ characterizes the model's intrinsic bias in how the model's endogenous mechanisms would impact the outcomes of counterfactual experiments.

4.2 A general characterization of aggregate comparative statics

That said, counterfactual implications in QSMs are inherently model-dependent, and the choice of model class can alter comparative statics results. To formalize this, we analytically characterize the response of ρ in economic geography models under Assumption RE. For illustration, suppose two regions have the same local characteristics and assume that $\bar{\mathbf{x}} = (\bar{x}, \bar{x})$ is stable. Consider a marginal regional asymmetry of the form $\mathbf{a} = (\bar{a} + \epsilon, \bar{a} - \epsilon)$ with small ϵ , so that $\bar{\mathbf{x}}$ is perturbed to a new equilibrium $\mathbf{x} = (\bar{x} + \xi, \bar{x} - \xi)$ with small



(A) The Krugman model (Class I) (B) The Redding–Sturm model (Class II)

Figure 8: The curve of the gain ω for the two-region case. This section considers the gray region where the uniform distribution $\bar{\mathbf{x}}$ is stable.

ξ . We can assume that $\xi > 0$ and $\epsilon > 0$. By definition, we have

$$\rho = (a_1 - \bar{a})(x_1 - \bar{x}) + (a_2 - \bar{a})(x_2 - \bar{x}) = \epsilon\xi + (-\epsilon)(-\xi) = 2\epsilon\xi > 0. \quad (47)$$

We can obtain the analytical expression for ρ . As we have seen in Section 2.2, we can measure the payoff gain of marginal migrants ξ at $\bar{\mathbf{x}}$ by the elasticity of the payoff difference ω (3). We have $\omega < 0$ as we assume $\bar{\mathbf{x}}$ is stable. On the other hand, the payoff gain induced by the marginal regional asymmetry in \mathbf{a} can be evaluated by the elasticity of the payoff difference concerning region 1's exogenous advantage:

$$\alpha \equiv \frac{\bar{a}}{\bar{v}} \left(\frac{\partial v_1(\bar{\mathbf{x}}, \bar{\mathbf{a}})}{\partial a_1} - \frac{\partial v_2(\bar{\mathbf{x}}, \bar{\mathbf{a}})}{\partial a_1} \right), \quad (48)$$

where we make the dependence of \mathbf{v} on \mathbf{a} explicit and $\bar{v} = v_i(\bar{\mathbf{x}}, \bar{\mathbf{a}})$. As the new spatial distribution \mathbf{x} is an equilibrium, we require $v_1(\mathbf{x}) = v_2(\mathbf{x})$. That is, $\omega < 0$ and $\alpha > 0$ should counterweight each other. Specifically, we must have $\frac{\omega}{\bar{x}}\xi + \frac{\alpha}{\bar{a}}\epsilon = 0$, implying

$$\rho = 2\epsilon\xi = -c\frac{\alpha}{\omega} = c\frac{\alpha}{|\omega|} \quad (49)$$

where $c \equiv 2\epsilon^2\frac{\bar{x}}{\bar{a}}$.²⁰ Then, the response of ρ in the course of decreasing transport costs is

$$\rho' = \frac{c}{\omega^2} (\alpha\omega' - \omega\alpha') = \frac{c}{\omega^2} (\alpha\omega' + |\omega|\alpha'), \quad (50)$$

where $'$ denotes the differentiation by ϕ . We recall that an increase of ϕ means a decrease in the transport cost level. Obviously, the sign of ρ' is thus generally model-dependent.

In the simplest case, α is constant. If $v_i(\mathbf{x}, \mathbf{a}) = a_i v_i(\mathbf{x})$ where $v_i(\mathbf{x})$ does not include \mathbf{a} , we see $\alpha = \frac{\bar{a}}{\bar{v}}(v_1(\bar{\mathbf{x}}) - 0) = \bar{a} > 0$. Then, (50) reduces to $\rho' = \frac{c\bar{a}}{\omega^2}\omega'$, that is,

$$\text{sgn } \rho' = \text{sgn } \omega'. \quad (51)$$

²⁰With $x := x_1$ and $a := a_1$, let $f(x, a) \equiv v_1(x, a) - v_2(x, a)$. Then, at $(x, a) = (\bar{x}, \bar{a})$ and on the equilibrium curve $f(x, a) = 0$, we have $f_x(x, a)\xi + f_a(x, a)\epsilon = \frac{\bar{x}}{\bar{v}}f_x(x, a)\frac{\bar{v}}{\bar{x}}\xi + \frac{\bar{a}}{\bar{v}}f_a(x, a)\frac{\bar{v}}{\bar{a}}\epsilon = \omega\frac{\bar{v}}{\bar{x}}\xi + \alpha\frac{\bar{v}}{\bar{a}}\epsilon = 0$.

In Class I models, agglomeration occurs when ϕ increases. Reflecting this, for Class I models in the literature, we have $\omega'(\phi) > 0$ if $\bar{\mathbf{x}}$ is stable. Converse is true for Class II models, for which dispersion occurs when transport access improves and $\omega'(\phi) < 0$ if $\bar{\mathbf{x}}$ is stable. Figure 8 shows the curves of ω for the Krugman model (Class I) and the Redding–Sturm model (Class II). It is evident from the figure that Classes I and II come to the opposite conclusions in the two-region economy: when interregional access improves, if a model has only a global (local) dispersion force, its mechanisms strengthen (weaken) the effects of exogenous local advantages. If exogenous heterogeneity causes one region to attract more population, such effects will be magnified in Class I models, while they are reduced in Class II models.

We provide a general characterization of the response of ρ in the case of the symmetric racetrack economy. Several notations and assumptions are in order. As we have seen in Section 3, the payoff elasticity matrix $\mathbf{V} = \frac{\bar{\mathbf{x}}}{v} [\frac{\partial v_i}{\partial x_j}(\bar{\mathbf{x}})]$ at $\bar{\mathbf{x}}$ is simply represented by the row-normalized proximity matrix \mathbf{D} . Suppose $\mathbf{V} = G(\mathbf{D})$ where G is a polynomial continuous over $[0, 1]$.²¹ In an analogous manner, let $\mathbf{A} = \frac{\bar{\mathbf{a}}}{v} [\frac{\partial v_i}{\partial a_j}(\bar{\mathbf{x}})]$ be the payoff elasticity matrix with respect to the local characteristic vector \mathbf{a} of interest, and suppose that \mathbf{A} can be represented by \mathbf{D} . Specifically, let $\mathbf{A} = G^h(\mathbf{D})$ where $G^h(\cdot)$ is another polynomial continuous over $[0, 1]$. In fact, regional heterogeneities in \mathbf{a} can be seen as deviations from $\bar{\mathbf{a}}$, so the effects of such deviations on the payoff vector can be evaluated exactly the same manner as population deviations from $\bar{\mathbf{x}}$ considered in the previous sections. Let

$$\delta(\chi) = -\frac{G^h(\chi)}{G(\chi)}. \quad (52)$$

For the two-region example discussed above, $\alpha = G^h(\chi)$ and $\omega = G(\chi)$ with $\chi = \frac{1-\phi}{1+\phi}$ as in (7), so that $\rho = -c\frac{\alpha}{\omega} = c\delta(\chi)$. We already considered the simple case where $\alpha = \bar{\alpha}$. In general, α is nonconstant. However, it is easy to see that the sign of $\delta'(\chi)$ determines the sign of $\rho'(\phi)$ because $\rho'(\phi) \propto \delta'(\chi)\chi'(\phi)$ and $\chi'(\phi) < 0$ for all ϕ .²² In fact, this observation generalizes to the many-region economy:

Proposition 2. *Suppose Assumption RE and assume that $\bar{\mathbf{x}}$ is stable. Then, the following hold true for ρ defined by (45):*

(a) $\rho'(\phi) > 0$, if $\delta'(\chi) < 0$ for all $\chi \in (0, 1)$ such that $G(\chi) < 0$.

(b) $\rho'(\phi) < 0$, if $\delta'(\chi) > 0$ for all $\chi \in (0, 1)$ such that $G(\chi) < 0$.

²¹Alternatively, G and G^h can be *rational functions* (the ratio of two polynomials). In fact, G is a rational function for the Redding–Sturm model in Section 3.2 and the Krugman model in Section 3.3.

²²For example, if the local characteristics of interest affect trade flows, α is nonconstant in ϕ . In (44), region i 's parameter b_i affects all trade flows and thus the payoffs in other regions. When α can vary in ϕ , the relative magnitudes of the terms in (50) matters. If the growth rate of the gain from exogenous asymmetry α is higher than that of the loss from migration $|\omega|$, then ρ increases, and vice versa. The function δ is the ratio of α and $|\omega|$.

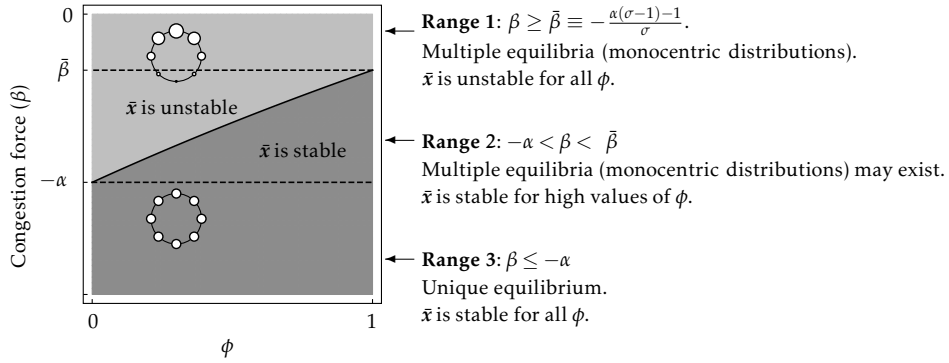


Figure 9: Uniqueness and stability of equilibria in the Allen–Arkolakis model.

For this general case, the three model classes we discussed in Section 3.4 are not precisely mapped to **Proposition 2** (a) or (b). However, there is a rough tendency that initial advantages are amplified (diminished) in Class I (II) models. For example, the regional model considered in Redding and Rossi-Hansberg (2017) is Class II. If we consider local productivity parameters as regional characteristic vector \mathbf{a} , then the model satisfies $\delta'(\chi) > 0$ for all $\chi \in (0, 1)$ when equilibrium is unique (see Remark D.7 in Appendix D). Likewise, the Krugman model considered in Section 3.3 is Class I and we show $\delta'(\chi) < 0$ for all $\chi \in (0, 1)$ if we consider immobile demand l_i as regional characteristics (see Remark D.3 in Appendix D). See also Appendix F for numerical examples under Assumption RE.

4.3 A quantitative example

To explore the empirical relevance of **Proposition 2**, we provide a quantitative example. Specifically, we apply the Allen and Arkolakis (2014) model ((43) and (44)) to Japanese Census population data (see Appendix F for details) to examine the impact of counterfactual reduction in transport costs in this framework. We show that, while **Proposition 2** is not obtained for asymmetric geography, counterfactual responses (in terms of $\Delta\rho$ and the counterfactual growth pattern) are consistent with our theoretical result.

The model is Class II. Then, by imposing a sufficiently strong local dispersion force, equilibrium is unique regardless of the level of transport costs. For reference, Figure 9 provides the classification of possible spatial patterns and their stability in the racetrack economy.²³ A sufficient condition for the equilibrium uniqueness is $\alpha + \beta \leq 0$ (Range 3 in Figure 9), which means there is *net* local dispersion force. In the racetrack economy, \bar{x} is the only equilibrium, and no endogenous asymmetry can emerge if $\alpha + \beta \leq 0$.

We set $\alpha = 0.1$ and $\beta = -0.3$ following Allen and Arkolakis (2014). Then, $\alpha + \beta < 0$ and the region-specific parameters are uniquely obtained by solving the equilibrium conditions given the observed population data. Figure 10A plots the observed population

²³Figure 9 can be seen as a refinement of Figure I in Allen and Arkolakis (2014) under Assumption RE.

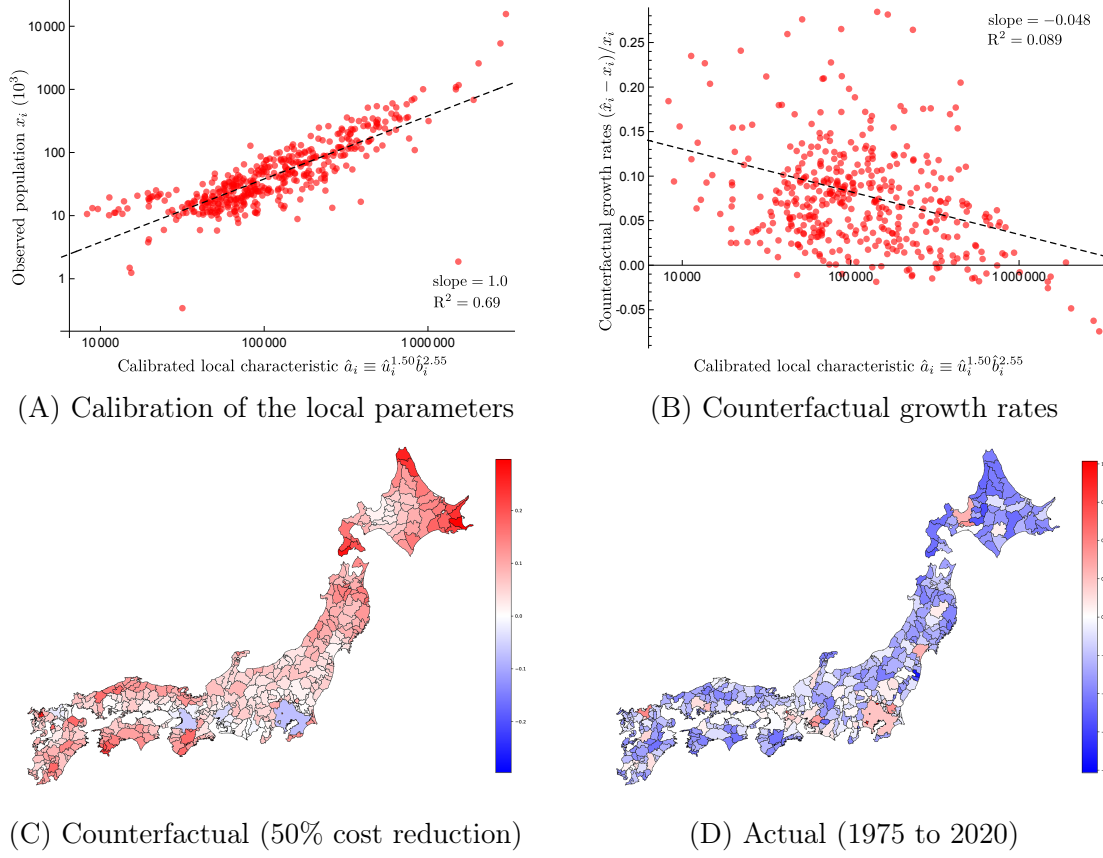


Figure 10: Counterfactual and actual growth of Japanese regions.

x_i in 2020 against the aggregated local characteristic parameter $\hat{a}_i = \hat{u}_i^{1.50} \hat{b}_i^{2.55}$, where the power coefficients are obtained by a logarithmic regression. By definition, the slope is unity on the log–log plot. We see 69 % of the actual log population variations are represented by the region-specific parameters $\{u_i\}$ and $\{b_i\}$, with locations with higher population obtaining higher exogenous unobserved advantages.

Figures 10B and 10C show the result of reducing interregional transportation costs by 50%.²⁴ We confirmed $\Delta\rho < 0$, which is consistent with **Proposition 2** (b) although the example does not satisfy Assumption RE. Figure 10B plots the counterfactual growth rate $(x'_i - x_i)/x_i$ against the aggregated local parameter \hat{a}_i . On average, more highly populated areas, which on average have higher \hat{a} , lost population by the transport cost reduction. As Figure 10C indicates, the model predicts that central locations such as Tokyo, Osaka, Nagoya, and Fukuoka lose population, which is consistent with local dispersion behaviour of Class II models (Figure C.2B). Figure 10D shows the actual growth rates of Japanese regions. There is a remarkable contrast between Figure 10C and Figure 10D, suggesting that the Class II model does not reproduce the evolution of Japanese cities.²⁵ It is also

²⁴The freeness of transport between region i and j is given as $\phi_{ij} \equiv \exp(-\tau t_{ij})$ where t_{ij} is the transport cost between i and j . In Figure 10B and C, we reduce τ by 50%.

²⁵Figure 10D reflects the result of the actual transport cost reduction from 1975 to 2020, whereas Figure 10C shows the result of 50% transport cost reduction. Thus, to make the comparison more

expected that Class II models, in general, would not reproduce the overall spatial pattern of the actual growth rates since these models result in dispersion toward peripheral regions as transport costs decrease.

As seen, the quantitative prediction of the Allen–Arkolakis model is consistent with **Proposition 2**, despite the example considers the real-world geography. Also, this behavior is in line with the general implications of Class II models in that dispersion toward “periphery” proceeds when transport costs decrease. In contrast, in Class I models, the numerical examples so far (e.g, Figure 7) suggest that the opposite result should occur as they generally predict agglomeration toward central locations as transport costs decrease. It is a challenging open question to what extent **Proposition 2** quantitatively matter when there are large regional asymmetries as in reality. However, Figure 10 (and Figure F.2) suggests that **Proposition 2** may be generalized to asymmetric settings.

5 Concluding remarks

This study showed that the spatial scale (local or global) of dispersion forces within a many-region model of endogenous agglomeration determines the equilibrium spatial patterns of economic activities and their comparative statics. We identified three prototypical model classes based on the spatial scale of their dispersion forces. In the following, we discuss connections to the empirical literature and highlight directions for future research.

While our approach is purely theoretical, various connections can be found between our results and the empirical literature. The evidence on regional agglomeration presented by [Duranton and Turner \(2012\)](#) and [Faber \(2014\)](#) is in line with the predictions of Class I models. The former study focused on the growth of large metropolitan areas in the US, whereas the latter analyzed the growth of peripheral counties in China. The former (latter) study revealed a positive (negative) correlation between the magnitude of growth and the interregional transport infrastructure level of a given region. These opposite responses can be interpreted as different sides of the same coin for Class I models, as both results indicate a tendency of selective concentration towards bigger regions when interregional transport access improves.²⁶ [Baum-Snow et al. \(2020\)](#) also provided an evidence for global concentration across Chinese prefectures due to the introduction of the Chinese national highway system by showing that hinterland prefectures experienced slower growth rates compared to regional primates.

precise, we should calibrate the model to the 1975 population distribution and then consider the actual transport cost changes. The exercise here focuses on demonstrating that the asymmetry of the transport network does not alter overall implication of our theoretical result, rather than to focus on reproducing the real population growth pattern.

²⁶The number of interregional highway linkages (e.g., the number and total length) within a given region is often used as a measure of *intra*-urban transport infrastructure (e.g., [Baum-Snow, 2007](#); [Duranton and Turner, 2012](#)). For [Duranton and Turner \(2012\)](#), we here interpret it as a measure of *inter*-regional transport infrastructure so that we can understand their results in the context of Class I models.

On the other hand, the behavior of Class II and III models corroborates with empirical evidence for the local dispersion of economic agglomerations when interregional access improves. [Baum-Snow \(2007\)](#) and [Baum-Snow et al. \(2017\)](#) presented evidence for US metro areas during 1950–1990 and Chinese prefectures during 1990–2010, respectively. These studies addressed the changes in the population or production size of the central area within the bigger region, both reporting a negative effect of improved interregional access. The local flattening of cities can also be interpreted as suburbanization in response to the improved intraurban transport infrastructure in classical urban economic theory (e.g., [Alonso, 1964](#)). As discussed in Section 1, the behavior of Class III models provides a consistent interpretation of several characteristic tendencies observed in Japan’s population distribution evolution from 1970 to 2020.

Our results call for reconsideration of the role of endogenous economic forces in the quantitative application of economic geography models. The defining survey of quantitative spatial economics states that this literature “does not aim to provide a fundamental explanation for the agglomeration of economic activity” ([Redding and Rossi-Hansberg, 2017](#), §1). Building on this premise, the models typically absorb most interregional variations in endogenous variables, such as populations and wages, into structural residuals. These residuals are then interpreted as unobserved location fundamentals, which are not accounted for by either the endogenous forces within the model or the observable exogenous factors. For example, in [Redding and Sturm \(2008\)](#) and [Allen and Arkolakis \(2014\)](#), the replication data indicate that the structural residuals (“housing stock” in the former and “unobserved amenity and productivity” in the latter) account for 90% and 78% of the log-city size variation when the models are calibrated to rationalize observed German city sizes and the US county sizes, respectively. In other words, in these models, endogenous forces and the observable topography explain 10% and 22% of the observed population-size variation in Germany and the US, respectively. Greater emphasis on endogenous economic forces may be necessary to enhance the model fit in quantitative economic geography models. Toward this goal, it is important to accumulate results on the theoretical foundation of spatial models.

Several aspects deserve further research. First, generalizing our theoretical results to different proximity structures is important. An efficient strategy would be to consider representative models and identify general insights when the proximity structure systematically varies ([Matsuyama, 2017](#)). As Appendix E suggests, the main conclusion of **Proposition 1**, whether a model produces monocentric or polycentric patterns, may be robust to generalizations concerning geography.

Second, it is important to consider multiple types of mobile agents subject to different proximity matrices and/or degrees of increasing returns. Such a structure is ubiquitous in multiple-sector models ([Fujita et al., 1999b](#); [Hsu, 2012](#); [Gaubert, 2018](#); [Davis and Dingel, 2020](#)) and intra-city models with both firms and households (e.g., [Fujita and Ogawa,](#)

1982; Lucas and Rossi-Hansberg, 2002; Ahlfeldt et al., 2015; Heblich et al., 2020). The racetrack economy provides a good starting point for analyzing these models (Tabuchi and Thisse, 2011; Osawa and Akamatsu, 2020). Multiple-sector models are also important for understanding the mechanisms behind the remarkable regularities in size and spatial variations of economic agglomerations in the real world. For example, Mori et al. (2020) use the data from six countries, including the US, to demonstrate that the spatial *common power law* holds, that is, city-size distributions exhibit similar power laws both in the country and its spatial sub-regions. Notably, a multi-sector economic geography model can replicate common power laws in a symmetric racetrack economy (Mori et al., 2022).²⁷

Finally, models featuring a continuum of agents, as in this study, are complementary to the recent development of *granular spatial models* (e.g., Ahlfeldt et al., 2022) in which endogenous agglomeration arises from the increasing returns and indivisibility of agents. While continuum models (e.g., Hsu, 2012; Tabuchi and Thisse, 2011; Mori et al., 2022) can endogenously replicate the systematic regularities such as the periodic agglomeration patterns, and city-size power laws including their fractal structure (Mori et al., 2020), granular spatial models are better at explaining idiosyncratic location choice behavior by superstar firms and plants (e.g., Greenstone et al., 2010). Combining these two approaches may provide a fundamental explanation for the spatial economy through endogenous mechanisms.

²⁷In the context of single-sector models, Behrens et al. (2017) incorporated a wide range of observed heterogeneity in location-specific factors such as the natural advantages (e.g., climate and landscape) and exogenous economic fundamentals (e.g., firm productivity and commuting technology). Their results in the case of the US indicate that the city-size variation accruing from these asymmetries is still less than 10% (Berliant and Mori, 2017, §3.3). Using multi-sector models that can replicate robust empirical regularities may be a possible remedy in improving the fit of quantitative spatial models.

A Proofs

A.1 Proof of Proposition 1

We assume that the payoff function $\mathbf{v}(\mathbf{x}) \equiv (v_i(\mathbf{x}))_{i \in \mathcal{N}}$ is differentiable if $x_i > 0$ for all $i \in \mathcal{N}$. As discussed in the main text, we impose a specific symmetry assumption on \mathbf{v} . The precise definition of Assumption S is the following.

Assumption S (full) (Symmetry of payoff function). *Assume Assumption RE. Let $\bar{\mathbf{D}} \equiv [\phi_{ij}]$ be the proximity matrix. For all \mathbf{x} , payoff function \mathbf{v} satisfies $\mathbf{v}(\mathbf{P}\mathbf{x}) = \mathbf{P}\mathbf{v}(\mathbf{x})$ for all permutation matrices \mathbf{P} with $\mathbf{P}\bar{\mathbf{D}} = \bar{\mathbf{D}}\mathbf{P}$.*

Example A.1. Suppose $N = 4$. The proximity matrix is given by (10). The geometry of the four-region circular economy is invariant even if we swap the indices of regions 1 and 3. The following *permutation matrix*

$$\mathbf{P} = \begin{bmatrix} & & 1 & \\ & 1 & & \\ 1 & & & \\ & & & 1 \end{bmatrix} \quad (\text{A.1})$$

represents this re-indexing, as we confirm the vector $(1, 2, 3, 4)$ is mapped to $(3, 2, 1, 4)$ by multiplication of \mathbf{P} . The condition $\mathbf{P}\bar{\mathbf{D}} = \bar{\mathbf{D}}\mathbf{P}$ means that the adjacency relationships between regions remain invariant under the regional index permutation represented by \mathbf{P} . Given a spatial distribution $\mathbf{x} = (x_1, x_2, x_3, x_4)$, the re-indexed spatial distribution becomes $\mathbf{x}' = (x_3, x_2, x_1, x_4) = \mathbf{P}\mathbf{x}$. If \mathbf{v} does not include any region-specific exogenous advantages, we must have $v_1(\mathbf{x}') = v_3(\mathbf{x})$, $v_2(\mathbf{x}') = v_2(\mathbf{x})$, $v_3(\mathbf{x}') = v_1(\mathbf{x})$, and $v_4(\mathbf{x}') = v_4(\mathbf{x})$, that is, $\mathbf{v}(\mathbf{x}') = \mathbf{v}(\mathbf{P}\mathbf{x}) = \mathbf{P}\mathbf{v}(\mathbf{x})$. ■

Such mathematical properties for \mathbf{v} is called *equivariance* and allows us to employ the powerful machineries developed in group-theoretic bifurcation theory (see, e.g., Golubitsky and Stewart, 2003; Golubitsky et al., 2012; Ikeda and Murota, 2014).

We characterize the stability of $\bar{\mathbf{x}} = (\bar{x}, \dots, \bar{x})$ and bifurcation from it. Following the literature, we assume some myopic evolutionary dynamics to define the stability of $\bar{\mathbf{x}}$. A myopic dynamic describes the rate of change in \mathbf{x} . Denote the dynamic that adjusts \mathbf{x} over the set of possible spatial distributions $\mathcal{X} \equiv \{\mathbf{x} \geq \mathbf{0} \mid \sum_{i \in \mathcal{N}} x_i = 1\}$ by $\dot{\mathbf{x}} = \mathbf{f}(\mathbf{x})$, where $\dot{\mathbf{x}}$ represents the time derivative. For the majority of myopic dynamics in the literature, $\mathbf{f}(\mathbf{x}) \equiv \tilde{\mathbf{f}}(\mathbf{x}, \mathbf{v}(\mathbf{x}))$ where $\tilde{\mathbf{f}}$ maps each pair $(\mathbf{x}, \mathbf{v}(\mathbf{x}))$ of a state and its associated payoff to a motion vector $\dot{\mathbf{x}}$ that satisfies $\mathbf{1}^\top \dot{\mathbf{x}} = 0$. We will focus exclusively on such dynamics. Let *restricted equilibrium* be a state $\mathbf{x}^* \in \mathcal{X}$ such that $v_j(\mathbf{x}^*) = v_k(\mathbf{x}^*)$ for all $j, k \in \{i \in \mathcal{N} \mid x_i^* > 0\}$, a spatial distribution in which all populated regions earn the same payoff level. A spatial equilibrium is always a restricted equilibrium.

We assume that \mathbf{f} and $\tilde{\mathbf{f}}$ are differentiable and satisfy the following conditions:

$$\mathbf{f}(\mathbf{x}) = \mathbf{0} \text{ if } \mathbf{x} \text{ is a Nash equilibrium,} \quad (\text{RS})$$

$$\text{if } \mathbf{f}(\mathbf{x}) \neq \mathbf{0}, \text{ then } \mathbf{v}(\mathbf{x})^\top \mathbf{f}(\mathbf{x}) > 0, \text{ and} \quad (\text{PC})$$

$$\mathbf{P}\tilde{\mathbf{f}}(\mathbf{x}, \mathbf{v}(\mathbf{x})) = \tilde{\mathbf{f}}(\mathbf{P}\mathbf{x}, \mathbf{P}\mathbf{v}(\mathbf{x})) \text{ for all permutation matrices } \mathbf{P}. \quad (\text{Sym})$$

We call dynamics that satisfy (RS), (PC), and (Sym) *admissible dynamics*.²⁸

Example A.2. Admissible dynamics include the Brown–von Neumann–Nash dynamic (Brown and von Neumann, 1950; Nash, 1951), the Smith dynamic (Smith, 1984), and Riemannian game dynamics (Mertikopoulos and Sandholm, 2018) that satisfy (Sym), e.g., the projection dynamic (Dupuis and Nagurney, 1993) and the replicator dynamic (Taylor and Jonker, 1978). ■

Consider $\bar{\mathbf{x}}$. Since $\bar{\mathbf{x}}$ is a spatial equilibrium, $\mathbf{f}(\bar{\mathbf{x}}) = \mathbf{0}$ by assumption (RS). Denote the Jacobian matrix of \mathbf{f} at $\bar{\mathbf{x}}$ by $\nabla \mathbf{f}(\bar{\mathbf{x}}) = [\frac{\partial f_i}{\partial x_j}(\bar{\mathbf{x}})]$. Assume that $\nabla \mathbf{f}(\bar{\mathbf{x}})$ has no eigenvalues with zero real parts. Then, $\bar{\mathbf{x}}$ is *linearly stable* if all the eigenvalues of $\nabla \mathbf{f}(\bar{\mathbf{x}})$, which we denote by $\{\eta_k\}$, have negative real parts (Hirsch et al., 2012). Spatial equilibrium $\bar{\mathbf{x}}$ is said to be *stable* (*unstable*) if it is linearly stable (unstable) under admissible dynamics.

Suppose $\bar{\mathbf{x}}$ is an isolated spatial equilibrium, that is, there is no equilibrium that is close to $\bar{\mathbf{x}}$. Then, (PC) implies that there is a neighborhood $\mathcal{O} \subset \mathcal{X}$ of $\bar{\mathbf{x}}$ such that $\mathbf{v}(\mathbf{x})^\top \mathbf{f}(\mathbf{x}) > 0$ for all $\mathbf{x} \in \mathcal{O} \setminus \{\bar{\mathbf{x}}\}$. By expanding \mathbf{v} and \mathbf{f} about $\bar{\mathbf{x}}$, we have

$$(\mathbf{v}(\bar{\mathbf{x}}) + \nabla \mathbf{v}(\bar{\mathbf{x}})\mathbf{z})^\top (\mathbf{f}(\bar{\mathbf{x}}) + \nabla \mathbf{f}(\bar{\mathbf{x}})\mathbf{z}) > 0 \quad (\text{A.2})$$

as we have $\mathbf{v}(\bar{\mathbf{x}}) = \bar{v}\mathbf{1}$, $\nabla \mathbf{v}(\bar{\mathbf{x}}) = \frac{\bar{v}}{\bar{x}}\mathbf{V}$, $\mathbf{f}(\bar{\mathbf{x}}) = \mathbf{0}$ by (RS), and $\mathbf{1}^\top \nabla \mathbf{f}(\bar{\mathbf{x}})\mathbf{z} = 0$, where the last equality $\mathbf{1}^\top \nabla \mathbf{f}(\bar{\mathbf{x}})\mathbf{z} = 0$ follows from $\dot{\mathbf{x}} = \mathbf{f}(\mathbf{x}) \approx \mathbf{f}(\bar{\mathbf{x}}) + \nabla \mathbf{f}(\bar{\mathbf{x}})\mathbf{z} = \nabla \mathbf{f}(\bar{\mathbf{x}})\mathbf{z}$ and $\mathbf{1}^\top \dot{\mathbf{x}} = \sum_{i \in \mathcal{N}} \dot{x}_i = 0$. From (A.2), we then see

$$\frac{\bar{v}}{\bar{x}} (\mathbf{V}\mathbf{z})^\top (\nabla \mathbf{f}(\bar{\mathbf{x}})\mathbf{z}) > 0 \quad (\text{A.3})$$

for any infinitesimal deviation $\mathbf{z} = \mathbf{x} - \bar{\mathbf{x}}$ from the uniform distribution.

We consider a sufficiently large class of models, which we call *canonical models*, that include the three model classes discussed in the main text.

Definition 1 (Canonical models and gain functions). Consider an economic geography model with payoff function \mathbf{v} parametrized by proximity matrix $[\phi_{ij}]$. Suppose Assumptions RE and S. Let \mathbf{D} be the row-normalized proximity matrix, whose (i, j) th element

²⁸The conditions (RS) and (PC) are, respectively, called *restricted stationarity* and *positive correlation* (Sandholm, 2010). The condition (Sym) implies \mathbf{f} does not feature ex-ante preference over alternatives in \mathcal{N} . We assume \mathbf{f} is defined for all nonnegative orthant $\mathbb{R}_{\geq 0}^{\mathcal{N}}$ for simplicity. We suppose \mathbf{f} is differentiable to conduct linear stability analysis.

is $\frac{\phi_{ij}}{\sum_{k \in \mathcal{N}} \phi_{ik}}$. Let $\mathbf{V} = \frac{\bar{x}}{v} \nabla \mathbf{v}(\bar{\mathbf{x}})$ be the payoff elasticity matrix at the uniform state $\bar{\mathbf{x}}$. A *canonical model* is a model for which there exists a rational function G that is continuous over $[0, 1]$ and satisfies $\mathbf{V} = G(\mathbf{D})$. We call G the *gain function* of the model.

In Definition 1, for a rational function of form $G(\cdot) = \frac{G^\sharp(\cdot)}{G^\flat(\cdot)}$ with polynomials $G^\sharp(\cdot)$ and $G^\flat(\cdot) \neq 0$, we let $G(\mathbf{D}) = G^\flat(\mathbf{D})^{-1} G^\sharp(\mathbf{D})$, where, for a polynomial $P(\chi) = c_0 + c_1\chi + c_2\chi^2 + \dots$, we define $P(\mathbf{D}) = c_0\mathbf{I} + c_1\mathbf{D} + c_2\mathbf{D}^2 + \dots$, with \mathbf{I} being the identity matrix.

Below, we assume canonical models so that there is a rational function $G(\cdot) = \frac{G^\sharp(\cdot)}{G^\flat(\cdot)}$ with some polynomials G^\sharp and $G^\flat(\cdot) > 0$ such that $\mathbf{V} = G(\mathbf{D}) = G^\flat(\mathbf{D})^{-1} G^\sharp(\mathbf{D})$. We assume $G^\flat(\cdot) > 0$, so that $G^\sharp(\cdot)$ governs the stability of $\bar{\mathbf{x}}$, as discussed in the main text. Under Assumption RE, \mathbf{D} is real, symmetric, and *circulant matrix* (Horn and Johnson, 2012, §0.9.6). Then, \mathbf{V} is also a real, symmetric, and circulant matrix. Because of (Sym), $\nabla \mathbf{f}(\bar{\mathbf{x}})$ is also real, symmetric, and circulant. Then, due to the standard properties of circulant matrices, we can choose the same set of eigenvectors for \mathbf{D} , \mathbf{V} , and $\nabla \mathbf{f}(\bar{\mathbf{x}})$.

For each eigenvector \mathbf{z}_k of \mathbf{D} , \mathbf{V} , or $\nabla \mathbf{f}(\bar{\mathbf{x}})$, (A.3) implies that

$$(\mathbf{V} \mathbf{z}_k)^\top (\nabla \mathbf{f}(\bar{\mathbf{x}}) \mathbf{z}_k) = \omega_k \eta_k > 0, \quad (\text{A.4})$$

where ω_k and η_k are the eigenvalues of \mathbf{V} and $\nabla \mathbf{f}(\bar{\mathbf{x}})$ associated with \mathbf{z}_k . Since η_k and ω_k are both real as $\nabla \mathbf{f}(\bar{\mathbf{x}})$ and \mathbf{V} are both symmetric, $\text{sgn}[\eta_k] = \text{sgn}[\omega_k] = \text{sgn}[G(\chi_k(\phi))] = \text{sgn}[G^\sharp(\chi_k(\phi))]$. Therefore, $\bar{\mathbf{x}}$ is stable spatial equilibrium under any admissible dynamic if and only if $\omega_k^\sharp \equiv G^\sharp(\chi_k(\phi)) < 0$ for all k .

The eigenpairs $\{(\chi_k, \mathbf{z}_k)\}$ of the row-normalized proximity matrix \mathbf{D} are derived in Akamatsu et al. (2012), where χ_k is the eigenvalue of \mathbf{D} associated to \mathbf{z}_k .

Lemma A.1 (Akamatsu et al. (2012), Lemma 4.2). *Assume that N is an even and let $M \equiv \frac{N}{2}$. Then, \mathbf{D} satisfies the following properties:*

(a) \mathbf{D} has $M + 1$ distinct eigenvalues $\{\chi_k\}_{k=0}^M$ whose formulae given by:

$$\chi_k(\phi) = \begin{cases} \Psi_k(\phi) \Psi_M(\phi) & (k: \text{even}) \\ \Psi_k(\phi) \Psi_M(\phi) \bar{\Psi}(\phi) & (k: \text{odd}) \end{cases} \quad k = 0, 1, 2, \dots, M, \quad (\text{A.5})$$

$$\text{where } \Psi_k(\phi) \equiv \frac{1 - \phi^2}{1 - 2\phi \cos(\theta k) + \phi^2}, \bar{\Psi}(\phi) \equiv \frac{1 + \phi^M}{1 - \phi^M}, \theta = \frac{2\pi}{N}.$$

(b) χ_k ($k \neq 0$) is strictly decreasing in ϕ , and $\lim_{\phi \rightarrow 0} \chi_k = 1$ and $\lim_{\phi \rightarrow 1} \chi_k = 0$.

(c) For any given $\phi \in (0, 1)$, $\{\chi_k\}$ ($k = 0, 1, 2, \dots, M$) are ordered as

$$\begin{cases} 1 = \chi_0 > \chi_2 > \dots > \chi_{2k} > \dots > \chi_M > 0, \\ 1 > \chi_1 > \chi_3 > \dots > \chi_{2k+1} > \dots > \chi_{M-1} > 0, \end{cases} \quad (\text{A.6})$$

with $\chi_1 > \chi_2$. Thus, $\max_{k \geq 1} \{\chi_k\} = \chi_1$ and $\min_{k \geq 1} \{\chi_k\} = \min\{\chi_{M-1}, \chi_M\}$.

(d) If N is a multiple of four, $\min_k \{\chi_k\} = \chi_M = \left(\frac{1-\phi}{1+\phi}\right)^2$.

(e) Denote a normalized vector by $\langle z_i \rangle_{i=0}^{N-1} \equiv \frac{1}{\|z\|} (z_i)_{i=0}^{N-1}$. The eigenpairs $\{(\chi_k, \mathbf{z}_k)\}$ are

$$\chi_0 = 1, \quad \mathbf{z}_0 \equiv \langle 1 \rangle_{i=0}^{N-1}, \quad (\text{A.7})$$

$$\chi_k, \quad \begin{cases} \mathbf{z}_k^+ \equiv \langle \cos(\theta k i) \rangle_{i=0}^{N-1}, \\ \mathbf{z}_k^- \equiv \langle \sin(\theta k i) \rangle_{i=0}^{N-1}, \end{cases} \quad \theta = \frac{2\pi}{N}, k = 1, 2, \dots, M-1 \quad (\text{A.8})$$

$$\chi_M, \quad \mathbf{z}_M \equiv \langle (-1)^i \rangle_{i=0}^{N-1}. \quad (\text{A.9})$$

The eigenpairs of $\mathbf{V} = G(\mathbf{D})$ are given by $\{(G(\chi_k), \mathbf{z}_k)\}$ (see, e.g., [Horn and Johnson, 2012](#), Section 1.1). Thus, letting $\mathcal{K} \equiv \{1, 2, \dots, M\}$ with $M = \frac{N}{2}$, $\bar{\mathbf{x}}$ is stable if $\omega_k^\sharp \equiv G^\sharp(\chi_k(\phi)) < 0$ for all $k \in \mathcal{K}$. If either agglomeration force or dispersion force in a model is too strong, $\bar{\mathbf{x}}$ can be (un)stable for all ϕ . As we are interested in endogenous agglomeration, we assume that $\bar{\mathbf{x}}$ can be stable and unstable depending on ϕ .

Assumption E (Endogenous agglomeration occurs). *The values of the model parameters are such that G switches its sign at least once in $(0, 1)$.*

Under Assumption E, we introduce a formal classification of canonical models based on three prototypical shapes of G found in the literature. The classification corresponds to the composition of the dispersion forces in the model (see Table 1 in Section 1).

Definition 2. Under Assumption E, a canonical model with gain function G is

- (a) *Class I*, if there is one and only one root $\chi^* \in (0, 1)$ for G such that $G(\chi) > 0$ for $\chi \in (0, \chi^*)$, $G(\chi^*) = 0$, and $G(\chi) < 0$ for $\chi \in (\chi^*, 1)$.
- (b) *Class II*, if there is one and only one $\chi^{**} \in (0, 1)$ such that $G(\chi) < 0$ for $\chi \in (0, \chi^{**})$, $G(\chi^{**}) = 0$, and $G(\chi) > 0$ for $\chi \in (\chi^{**}, 1)$.
- (c) *Class III*, if there are two and only two $\chi^*, \chi^{**} \in (0, 1)$ such that $G(\chi^*) = G(\chi^{**}) = 0$ and $\chi^{**} < \chi^*$, with $G(\chi) < 0$ for $\chi \in (0, \chi^{**}) \cup (\chi^*, 1)$ and $G(\chi) > 0$ for $\chi \in (\chi^{**}, \chi^*)$.

Example A.3. The gain function of the Beckmann model is $G(\chi) = -\gamma + \chi$. If $\gamma \in (0, 1)$, then G has one and only one root $\chi^* = \gamma \in (0, 1)$ and $G(\chi) < 0$ for all $\chi < \chi^*$ and $G(\chi) > 0$ for all $\chi > \chi^*$, satisfying Definition 2 (a). If $\gamma \geq 1$ ($\gamma \leq 0$), then G has no root in $(0, 1)$ and violates Assumption E, and $\bar{\mathbf{x}}$ is always stable (unstable). The gain functions of the Krugman and Redding–Sturm models have two parameters, $\mu \in (0, 1)$ and $\sigma > 1$. For the Krugman model, if $1 < (1 - \mu)\sigma$, G satisfies Definition 2 (a). If $1 \geq (1 - \mu)\sigma$, then $G(\chi) > 0$ for all $\chi \in (0, 1)$. This violates Assumption E and $\bar{\mathbf{x}}$ is always unstable (agglomeration force is too strong). For this reason, $1 < (1 - \mu)\sigma$ is

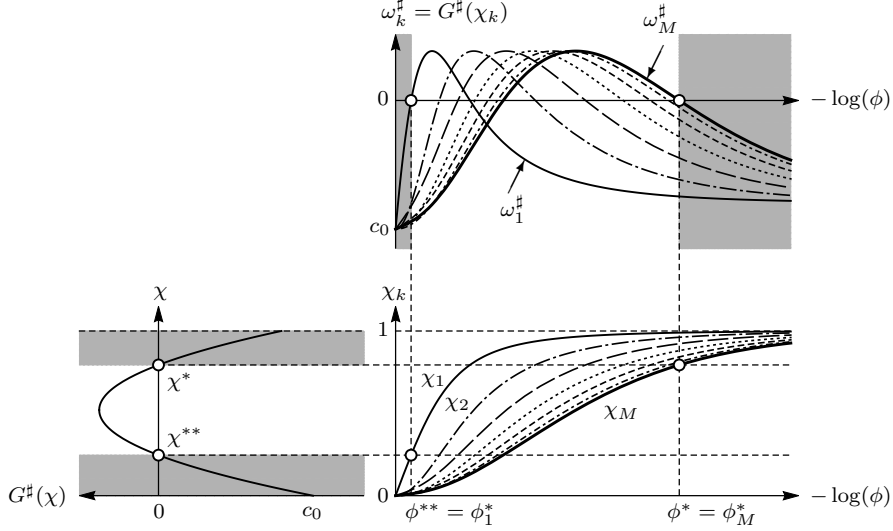


Figure A.1: The relationships between G^\sharp , $\{\chi_k\}$, and $\{\omega_k^\sharp\}$.

Top: Graphs of $\omega_k^\sharp = G^\sharp(\chi_k)$. Bottom left: Net gain function G^\sharp for a hypothetical Class III model with a quadratic net gain function of the form $G^\sharp(\chi) = c_0 + c_1\chi + c_2\chi^2$. Bottom right: The (model-independent) eigenvalues $\{\chi_k(\phi)\}$ of \mathbf{D} . In the shaded regions of ϕ or χ , $\bar{\mathbf{x}}$ is stable. For the ϕ axis, the negative log scale is used for better readability, with the transport cost level being high toward the right. Similar plots in the main text are shown in the simple ϕ axis. We have $\max\{\chi_k\} = \chi_1$ and $\min\{\chi_k\} = \chi_M$ at any given level of ϕ .

called the “no-black-hole condition” (Fujita et al., 1999a). For the Redding–Sturm model, if $1 > (1 - \mu)\sigma$, G satisfies Definition 2 (b). If $1 \leq (1 - \mu)\sigma$, $G(\chi) < 0$ for all $\chi \in (0, 1)$. This violates Assumption E and $\bar{\mathbf{x}}$ is always stable as dispersion force is strong. ■

We focus on the three model classes defined above²⁹ and consider the destabilization of $\bar{\mathbf{x}}$. Figure A.1 schematically shows connections between $\{\omega_k^\sharp\}$, $G^\sharp(\chi)$, and $\{\chi_k\}$ to help understanding the following arguments.

Class I. By definition, there is χ^* such that $G^\sharp(\chi) < 0$ for all $\chi \in (\chi^*, 1)$, that $G^\sharp(\chi^*) = 0$, and that $G^\sharp(\chi) > 0$ for all $\chi \in (0, \chi^*)$. By Lemma A.1, $\{\chi_k(\phi)\}$ are strictly decreasing from 1. Thus, $\bar{\mathbf{x}}$ is stable if and only if $\chi_k \in (\chi^*, 1)$, so that $\omega_k^\sharp \equiv G^\sharp(\chi_k) < 0$, for all $k \in \mathcal{K}$, i.e., if $\chi^* < \min_{k \in \mathcal{K}} \chi_k = \chi_M$. Thus, $\bar{\mathbf{x}}$ is stable for all $(0, \phi_M^*)$ where $\phi_M^* = \frac{1 - \sqrt{\chi^*}}{1 + \sqrt{\chi^*}}$ is the unique solution for $\chi_M(\phi) = \chi^*$. Because $G^\sharp(\chi) > 0$ for all $\chi \in (0, \chi^*)$ and χ_M is strictly decreasing, $\bar{\mathbf{x}}$ is unstable for all $(\phi_M^*, 1)$ because $\omega_M^\sharp > 0$ for the range.

Class II. By definition, there is χ^{**} such that $G^\sharp(\chi) < 0$ for all $\chi \in (0, \chi^{**})$, that $G^\sharp(\chi^{**}) = 0$, and that $G^\sharp(\chi^{**}) > 0$ for all $\chi \in (\chi^{**}, 1)$. Thus, $\bar{\mathbf{x}}$ is stable if and only if $\chi_k \in (0, \chi^{**})$, so that $\omega_k^\sharp = G^\sharp(\chi_k) < 0$, for all $k \in \mathcal{K}$, i.e., if $\chi^{**} > \max_{k \in \mathcal{K}} \chi_k = \chi_1$. Thus, $\bar{\mathbf{x}}$ is stable for all $(\phi_1^*, 1)$ where ϕ_1^* is the unique solution for $\chi_1(\phi) = \chi^{**}$. Because $G^\sharp(\chi) > 0$ for all $\chi \in (\chi^{**}, 1)$ and χ_1 is strictly decreasing, $\bar{\mathbf{x}}$ is unstable for all $(0, \phi_1^*)$.

Class III. Via a similar logic, we see $\bar{\mathbf{x}}$ is stable if $\phi \in (0, \phi_M^*) \cup (\phi_1^*, 1)$.

²⁹When we consider the quadratic form $\mathbf{V} \simeq c_0\mathbf{I} + c_1\mathbf{D}^1 + c_2\mathbf{D}^2$, there may be “Class IV” models for which $G(\chi) < 0$ if and only if $\chi \in (\chi^*, \chi^{**})$. However, we are not aware of any natural examples.

Consider a state where $\bar{\mathbf{x}}$ is stable. Suppose one and only one ω_k ($k \in \mathcal{K}$) switches its sign from negative to positive at ϕ_k^* . From (A.4), the corresponding eigenvalue of the dynamic \mathbf{f} , η_k , must switch its sign from negative to positive at ϕ_k^* . Then, we can invoke a fact in bifurcation theory that $\bar{\mathbf{x}}$ deviates towards the direction of associated eigenvector \mathbf{z}_k at such point. Specifically, \mathbf{z}_k is tangent to *unstable manifold* diverging from $\bar{\mathbf{x}}$ (see, e.g., Hirsch et al., 2012; Kuznetsov, 2004). Thus, a polycentric pattern with $M = \frac{N}{2}$ peaks emerges at ϕ_M^* , whereas a monocentric pattern emerges at ϕ_1^{**} .

Remark A.1. The bifurcation toward the monocentric direction ($k = 1$) is in fact a *double bifurcation* at which the relevant eigenvalue, ω_1 , has multiplicity two (A.8). For this case, possible migration patterns are linear combinations of the form $c^+ \mathbf{z}_1^+ + c^- \mathbf{z}_1^-$ with $c^+, c^- \in \mathbb{R}$. Under Assumptions RE and S, we have $(c^+, c^-) = (c, 0)$ or (c, c) for some $c \in \mathbb{R}$ (Ikeda et al., 2012b). Although which of the two possibilities occur depends on the specific functional form of \mathbf{v} , the implication of **Proposition 1** is unaffected because any linear combination of \mathbf{z}_1^+ and \mathbf{z}_1^- is a monocentric pattern. ■

Remark A.2. We suppose N is a multiple of four so that $\min_{k \in \mathcal{K}} \{\chi_k\} = \chi_M$. This assumption is inconsequential for the essential implication of **Proposition 1** on the overall shape of endogenous spatial patterns. If N is an even, $\min_{k \in \mathcal{K}} \{\chi_k\} = \min\{\chi_{M-1}, \chi_M\}$. If N is an odd, $\min_{k \in \mathcal{K}} \{\chi_k\} = \min\{\chi_{\lfloor N/2 \rfloor}, \chi_{\lfloor N/2 \rfloor - 1}\}$. Except for $N = 2$ or 3 where polycentric patterns cannot occur, $\min_{k \in \mathcal{K}} \{\chi_k\}$ corresponds to a polycentric direction. ■

Remark A.3. Beyond the local result of the proposition, Ikeda et al. (2012b) characterized the possible equilibrium configurations and bifurcations in symmetric racetrack economy by group-theoretic analysis. Two formal predictions are worth mentioning. One is that no symmetry-breaking bifurcations occur after a single-peaked spatial configuration emerges. For Class II models, this implies that the spatial configuration remains monocentric for the whole range of ϕ after the bifurcation characterized by **Proposition 1** (b). The other prediction is that, if $M \geq 2$ same-sized agglomerations are equidistantly placed over a racetrack economy, then a symmetry-breaking bifurcation can occur, resulting in a smaller number of symmetric agglomerations with a larger average distance between them. If $M < N$ distinct, same-sized agglomerations exist equidistantly in the racetrack economy (i.e., M is a divisor of N), then a bifurcation can occur so that only K among M agglomerations grow (where K is a divisor of M and hence N) and they are again equidistantly placed. **Proposition 1** (a) shows that Class I models produce $\frac{N}{2}$ agglomerations, that is, the evolution after the bifurcation from $\bar{\mathbf{x}}$ starts with $M = \frac{N}{2}$ and successive bifurcations is expected if this M is a composite number. For the analysis of specific Class I models, see (Akamatsu et al., 2012; Ikeda et al., 2012b; Osawa et al., 2017). For Class II models, Takayama et al. (2020) provided a detailed analysis of Murata and Thisse (2005)'s model in a racetrack economy to demonstrate single-peaked spatial distributions emerge. Akamatsu et al. (2016) showed that Helpman (1998)'s Class II

model produces monocentric configuration and polycentric patterns cannot become stable in the four-region racetrack economy. All available formal results in the literature corroborates with **Proposition 1** and the numerical examples presented in Figure 7. ■

Remark A.4. Definition 2 identifies three prototypical model classes found in the literature. However, there are flexible models that can change their behavior. For example, the model by Pflüger and Tabuchi (2010) can fall into both Classes II and III depending on the parameter values. For such a model, one can split its parameter space to understand the model behavior in light of the three prototypical classes. Extant models often have presumed parametric restrictions that unambiguously determine the model class each belongs to. However, it may be plausible to use a flexible model because we can see which model class the observed data support by estimating the model's key parameters. ■

A.2 Proof of Proposition 2

The equilibrium condition when all regions are populated is given by

$$\mathbf{v}(\mathbf{x}, \mathbf{a}) - \bar{v}(\mathbf{x}, \mathbf{a})\mathbf{1} = \mathbf{0}, \quad (\text{A.10})$$

where we make the dependence of \mathbf{v} on \mathbf{a} explicit, $\bar{v}(\mathbf{x}, \mathbf{a}) \equiv \sum_{i \in \mathcal{N}} v_i(\mathbf{x}, \mathbf{a})x_i$ is the average payoff, and $\mathbf{1}$ is N -dimensional all-one vector. The pair $(\bar{\mathbf{x}}, \bar{\mathbf{a}})$ is a solution to (A.10). Suppose that there is a spatial equilibrium nearby $\bar{\mathbf{x}}$ when \mathbf{a} is marginally different from $\bar{\mathbf{a}}$. Let $\mathbf{x}(\mathbf{a})$ denote the perturbed version of $\bar{\mathbf{x}}$, which is a function in \mathbf{a} . We assume $\bar{\mathbf{x}}$ is stable so that studying a perturbed version of it makes sense.

The covariance ρ discussed in Section 4 is represented as follows:

$$\rho \equiv (\mathbf{a} - \bar{\mathbf{a}})^\top (\mathbf{x}(\mathbf{a}) - \bar{\mathbf{x}}) = (\mathbf{C}\mathbf{a})^\top \mathbf{C}\mathbf{x}(\mathbf{a}) = \mathbf{a}^\top \mathbf{C}\mathbf{x}(\mathbf{a}) \quad (\text{A.11})$$

where $\mathbf{C} \equiv \mathbf{I} - \frac{1}{N}\mathbf{1}\mathbf{1}^\top$. Let $\mathbf{X} \equiv [\frac{\partial x_i}{\partial a_j}(\bar{\mathbf{a}})]$ be the Jacobian matrix of \mathbf{x} with respect to \mathbf{a} at $(\bar{\mathbf{x}}, \bar{\mathbf{a}})$. Then, $\mathbf{x}(\mathbf{a}) \approx \bar{\mathbf{x}} + \mathbf{X}(\mathbf{a} - \bar{\mathbf{a}}) = \bar{\mathbf{x}} + \mathbf{X}\mathbf{C}\mathbf{a}$ and thus $\rho = \mathbf{a}^\top \mathbf{C}\mathbf{X}\mathbf{C}\mathbf{a}$ as $\mathbf{C}\bar{\mathbf{x}} = \mathbf{0}$. The implicit function theorem regarding (A.10) at $(\bar{\mathbf{x}}, \bar{\mathbf{a}})$ gives:

$$\mathbf{X} = -(\mathbf{V}_x - \mathbf{1}\bar{\mathbf{x}}^\top \mathbf{V}_x - \mathbf{1}\mathbf{v}(\bar{\mathbf{x}})^\top)^{-1} (\mathbf{V}_a - \mathbf{1}\bar{\mathbf{x}}^\top \mathbf{V}_a) \quad (\text{A.12})$$

$$= \left(\frac{\bar{v}}{\bar{\mathbf{x}}}\frac{1}{N}\mathbf{1}\mathbf{1}^\top - \left(\mathbf{I} - \frac{1}{N}\mathbf{1}\mathbf{1}^\top\right)\mathbf{V}_x\right)^{-1} \left(\mathbf{I} - \frac{1}{N}\mathbf{1}\mathbf{1}^\top\right)\mathbf{V}_a \quad (\text{A.13})$$

$$= \frac{\bar{\mathbf{x}}}{\bar{v}} \left(\left(\mathbf{I} - \mathbf{C}\right) - \mathbf{C}\frac{\bar{\mathbf{x}}}{\bar{v}}\mathbf{V}_x\right)^{-1} \mathbf{C}\frac{\bar{\mathbf{a}}}{\bar{v}}\mathbf{V}_a \quad (\text{A.14})$$

$$= \frac{\bar{\mathbf{x}}}{\bar{\mathbf{a}}} \left(\left(\mathbf{I} - \mathbf{C}\right) - \mathbf{C}\mathbf{V}\right)^{-1} \mathbf{C}\mathbf{A} \quad (\text{A.15})$$

where \bar{v} is the payoff level, $\mathbf{V}_x \equiv [\frac{\partial v_i}{\partial x_j}(\bar{\mathbf{x}}, \bar{\mathbf{a}})]$, $\mathbf{V}_a \equiv [\frac{\partial v_i}{\partial a_j}(\bar{\mathbf{x}}, \bar{\mathbf{a}})]$, $\mathbf{V} \equiv \frac{\bar{\mathbf{x}}}{\bar{v}}\mathbf{V}_x$, and $\mathbf{A} \equiv \frac{\bar{\mathbf{a}}}{\bar{v}}\mathbf{V}_a$.

For tractability, we focus on a specific form of \mathbf{A} which covers many relevant cases.

Assumption A. Suppose Assumption RE. Let $\mathbf{A} \equiv \frac{\bar{a}}{\bar{v}} \left[\frac{\partial v_i}{\partial a_j} \right]$ be the elasticity matrix of the payoff with respect to the local characteristic \mathbf{a} under consideration, evaluated at $(\bar{\mathbf{x}}, \bar{\mathbf{a}})$. There is a rational function G^{\natural} that is continuous over $[0, 1]$, positive whenever $\bar{\mathbf{x}}$ is stable, and satisfies $\mathbf{A} = G^{\natural}(\mathbf{D})$.

The simplest example is local amenity differences.

Example A.4. Suppose $v_i(\mathbf{x}, \mathbf{a}) = a_i v_i(\mathbf{x})$, where $a_i > 0$ is the exogenous level of local amenities and $\mathbf{v}(\mathbf{x}) = (v_i(\mathbf{x}))_{i \in \mathcal{N}}$ is the homogeneous component of the payoff function satisfying Assumption S. Then, $\mathbf{A} = \frac{\bar{a}}{\bar{v}} \bar{\mathbf{v}} \mathbf{I} = \bar{a} \mathbf{I}$ and $G^{\natural}(\cdot) = \bar{a} > 0$. ■

Under Assumptions RE, S, and A, \mathbf{X} is real, symmetric, and circulant. Thus, the set of eigenvectors of \mathbf{CXC} can be chosen as in Lemma A.1 (a) because it is a circulant matrix of the same size as \mathbf{D} . Let $\{\lambda_k\}_{k=0}^M$ be the distinct eigenvalues of \mathbf{CXC} . As \mathbf{CXC} is symmetric, it admits the eigenvalue decomposition

$$\mathbf{CXC} = \lambda_0 \mathbf{1}\mathbf{1}^\top + \sum_{k=1}^{M-1} \lambda_k \left(\mathbf{z}_k^+ \mathbf{z}_k^{+\top} + \mathbf{z}_k^- \mathbf{z}_k^{-\top} \right) + \lambda_M \mathbf{z}_M \mathbf{z}_M^\top. \quad (\text{A.16})$$

This fact yields the following representation of ρ :

$$\rho = \mathbf{a}^\top \mathbf{CXC} \mathbf{a} = \sum_{k \neq 0} \tilde{a}_k^2 \lambda_k, \quad (\text{A.17})$$

where $\tilde{\mathbf{a}} \equiv (\tilde{a}_k)$ is the representation of \mathbf{a} in the new coordinate system $\{\mathbf{z}_k\}$. We drop $k = 0$ since $\lambda_0 = 0$, which reflects that $\mathbf{z}_0 = \mathbf{1}$ is a uniform increase in \mathbf{a} and thus does not affect spatial equilibria. All the matrices in (A.15) are circulant and hence shares the same set of eigenvectors. Thus, λ_k is obtained from (A.15) as follows:

$$\lambda_k = \frac{\bar{x}}{\bar{a}} \frac{\kappa_k \alpha_k}{((1 - \kappa_k) - \kappa_k \omega_k)} = -\frac{\bar{x}}{\bar{a}} \frac{\alpha_k}{\omega_k} \quad \forall k \in \mathcal{K}, \quad (\text{A.18})$$

where κ_k , ω_k , and α_k are the k th eigenvalues of \mathbf{C} , \mathbf{V} , and \mathbf{A} , respectively, with $\kappa_0 = 0$ and $\kappa_k = 1$ for all $k \neq 0$. As $\omega_k = G(\chi_k)$ and $\alpha_k = G^{\natural}(\chi_k)$ with $\{\chi_k\}_{k \in \mathcal{K}}$ are the eigenvalues of \mathbf{D} because we assume $\mathbf{G} = G(\mathbf{D})$ and $\mathbf{A} = G^{\natural}(\mathbf{D})$,

$$\lambda_k = -\frac{\bar{x}}{\bar{a}} \frac{G^{\natural}(\chi_k)}{G(\chi_k)} = \frac{\bar{x}}{\bar{a}} \delta(\chi_k) \quad \forall k \in \mathcal{K} \quad (\text{A.19})$$

and $\lambda_0 = 0$ where $\delta(\chi) \equiv -\frac{G^{\natural}(\chi)}{G(\chi)}$.

From (A.17), $\rho > 0$ for all \mathbf{a} if all $\{\lambda_k\}$ are positive except for $\lambda_0 = 0$. The denominator of (A.19), $G(\chi_k)$, must be negative for all k because $\bar{\mathbf{x}}$ is stable by assumption. Thus, we see that $\rho > 0$ if $G^{\natural}(\chi) > 0$ for all χ since $\chi_k \in (0, 1)$ for all $k \in \mathcal{K}$.

Proposition 2 follows by noting

$$\rho'(\phi) = \sum_{k \neq 0} \tilde{a}_k^2 \frac{d\lambda_k}{d\phi} = \frac{\bar{x}}{\bar{a}} \sum_{k \neq 0} \tilde{a}_k^2 \delta'(\chi_k) \frac{d\chi_k}{d\phi} = -\frac{\bar{x}}{\bar{a}} \sum_{k \neq 0} \tilde{a}_k^2 \delta'(\chi_k) \left| \frac{d\chi_k}{d\phi} \right|.$$

From Lemma A.1, $\{\chi_k\}_{k \in \mathcal{K}}$ are strictly decreasing in ϕ . Thus, for $\rho'(\phi) > 0$ ($\rho'(\phi) < 0$), it is sufficient that $\delta'(\chi) < 0$ ($\delta'(\chi) > 0$) for all χ such that $G(\chi) < 0$.

References

- Ahlfeldt, Gabriel M., Stephen J. Redding, Daniel M. Sturm, and Nikolaus Wolf, “The economics of density: Evidence from the Berlin Wall,” *Econometrica*, 2015, 83 (6), 2127–2189.
- , Thilo Albers, and Kristian Behrens, “A granular spatial model,” 2022. CEPR Discussion Paper No. 17126.
- Akamatsu, Takashi, Tomoya Mori, and Yuki Takayama, “Agglomerations in a Multi-region Economy: Polycentric versus monocentric patterns,” Discussion papers, Research Institute of Economy, Trade and Industry (RIETI) 2016.
- , —, Minoru Osawa, and Yuki Takayama, “Spatial scale of agglomeration and dispersion: Theoretical foundations and empirical implications,” 2017. Unpublished manuscript, MPRA Paper No. 84145.
- , Yuki Takayama, and Kiyohiro Ikeda, “Spatial discounting, Fourier, and racetrack economy: A recipe for the analysis of spatial agglomeration models,” *Journal of Economic Dynamics and Control*, 2012, 99 (11), 32–52.
- Allen, Treb and Costas Arkolakis, “Trade and the topography of the spatial economy,” *The Quarterly Journal of Economics*, 2014, 129 (3), 1085–1140.
- , —, and Yuta Takahashi, “Universal gravity,” *Journal of Political Economy*, 2019, *Forthcoming*.
- Alonso, Wiliam, *Location and Land Use: Toward a General Theory of Land Rent*, Cambridge, MA: Harvard University Press, 1964.
- Anas, Alex and Ikki Kim, “General equilibrium models of polycentric urban land use with endogenous congestion and job agglomeration,” *Journal of Urban Economics*, 1996, 40 (2), 232–256.
- , Richard Arnott, and Kenneth A Small, “Urban spatial structure,” *Journal of Economic Literature*, 1998, 36 (3), 1426–1464.
- Anderson, Simon P., Andre de Palma, and Jacques François Thisse, *Discrete Choice Theory of Product Differentiation*, MIT Press, 1992.
- Armington, Paul S., “A theory of demand for product distinguished by place of production,” *International Monetary Fund Staff Papers*, 1969, 16 (1), 159–178.
- Arthur, W. Brian, *Increasing Returns and Path Dependence in the Economy*, Ann Arbor, MI: University of Michigan Press, 1994.

- Baldwin, Richard E., Rikard Forslid, Philippe Martin, Gianmarco I. P. Ottaviano, and Frederic Robert-Nicoud**, *Economic Geography and Public Policy*, Princeton University Press, 2003.
- Baum-Snow, Nathaniel**, “Did highways cause suburbanization?,” *The Quarterly Journal of Economics*, May 2007, *122* (2), 775–805.
- , **J. Vernon Henderson, Matthew A. Turner, Qinghua Zhang, and Loren Brandt**, “Does investment in national highways help or hurt hinterland city growth?,” *Journal of Urban Economics*, 2020, *115*, 103124.
- , **Loren Brandt, J. Vernon Henderson, Matthew A. Turner, and Qinghua Zhang**, “Roads, railroads and decentralization of Chinese cities,” *Review of Economics and Statistics*, 2017, *99* (3), 435–448.
- Beckmann, Martin J.**, “Spatial equilibrium in the dispersed city,” in Yorgos Papageorgiou, ed., *Mathematical Land Use Theory*, Lexington Book, 1976, pp. 117–125.
- Behrens, Kristian and Yasusada Murata**, “On quantitative spatial economic models,” *Journal of Urban Economics*, 2021, *123*, 103348.
- , **Giordano Mion, Yasusada Murata, and Jens Südekum**, “Spatial frictions,” *Journal of Urban Economics*, 2017, *97*, 40–70.
- Berliant, Marcus and Tomoya Mori**, “Beyond urban form: How Masahisa Fujita shapes us,” *International Journal of Economic Theory*, February 2017, *13*, 5–28.
- Blanchet, Adrien, Pascal Mossay, and Filippo Santambrogio**, “Existence and uniqueness of equilibrium for a spatial model of social interactions,” *International Economic Review*, 2016, *57* (1), 36–60.
- Brown, George W. and John von Neumann**, “Solutions of games by differential equations,” in Harold W. Kuhn and Albert W. Tucker, eds., *Contributions to the Theory of Games I*, Princeton University Press, 1950, pp. 73–80.
- Combes, Pierre-Philippe, Gilles Duranton, Laurent Gobillon, and Fré**, “The emergence, growth, and stagnation of cities: France 1760-2020,” 2020. Unpublished manuscript.
- Davis, Donald R. and Jonathan I. Dingel**, “The Comparative Advantage of Cities,” *Journal of International Economics*, 2020, *123*, 1032–91.
- Diamond, Rebecca**, “The determinants and welfare implications of US workers’ diverging location choices by skill: 1980-2000,” *American Economic Review*, 2016, *106* (3), 479–524.
- Dupuis, Paul and Anna Nagurney**, “Dynamical systems and variational inequalities,” *Annals of Operations Research*, 1993, *44* (1), 7–42.
- Duranton, Gilles and Diego Puga**, “Micro-foundations of urban agglomeration economies,” in J. Vernon Henderson and Jacques-François Thisse, eds., *Handbook of Regional and Urban Economics*, Vol. 4, North-Holland, 2004, pp. 2063–2117.
- **and Matthew A. Turner**, “Urban growth and transportation,” *Review of Economic Studies*, 2012, *79* (4), 1407–1440.

- Faber, Benjamin**, “Trade integration, market size, and industrialization: Evidence from China’s national trunk highway system,” *Review of Economic Studies*, 2014, 81 (3), 1046–1070.
- Facchinei, Francisco and Jong-Shi Pang**, *Finite-dimensional Variational Inequalities and Complementarity Problems*, Springer Science & Business Media, 2007.
- Forslid, Rikard and Gianmarco I. P. Ottaviano**, “An analytically solvable core-periphery model,” *Journal of Economic Geography*, 2003, 33 (3), 229–240.
- Fujita, Masahisa and Hideaki Ogawa**, “Multiple equilibria and structural transformation of non-monocentric urban configurations,” *Regional Science and Urban Economics*, 1982, 12, 161–196.
- and **Jacques-François Thisse**, *Economics of Agglomeration: Cities, Industrial Location, and Regional Growth (Second Edition)*, Cambridge University Press, 2013.
- and **Paul R. Krugman**, “When is the economy monocentric?: von Thuünen and Chamberlin unified,” *Regional Science and Urban Economics*, 1995, 25 (4), 505–528.
- , – , and **Anthony Venables**, *The Spatial Economy: Cities, Regions, and International Trade*, Princeton University Press, 1999.
- , – , and **Tomoya Mori**, “On the evolution of hierarchical urban systems,” *European Economic Review*, February 1999, 43 (2), 209–251.
- Gaubert, Cecile**, “Firm sorting and agglomeration,” *American Economic Review*, 2018, 108 (11), 3117–3153.
- Golubitsky, Martin and Ian Stewart**, *The Symmetry Perspective: From Equilibrium to Chaos in Phase Space and Physical Space*, Vol. 200, Springer Science & Business Media, 2003.
- , – , and **David G. Schaeffer**, *Singularities and Groups in Bifurcation Theory*, Vol. 2, Springer Science & Business Media, 2012.
- Greenstone, Michael, Richard Hornbeck, and Enrico Moretti**, “Identifying agglomeration spillovers: Evidence from winners and losers of large plant openings,” *Journal of Political Economy*, 2010, 118 (3), 536–598.
- Harris, Britton and Alan G. Wilson**, “Equilibrium values and dynamics of attractiveness terms in production-constrained spatial-interaction models,” *Environment and Planning A*, 1978, 10 (4), 371–388.
- Heblich, Stephan, Stephen J Redding, and Daniel M Sturm**, “The making of the modern metropolis: Evidence from London,” *The Quarterly Journal of Economics*, 2020, 135 (4), 2059–2133.
- Helpman, Elhanan**, “The size of regions,” in David Pines, Efraim Sadka, and Itzhak Zilcha, eds., *Topics in Public Economics: Theoretical and Applied Analysis*, Cambridge University Press, 1998, pp. 33–54.
- Hirsch, Morris W., Stephen Smale, and Robert L. Devaney**, *Differential Equations, Dynamical Systems, and an Introduction to Chaos*, Academic Press, 2012.
- Hofbauer, Josef and William H Sandholm**, “Evolution in games with randomly disturbed payoffs,” *Journal of economic theory*, 2007, 132 (1), 47–69.

- Horn, Roger A. and Charles R. Johnson**, *Matrix Analysis (Second Edition)*, Cambridge University Press, 2012.
- Hsu, Wen-Tai**, “Central place theory and city size distribution,” *The Economic Journal*, 2012, *122*, 903–932.
- Ikeda, Kiyohiro and Kazuo Murota**, *Bifurcation Theory for Hexagonal Agglomeration in Economic Geography*, Springer, 2014.
- , – , and **Takashi Akamatsu**, “Self-organization of Lösch’s hexagons in economic agglomeration for core-periphery models,” *International Journal of Bifurcation and Chaos*, 2012, *22* (08), 1230026.
- , – , and **Yuki Takayama**, “Stable economic agglomeration patterns in two dimensions: Beyond the scope of central place theory,” *Journal of Regional Science*, 2017, *57* (1), 132–172.
- , – , **Takashi Akamatsu**, and **Yuki Takayama**, “Agglomeration patterns in a long narrow economy of a new economic geography model: Analogy to a racetrack economy,” *International Journal of Economic Theory*, 2017, *13*, 113–145.
- , – , – , **Tatsuhito Kono**, and **Yuki Takayama**, “Self-organization of hexagonal agglomeration patterns in new economic geography models,” *Journal of Economic Behavior & Organization*, 2014, *99*, 32–52.
- , **Mikihisa Onda**, and **Yuki Takayama**, “Spatial period doubling, invariant pattern, and break point in economic agglomeration in two dimensions,” *Journal of Economic Dynamics and Control*, 2018, *92*, 129–152.
- , **Takashi Akamatsu**, and **Tatsuhito Kono**, “Spatial period-doubling agglomeration of a core-periphery model with a system of cities,” *Journal of Economic Dynamics and Control*, 2012, *36* (5), 754–778.
- Krugman, Paul R.**, “Increasing returns and economic geography,” *Journal of Political Economy*, 1991, *99* (3), 483–499.
- , “On the number and location of cities,” *European Economic Review*, 1993, *37* (2), 293–298.
- Kuznetsov, Yuri A.**, *Elements of Applied Bifurcation Theory (3rd Eds.)*, Springer-Verlag, 2004.
- Lucas, Robert E. and Esteban Rossi-Hansberg**, “On the internal structure of cities,” *Econometrica*, 2002, *70* (4), 1445–1476.
- Matsuyama, Kiminori**, “Geographical advantage: Home market effect in a multi-region world,” *Research in Economics*, 2017, *71*, 740–758.
- Mertikopoulos, Panayotis and William H. Sandholm**, “Riemannian game dynamics,” *Journal of Economic Theory*, 2018, *177*, 315–364.
- Mori, Tomoya, Takashi Akamatsu, Yuki Takayama, and Minoru Osawa**, “Origin of power laws and their spatial fractal structure for city-size distributions,” 2022. arXiv:2207.05346.
- , **Tony E Smith**, and **Wen-Tai Hsu**, “Common power laws for cities and spatial fractal structures,” *Proceedings of the National Academy of Sciences*, 2020, *117* (12), 6469–6475.

- Mossay, Pascal and Pierre M. Picard**, “On spatial equilibria in a social interaction model,” *Journal of Economic Theory*, 2011, *146* (6), 2455–2477.
- Murata, Yasusada and Jacques-François Thisse**, “A simple model of economic geography à la Helpman–Tabuchi,” *Journal of Urban Economics*, 2005, *58* (1), 137–155.
- Nash, John**, “Non-cooperative games,” *Annals of Mathematics*, 1951, *54* (2), 286–295.
- Osawa, Minoru and Takashi Akamatsu**, “Equilibrium refinement for a model of non-monocentric internal structures of cities: A potential game approach,” *Journal of Economic Theory*, 2020, *187*, 105025.
- , – , and **Yuki Takayama**, “Harris and Wilson (1978) model revisited: The spatial period-doubling cascade in an urban retail model,” *Journal of Regional Science*, 2017, *57* (3), 442–466.
- Ottaviano, Gianmarco I. P., Takatoshi Tabuchi, and Jacques-François Thisse**, “Agglomeration and trade revisited,” *International Economic Review*, 2002, *43*, 409–436.
- Pflüger, Michael**, “A simple, analytically solvable, Chamberlinian agglomeration model,” *Regional Science and Urban Economics*, 2004, *34* (5), 565–573.
- and **Jens Südekum**, “Integration, agglomeration and welfare,” *Journal of Urban Economics*, March 2008, *63* (2), 544–566.
- Pflüger, Michael and Takatoshi Tabuchi**, “The size of regions with land use for production,” *Regional Science and Urban Economics*, 2010, *40* (6), 481–489.
- Picard, Pierre M. and Takatoshi Tabuchi**, “On microfoundations of the city,” *Journal of Economic Theory*, 2013, *148* (6), 2561–2582.
- Puga, Diego**, “The rise and fall of regional inequalities,” *European Economic Review*, 1999, *43* (2), 303–334.
- Redding, Stephen J. and Daniel Sturm**, “The cost of remoteness: Evidence from German division and reunification,” *American Economic Review*, 2008, *98* (5), 1766–1797.
- and **Esteban Rossi-Hansberg**, “Quantitative spatial economics,” *Annual Review of Economics*, 2017, *9*, 21–58.
- Sandholm, William H.**, *Population Games and Evolutionary Dynamics*, MIT Press, 2010.
- Smith, Michael J.**, “The stability of a dynamic model of traffic assignment: An application of a method of Lyapunov,” *Transportation Science*, 1984, *18* (3), 245–252.
- Sugimoto, Tatsuya, Mizuki Takada, Yuki Takayama, and Akiyoshi Takagi**, “Development of a long-run impact assessment methodology for interregional transportation improvements based on spatial economics,” *Journal of Japan Society of Civil Engineers*, 2023, *79* (4), 22–00115. in Japanese.
- Tabuchi, Takatoshi**, “Urban agglomeration and dispersion: A synthesis of Alonso and Krugman,” *Journal of Urban Economics*, 1998, *44* (3), 333–351.
- and **Jacques-François Thisse**, “A new economic geography model of central places,” *Journal of Urban Economics*, 2011, *69* (2), 240–252.

Takayama, Yuki and Takashi Akamatsu, “Emergence of polycentric urban configurations from combination of communication externality and spatial competition,” *Journal of JSCE Series D3: Infrastructure Planning and Management*, 2011, 67 (1), 001–020.

– , **Kiyohiro Ikeda, and Jacques-François Thisse**, “Stability and sustainability of urban systems under commuting and transportation costs,” *Regional Science and Urban Economics*, 2020, 84, 103553.

Taylor, Peter D. and Leo B. Jonker, “Evolutionarily stable strategies and game dynamics,” *Mathematical Biosciences*, 1978, 40, 145–156.

Supplementary Materials

for “Spatial Scale of Agglomeration and Dispersion: Number, Spacing, and the Spatial Extent of Cities”

August 30, 2024

By Takashi Akamatsu, Tomoya Mori, Minoru Osawa, and Yuki Takayama

We provide derivations and numerical examples omitted in the main text. Appendix B discusses the evolution of Japanese cities from 1970 to 2020. Appendix C provides numerical examples for the eight-region racetrack economy. Appendix D provides omitted derivations for the examples in the main text. Appendix E provides numerical examples where we relax the racetrack assumption (Assumption RE). Appendix F provides numerical examples for **Proposition 2**.

B Evolution of cities

B.1 Japanese cities

For Japan, we construct cities from the Grid Square Statistics of the Population Census in 1970–2020 (every five years). A *city* is defined as an *urban agglomeration (UA)*, which is a set of contiguous 1 km-by-1 km grid cells whose population density is at least 1000/km² and a total population of at least 10,000. The results are robust for alternative threshold values. Fig. B.1 shows the identified 431 UAs in 2020. They occupy 6% of land area while containing 80% of the national population. Populated cells with less than 1,000 residents are shown in grey with darker grey indicating a larger population. We use only the cells reachable by roads from four major islands (Hokkaido, Honshu, Shikoku, and Kyushu).

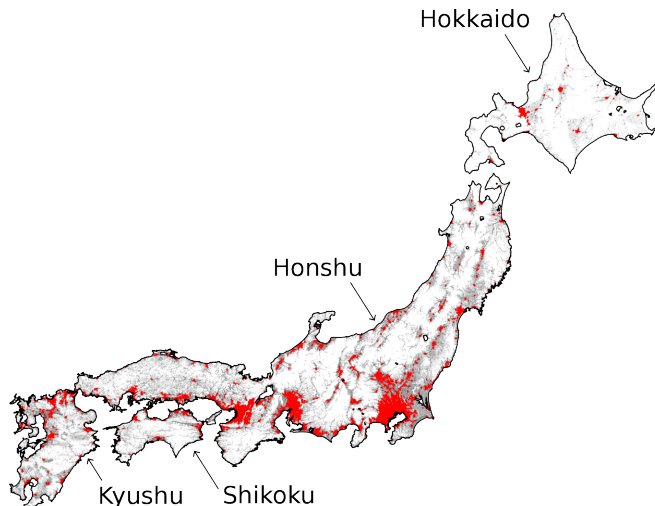


Figure B.1: Urban agglomerations of Japan in 2020

UAs are identified for each census year during the 1970–2020 period. Unique IDs throughout the period are assigned by the following steps.

1. IDs for the UAs in $t = 1970$ are set to be their city-size ranking in the year. In the case of ties, the UA with higher population density is ranked higher.

2. A UA in year t and a UA in year $t + 5$ are considered the same if they mutually have the largest population in their areal intersection. If there are ties, then the pair of UAs whose areal intersection has the largest population density is matched. In that case, their IDs in year $t + 5$ are inherited from year t .
3. If UA i in year t has the largest population (in year t) in the areal intersection with UA j in year $t + 5$, and UA j in year $t + 5$ has the largest population in the areal intersection with a UA other than i in year t , then UA i is absorbed to UA j in year $t + 5$.
4. If UA j in year $t + 5$ has no intersection with any UA in year t , then UA j is either a newly formed UA or a UA split from the existing UA. For a newly formed UA or a split UA with no predecessor in older years $< t$, a new ID is assigned in the order of their population size in year $t + 5$.
5. If a UA is split from the existing UA in year $t + 5$ but has a predecessor a year before t , the latest predecessor's ID is recovered. If there are multiple latest predecessors, the one with the largest population in the areal intersection with the UA is chosen. (Again, in the case of ties, the population density in the intersection is compared among the UA pairs.) Thus, a UA i , which was absorbed to another UA j and then split from UA j , will be named i again.

B.2 Development of high-speed transport networks in Japan

Figure B.2 depicts the development of high-speed railway and highway networks, respectively, in Japan between 1970 and 2020. The development of highways and high-speed railway networks in Japan was initiated by the Tokyo Olympics held in 1964. Between 1970 and 2020, the total highway (high-speed railway) length increased from 1,119 km (515 km) to 9,050 km (3,106 km), which is an increase of more than eight (six) times.

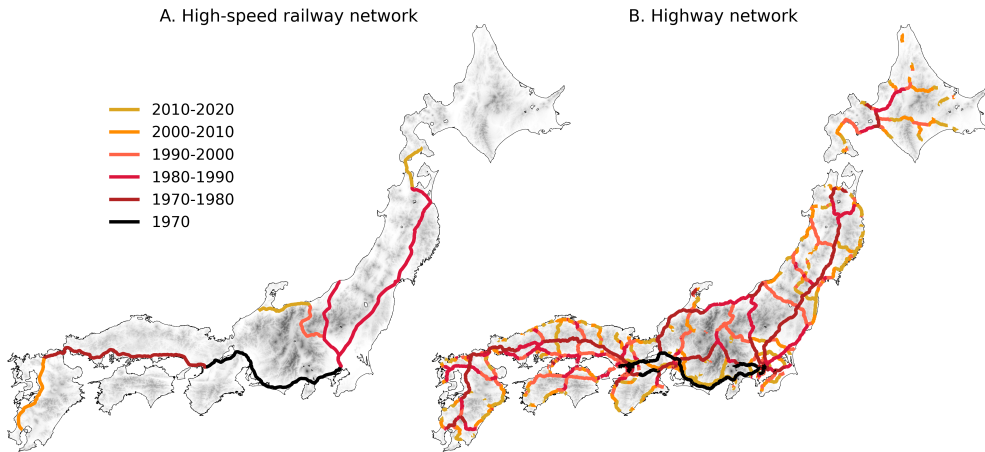


Figure B.2: The development of high-speed network in Japan

Notes: The shapefiles of highway and high-speed railway lines are obtained from the Digital National Land Information Download Service (Highway: <https://nlftp.mlit.go.jp/ksj/gml/datalist/KsjTmplt-N06-2023.html>, High-speed railway: <https://nlftp.mlit.go.jp/ksj/gml/datalist/KsjTmplt-N05-2023.html>).

Figure B.3A and B show the expansion of high-speed transport network over the period between 1964 and 2020 in terms of the increase in the total length of high-speed railway lines and that of highway. As both of these networks gradually expanded in the past half century, Japan is an ideal case to study the comparative statics regarding transport costs.

In the same period, the cities in Japan attracted substantial in-migration from across the country as the national population increased by only 21% between 1970 and 2020. At the same time, there was a clear tendency of concentration toward larger cities at the national (or global) level, as the city-size distribution is rotated clock-wisely (from the blue graph to the orange one in Figure 1A) so that larger cities grew more, while smaller cities declined more in the same period. In particular, the population of the largest city, Tokyo, has grown by 67% while the national population growth was only 22%. Tokyo's population increase was about the size of the second largest city, Osaka.

B.3 Cities in other countries

Figure 1 in Section 1 uses Japanese Census data. To allow a parallel comparison between different countries, we employ the the LandScan™ Global Population Database, developed by the Department of Energy's Oak Ridge National Laboratory (ORNL), as the basic grid population data to see the evolution of cities. Cities are defined in the same manner as for Japanese cities. To assess compatibility between the LandScan data and the census we compare Census and the LandScan data for Japan. Figure B.4A and Figure B.4B are, respectively, based on the Census and the the LandScan data (Figure B.4A is a reproduction of Figure 1B-C). The LandScan data is only available after 2000, and are only roughly in agreement with the precise data based on Census. It is also noted that, while the LandScan data is available every year, we employ 5-year steps to avoid noises due to its data generation procedure that incorporates various interpolations. Nonetheless, Figure B.4 confirms the general tendency of nationwide concentration and local flattening of the cities. To be consistent with our theory that assume a fixed total population, we normalize the total population in each country. In the cases of France, Germany and Japan, the local flattening is apparent even without the normalization.

B.4 Flattening of the employment distribution within cities

The tendency of local dispersion is observed in alternative indicator of agglomeration other than population. Figure B.5 shows the change in the mean values of the maximum and average employment density within a city across all cities in Japan from 1975 to 2014. Their long-run trend indicates that the geographical distribution of employment in a city has flattened over the past half century.

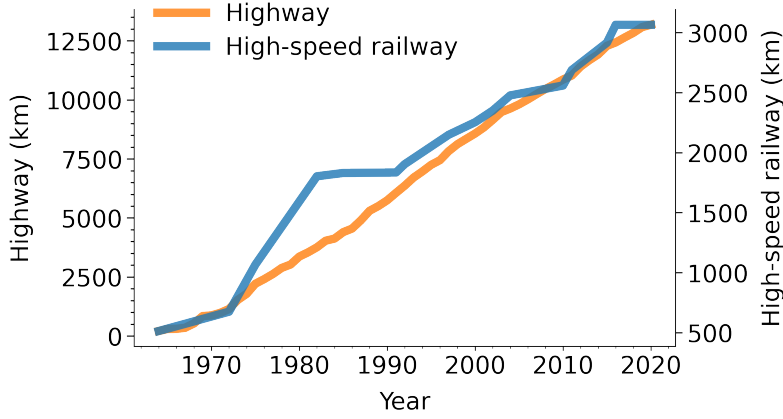


Figure B.3: Total length of high-speed high-speed network in Japan

Note: The length of highway and high-speed railway lines are computed from the line data provided by the Digital National Land Information Download Service. Specifically, <https://nlftp.mlit.go.jp/ksj/gml/datalist/KsjTmplt-N06-2023.html> for the highways and <https://nlftp.mlit.go.jp/ksj/gml/datalist/KsjTmplt-N05-2023.html> for the high-speed railways.

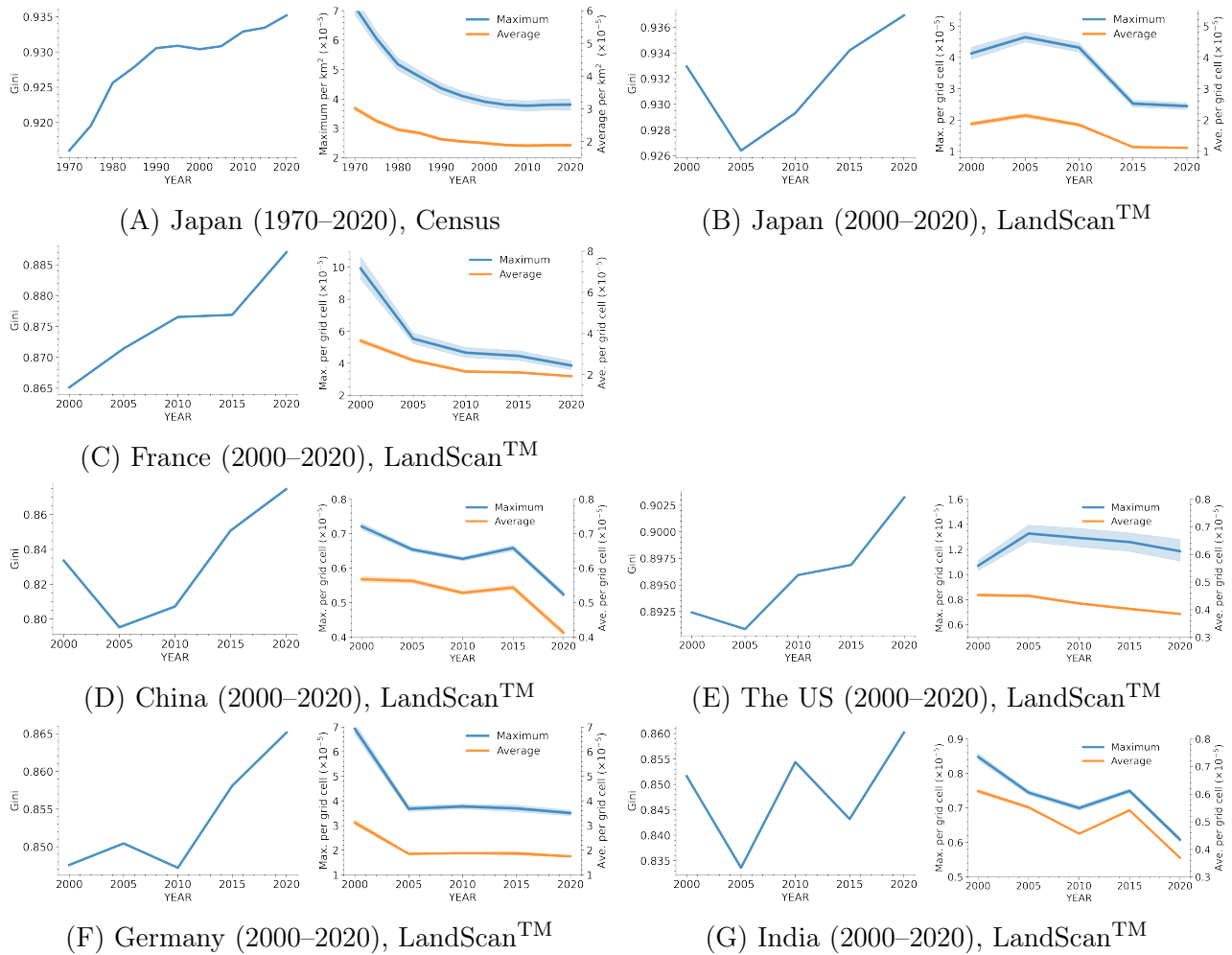


Figure B.4: Global concentration and local dispersion

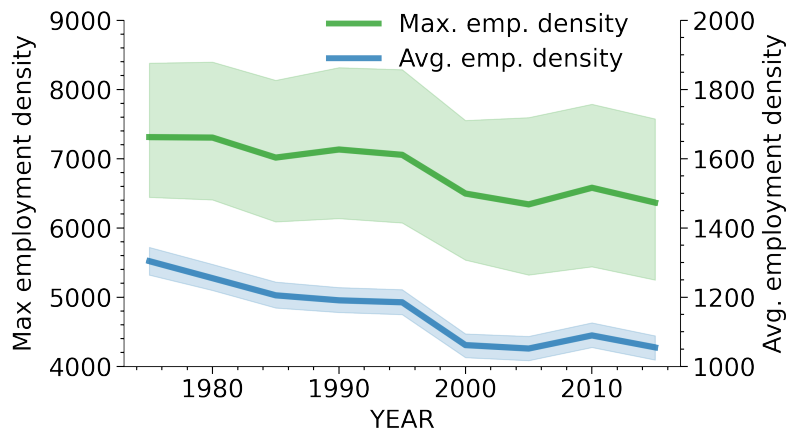


Figure B.5: Maximum and average employment density within a city in Japan in 1975–2014

Notes: The green and blue lines show the means of maximum and average employment densities within a city for years 1975, 1981, 1986, 1991, 1996, 2001, 2006, 2009, and 2014. The shaded area indicates the range covering 90% of the values for individual cities. The grid-cell data of employment are obtained from the Grid Square Statistics of the Census for Establishment (1975, 1981, 1986, 1991); Establishment and Enterprise census (1996, 2001, 2006); Economic Census for Business Frame (2009 and 2014) of Japan.

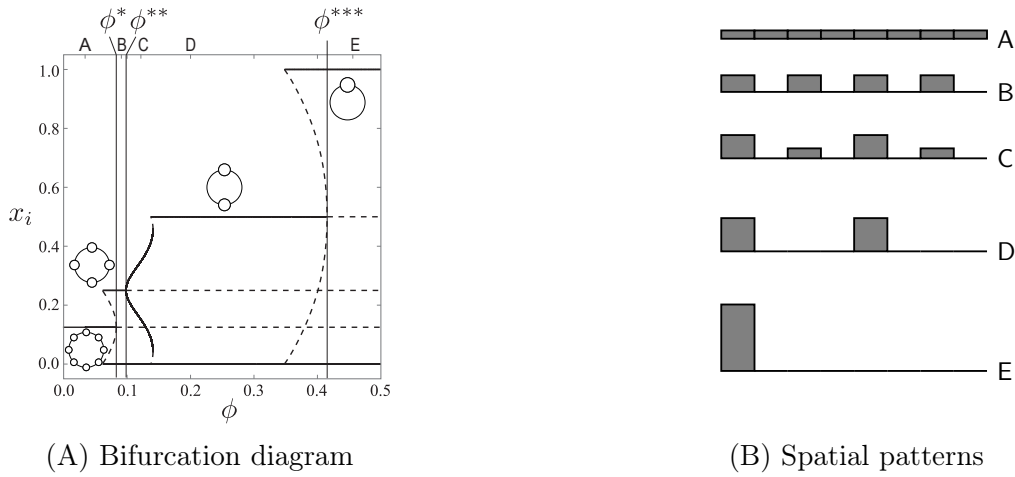


Figure C.1: Class I model (Krugman, 1991)

C Eight-region racetrack economy

We simulate an overall evolution of the spatial structure for a selected model from Classes I, II, and III in the $N = 8$ racetrack economy. We follow stationary equilibria branching from \bar{x} and then numerically check the local stability of those stationary equilibrium solutions under the replicator dynamic (Taylor and Jonker, 1978). See Appendix D for the details of the specific formulations and the parameter settings.

C.1 Class I model

Figure C.1 reports stable equilibrium patterns in the course of increasing ϕ for the Krugman (1991) model. In Figure C.1A, the black solid (dashed) curves depict the stable (unstable) equilibrium values of x_i at each ϕ . Figure C.1B is the schematic illustration of the stable spatial pattern on the path. The letters in Figure C.1B correspond to those in Figure C.1A. The global dispersion force in the Krugman model stems from competition between firms over consumers' demand. When ϕ is low (when transport costs are high), firms have few incentives to agglomerate, and the uniform distribution is stable. As ϕ increases, competition with firms in other regions becomes fiercer, as the markets of other regions become closer. At some point firms are better off forming small agglomerations so that each agglomeration has its dominant market area but is relatively remote from other agglomerations of firms. At the so-called “break point” ϕ^* , a bifurcation from \bar{x} occurs and the spatial pattern is pushed towards the formation of $\frac{8}{2} = 4$ distinct agglomerations [Proposition 1 (a)]. A further increase in ϕ causes the second and third bifurcations at ϕ^{**} and ϕ^{***} , respectively. These bifurcations sequentially double the spacing between agglomerations, each time halving their number, $4 \rightarrow 2 \rightarrow 1$, in a close analogy to the first bifurcation at ϕ^* . We can formally study the successive bifurcations at ϕ^{**} and ϕ^{***} if we assume a specific model. See, e.g., Ikeda et al. (2012b); Akamatsu et al. (2012); Osawa et al. (2017). At the higher extreme of ϕ , agents concentrate in a single region. This behavior can be understood as a gradual extension of the market area of each agglomeration. See also Ikeda et al. (2012b) for thorough numerical simulations for the Krugman (1991) model in a racetrack economy with various number of regions.

C.2 Class II model

Figure C.2 considers a Class II model by Allen and Arkolakis (2014) (Appendix D.2.4). The model incorporates a local dispersion force but no global dispersion force. The uniform equilibrium \bar{x} is stable

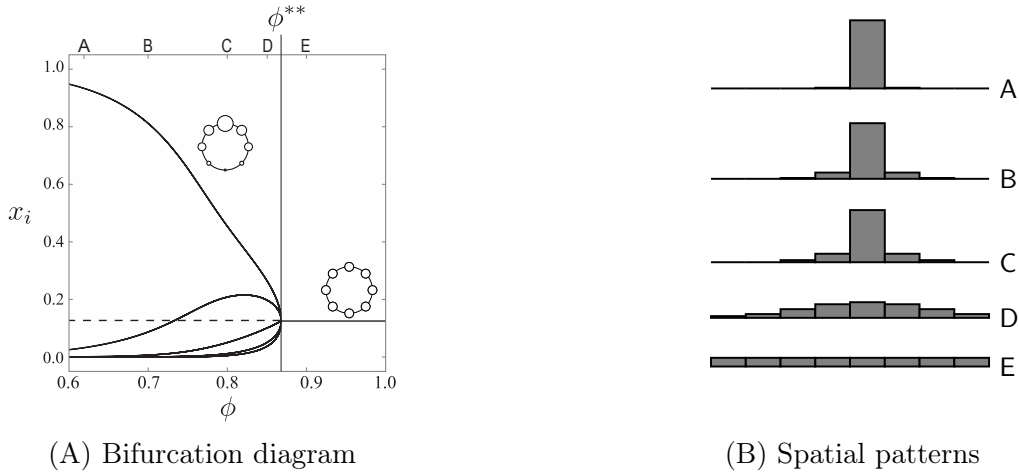


Figure C.2: Class II model (Allen and Arkolakis, 2014)

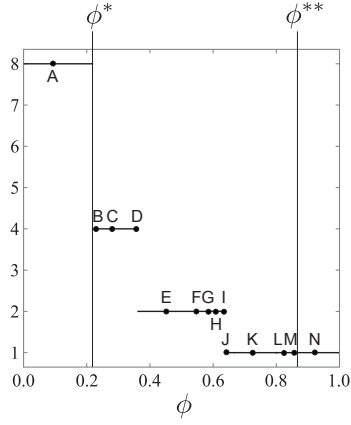
when transport costs are low (when ϕ is close to 1). If we start from \bar{x} and consider the process of a monotonic *decrease* in ϕ from $\phi \approx 1$, then a unimodal pattern emerges due to the bifurcation at ϕ^{**} . This is *the* bifurcation in the model. When ϕ decreases further, the spatial pattern smoothly converges to a full concentration in a single region in the lower extreme ($\phi \approx 0$). The local dispersion force is less important than the benefits of agglomeration when interregional transportation is prohibitively costly. Mobile agents prefer concentrating on a smaller number of regions because of the agglomeration forces. As ϕ increases, agglomeration force due to costly transportation diminishes, and the *relative* rise in the local dispersion force induces a crowding-out from the populated region to the adjacent regions. As a result, the spatial pattern gradually flattens and connects to \bar{x} at ϕ^{**} . We can interpret the region at the mode of population distribution (region i such that $x_i > x_{i-1}$ and $x_i > x_{i+1}$ where mod N for indices) as the location of an agglomeration. Then, this model endogenously produces at most one agglomeration.

C.3 Class III model

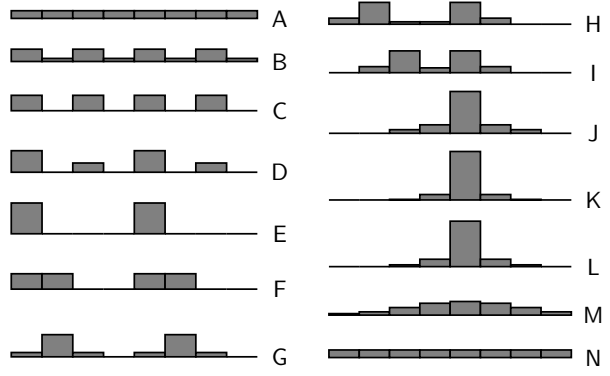
With both local and global dispersion forces, Class III models exhibit a realistic interplay between the number of agglomerations, spacing between them (as in Class I models), and the spatial extent of each agglomeration (as in Class II models).

Figure C.3A shows the evolution of the number of agglomerations in the course of increasing ϕ under the Pflüger and Südekum (2008)'s model (Appendix D.2.3). The number of agglomerations in a spatial distribution is defined by that of the local maxima therein. Figure C.3A exhibits the mixed characteristics of Figures C.1 and C.2, as expected. When $\phi < \phi^*$ or $\phi > \phi^{**}$, \bar{x} is stable. We interpret the number of agglomerations in \bar{x} as either 8 (for a low ϕ) or 1 (for a high ϕ) to acknowledge that \bar{x} at the low and high levels of ϕ are distinct. When ϕ gradually increases from $\phi \approx 0$, the number of agglomerations reduces from $8 \rightarrow 4 \rightarrow 2 \rightarrow 1$ as in the Class I models (Figure C.1), whereas it is always 1 in the latter stage as per the Class II models (Figure C.2). The initial stage is governed by a decline in the global dispersion force, while the later stage is marked by a relative rise of the local dispersion force.

Figure C.3B illustrates the spatial patterns associated with Figure C.3A. Uniform pattern \bar{x} is initially stable (Pattern A) and the first bifurcation at ϕ^* leads to a quad-modal agglomeration (B, C), whereas the second bifurcation to the formation of a bimodal agglomeration (D, E). These transitions are in line with Figure C.1 and are governed by the gradual decline in the global dispersion force. A further decline in the global dispersion force increases the relative importance of the local dispersion force. As a result, the



(A) Number of agglomerations



(B) Spatial patterns

Figure C.3: Class III model (Pfüger and Südekum, 2008)

bimodal agglomeration flattens out gradually (F, G). When ϕ increases further, it reduces to a unimodal agglomeration (J, K). The unimodal agglomeration flattens out as ϕ increases (L, M) until it converges to the complete dispersion (N) at ϕ^{**} . See also Appendix E.

In our framework, the payoff function is homogeneous across mobile agents. The effects of introducing idiosyncratic payoff shocks are of interest as it is a standard recipe in quantitative models (Redding and Rossi-Hansberg, 2017). The idiosyncratic payoff shocks should act as some dispersion force without connection to the underlying geography. In fact, such idiosyncratic heterogeneity is isomorphic to a *local dispersion force*. For example, for additive random utility models, the idiosyncratic payoff is defined by $\hat{v}_{ni}(\mathbf{x}) = \tilde{v}_i(\mathbf{x}) + \epsilon_{ni}$ where $\tilde{v}_i(\mathbf{x})$ is the homogeneous payoff for choosing region i and ϵ_{ni} is random shock drawn for each agent n in region i . A spatial equilibrium is defined by $x_i = P_i(\mathbf{x})$, where $P_i(\mathbf{x}) \equiv \Pr(i \in \arg \max_{j \in \mathcal{N}} \hat{v}_{nj}(\mathbf{x})) \in (0, 1)$ is the probability for an agent to choose region i when the current state is \mathbf{x} . Random utility models have deterministic interpretations (Anderson et al., 1992) in the sense that there is a deterministic (homogeneous) payoff function $\mathbf{v}(\mathbf{x}) = (v_i(\mathbf{x}))_{i \in \mathcal{N}}$, associated with the stochastic (heterogeneous) payoffs $(\hat{v}_{ni}(\mathbf{x}))$, such that \mathbf{x}^* is a deterministic spatial equilibrium under \mathbf{v} if and only if $x_i^* = P_i(\mathbf{x}^*)$. Thus, the two equilibrium concepts are isomorphic in terms of the equilibrium spatial distribution of agents (Behrens and Murata, 2021). For additive random utility models, Hofbauer and Sandholm (2007) demonstrates that the deterministic payoff is represented as $\mathbf{v}(\mathbf{x}) = \tilde{\mathbf{v}}(\mathbf{x}) - \nabla H(\mathbf{x})$, where H is a scalar-valued function. When ϵ_{ni} is Gumbel-distributed, $H(\mathbf{x}) = \eta \sum_{i \in \mathcal{N}} x_i \log x_i$, where η is a constant. Thus, $v_i(\mathbf{x}) = \tilde{v}_i(\mathbf{x}) - \eta \log x_i - \eta$, implying $\mathbf{V} \propto \tilde{\mathbf{V}} - \eta \mathbf{I}$, where \mathbf{V} and $\tilde{\mathbf{V}}$ are, respectively, the elasticity matrix for \mathbf{v} and $\tilde{\mathbf{v}}$ at $\bar{\mathbf{x}}$. In the context of Section 2.3, introducing payoff shocks is equivalent to adding a negative constant term (local dispersion force). As such, introducing payoff shocks to a Class I model changes the model to Class III.

D Derivations for examples

This section collects derivations for G and G^\sharp for the discussed examples. Below, $\mathbf{F}_x = [\frac{\partial f_i}{\partial x_j}]$ is the Jacobian matrix of a vector-valued function $\mathbf{f}(\mathbf{x})$ with respect to \mathbf{x} evaluated at $\bar{\mathbf{x}}$, unless otherwise noted. For example, $\mathbf{V}_x \equiv [\frac{\partial v_i}{\partial x_j}]$, $\tilde{\mathbf{V}}_w \equiv [\frac{\partial \tilde{v}_i}{\partial w_j}]$, and $\mathbf{W}_x \equiv [\frac{\partial w_i}{\partial x_j}]$. Throughout, \bar{v} , \bar{w} , \bar{e} and so on represent v_i , w_i , e_i evaluated at $\bar{\mathbf{x}}$ unless otherwise noted. \mathbf{D} denotes the row-normalized proximity matrix.

D.1 General derivations

D.1.1 The payoff elasticity matrix with respect to agents' distribution

The payoff functions for the models we referenced in the main text reduce to the following form:

$$\mathbf{v}(\mathbf{x}) = \tilde{\mathbf{v}}(\mathbf{x}, \mathbf{w}), \quad (\text{D.1})$$

$$\mathbf{s}(\mathbf{x}, \mathbf{w}) = \mathbf{0}. \quad (\text{D.2})$$

The condition (D.2) represents, for example, the market equilibrium conditions for a given \mathbf{x} that defines endogenous variable \mathbf{w} other than \mathbf{x} as an implicit function of \mathbf{x} . For $\mathbf{v}(\mathbf{x})$ to be well-defined, (D.2) must admit a unique solution of \mathbf{w} for all $\mathbf{x} \in \mathcal{X}$. We assume this throughout the analysis. Suppose \mathbf{s} and \mathbf{v} are continuously differentiable. Then, we have

$$\mathbf{V}_x(\mathbf{x}) = \tilde{\mathbf{V}}_x(\mathbf{x}) + \tilde{\mathbf{V}}_w(\mathbf{x})\mathbf{W}_x(\mathbf{x}), \quad (\text{D.3})$$

$$\mathbf{W}_x(\mathbf{x}) = -\mathbf{S}_w(\mathbf{x})^{-1}\mathbf{S}_x(\mathbf{x}), \quad (\text{D.4})$$

where $\mathbf{W}_x(\mathbf{x})$ is obtained by the implicit function theorem regarding (D.2).

Under Assumptions RE and S, if $\mathbf{x} = \bar{\mathbf{x}}$, $\mathbf{V}_x = \mathbf{S}_w^{-1}(\mathbf{S}_w \tilde{\mathbf{V}}_x - \tilde{\mathbf{V}}_w \mathbf{S}_x)$, since all matrices commute (they are real, symmetric, and circulant at $\bar{\mathbf{x}}$). In the Krugman and Helpman models, $G^\flat(\mathbf{D})$ arises from \mathbf{S}_w and represents general equilibrium effects through (D.2). For any model whose payoff function reduces to the equations of the form (D.1) and (D.2), $\mathbf{V} = G^\flat(\mathbf{D})^{-1}G^\sharp(\mathbf{D})$ where polynomials $G^\sharp(\cdot)$ and $G^\flat(\cdot)$ are such that $G^\sharp(\mathbf{D}) = \mathbf{S}_w \tilde{\mathbf{V}}_x - \tilde{\mathbf{V}}_w \mathbf{S}_x$ and $G^\flat(\mathbf{D}) = \mathbf{S}_w$.

Example D.1. For the Krugman model and Redding–Sturm model, (D.2) is given by

$$s_i(\mathbf{x}, \mathbf{w}) = w_i x_i - \sum_{j \in \mathcal{N}} m_{ij} e_j = 0, \quad (\text{D.5})$$

where $e_i = e(w_i, x_i)$ with some nonnegative function e and $\mathbf{M} = \mathbf{M}(\mathbf{x}) = [m_{ij}]$ is

$$m_{ij} = \frac{x_i w_i^{1-\sigma} \phi_{ij}}{\sum_{k \in \mathcal{N}} x_k w_k^{1-\sigma} \phi_{kj}}. \quad (\text{D.6})$$

In matrix form, we may write (D.5) as $\mathbf{y} - \mathbf{M}\mathbf{e} = \mathbf{0}$ where $\mathbf{y} = (w_i x_i)_{i \in \mathcal{N}}$. It gives

$$\mathbf{S}_x(\mathbf{x}) = \text{diag}[\mathbf{w}] - \left(\text{diag}[\mathbf{M}\mathbf{e}] - \mathbf{M} \text{diag}[\mathbf{e}]\mathbf{M}^\top \right) \text{diag}[\mathbf{x}]^{-1} - \mathbf{M}\mathbf{E}_x, \quad (\text{D.7a})$$

$$\mathbf{S}_w(\mathbf{x}) = \text{diag}[\mathbf{x}] + (\sigma - 1) \left(\text{diag}[\mathbf{M}\mathbf{e}] - \mathbf{M} \text{diag}[\mathbf{e}]\mathbf{M}^\top \right) \text{diag}[\mathbf{w}]^{-1} - \mathbf{M}\mathbf{E}_w. \quad (\text{D.7b})$$

Suppose Assumptions RE and S. Suppose $\mathbf{x} = \bar{\mathbf{x}}$ and let \bar{w} be the uniform level of $\{w_i\}$ at $\bar{\mathbf{x}}$. We have $\mathbf{M} = \mathbf{D}$ at $\mathbf{x} = \bar{\mathbf{x}}$. Suppose the scalars ϵ_x and ϵ_w are chosen to satisfy $\mathbf{E}_x = \epsilon_x \bar{w} \mathbf{I}$ and $\mathbf{E}_w = \epsilon_w \bar{\mathbf{x}} \mathbf{I}$

at $\bar{\mathbf{x}}$. Let $\bar{e} = e(\bar{w}, \bar{x})$ and $\zeta \equiv \frac{\bar{e}}{\bar{w}\bar{x}}$. We see that

$$\mathbf{S}_x = -\bar{w} \left((\zeta - 1)\mathbf{I} + \epsilon_x \mathbf{D} - \zeta \mathbf{D}^2 \right), \quad (\text{D.8a})$$

$$\mathbf{S}_w = \bar{x} \left((1 + \zeta(\sigma - 1))\mathbf{I} - \epsilon_w \mathbf{D} - \zeta(\sigma - 1)\mathbf{D}^2 \right). \quad (\text{D.8b})$$

If $e(w_i, x_i) = w_i x_i$, then $\epsilon_x = \epsilon_w = 1$ and $\zeta = 1$, thereby $\mathbf{W}_x = \frac{\bar{w}}{\bar{x}}(\sigma \mathbf{I} + (\sigma - 1)\mathbf{D})^{-1}\mathbf{D}$. \blacksquare

D.1.2 The payoff elasticity matrix with respect to local characteristics

In (A.15), $\mathbf{X} = \left[\frac{\partial x_i(\bar{\mathbf{a}})}{\partial a_i} \right] = \mathbf{X}_a$ acts as $\hat{\mathbf{X}} \equiv -\mathbf{V}_x^{-1}\mathbf{V}_a$ for \mathbf{z} such that $\mathbf{z}^\top \mathbf{1} = \mathbf{0}$. Thus, \mathbf{V}_a is of interest.

For purely local characteristics (Example A.4), since $v_i(\mathbf{x}, \mathbf{a}) = a_i v_i(\mathbf{x})$, it follows that $\mathbf{V}_a = \text{diag}[\mathbf{v}(\mathbf{x})]$. At $\bar{\mathbf{x}}$, we have $\mathbf{V}_a = \bar{v}\mathbf{I}$. Thus, $\hat{\mathbf{X}} = -\bar{v}\mathbf{V}_x^{-1}$.

For regional characteristics that affect trade flows, the payoff function and the market equilibrium condition are, respectively, modified to $\mathbf{v}(\mathbf{x}, \mathbf{a}) = \tilde{\mathbf{v}}(\mathbf{x}, \mathbf{w}, \mathbf{a})$ and $\mathbf{s}(\mathbf{x}, \mathbf{w}, \mathbf{a}) = \mathbf{0}$. By applying the implicit function theorem, we see $\mathbf{V}_a = \tilde{\mathbf{V}}_x + \tilde{\mathbf{V}}_w \mathbf{W}_a = \tilde{\mathbf{V}}_x - \tilde{\mathbf{V}}_w \mathbf{S}_w^{-1} \mathbf{S}_a$. As all matrices commute at $\bar{\mathbf{x}}$ under Assumptions RE and S, it is equivalent to consider

$$\hat{\mathbf{X}} = - \left(\tilde{\mathbf{V}}_x - \tilde{\mathbf{V}}_w \mathbf{S}_w^{-1} \mathbf{S}_x \right)^{-1} \left(\tilde{\mathbf{V}}_a - \tilde{\mathbf{V}}_w \mathbf{S}_w^{-1} \mathbf{S}_a \right) \quad (\text{D.9})$$

$$= \left(\mathbf{S}_w \tilde{\mathbf{V}}_x - \tilde{\mathbf{V}}_w \mathbf{S}_x \right)^{-1} \left(\tilde{\mathbf{V}}_w \mathbf{S}_a - \mathbf{S}_w \tilde{\mathbf{V}}_a \right). \quad (\text{D.10})$$

Example D.2. For the regional model by Redding and Rossi-Hansberg (2017), we have

$$s_i(\mathbf{x}, \mathbf{w}, \mathbf{a}) = w_i x_i - \sum_{j \in \mathcal{N}} \frac{x_i a_i w_i^{1-\sigma} \phi_{ij}}{\sum_{k \in \mathcal{N}} x_k a_k w_k^{1-\sigma} \phi_{kj}} e_j = 0. \quad (\text{D.11})$$

So, $\mathbf{S}_a = -(\text{diag}[\mathbf{M}\mathbf{e}] - \mathbf{M} \text{diag}[\mathbf{e}]\mathbf{M}^\top) \text{diag}[\mathbf{a}]^{-1} = -\frac{\bar{e}}{\bar{a}}(\mathbf{I} - \mathbf{D}^2)$. See Appendix D.2.2. \blacksquare

Example D.3. For the Krugman model, we have

$$s_i(\mathbf{x}, \mathbf{w}, \mathbf{a}) = w_i x_i - \sum_{j \in \mathcal{N}} \frac{x_i w_i^{1-\sigma} \phi_{ij}}{\sum_{k \in \mathcal{N}} x_k w_k^{1-\sigma} \phi_{kj}} e(w_j, x_j, a_j) = 0 \quad (\text{D.12})$$

where e maps the tuple (w_j, x_j, a_j) to the regional expenditure. Then, we have $\mathbf{S}_a = -\mathbf{M}\mathbf{E}_a$, or $\mathbf{S}_a = -\epsilon_a \mathbf{D}$ at $\bar{\mathbf{x}}$ where $\epsilon_a = \frac{\partial e(\bar{x}, \bar{w}, \bar{a})}{\partial a_i}$. See Appendix D.2.1. \blacksquare

D.2 Model-specific derivations

We provide omitted derivations of the gain functions G for the main examples. See Akamatsu et al. (2017) for derivations for other models mentioned in Section 3.4.

D.2.1 Krugman (1991) model

There are two types of workers, mobile and immobile, and their total masses are 1 and L , respectively. $\mathbf{x} \equiv (x_i)_{i \in \mathcal{N}}$ is the distribution of mobile workers. Each worker supplies one unit of labor inelastically.

There are two industrial sectors: agriculture (abbreviated as A) and manufacturing (abbreviated as M). The A-sector is perfectly competitive and a unit input of immobile labor is required to produce one unit of goods. The M-sector follows Dixit–Stiglitz monopolistic competition. M-sector goods are

horizontally differentiated and produced under increasing returns to scale using mobile labor as the input. The goods of both sectors are transported. Transportation of A-sector goods is frictionless, while that of M-sector goods is of an iceberg form. For each unit of M-sector goods transported from region i to j , only the proportion $1/\tau_{ij}$ arrives, where $\tau_{ij} > 1$ for $i \neq j$ and $\tau_{ii} = 1$.

All workers have an identical preference for both M- and A-sector goods. The utility of a worker in region i is given by a two-tier form. The upper tier is Cobb–Douglas over the consumption of A-sector goods C_i^A and that of M-sector constant-elasticity-of-substitution (CES) aggregate C_i^M with $\sigma > 1$

$$C_i^M \equiv \left(\sum_{j \in \mathcal{N}} \int_0^{n_j} q_{ji}(\xi)^{\frac{\sigma-1}{\sigma}} d\xi \right)^{\frac{\sigma}{\sigma-1}}, \quad (\text{D.13})$$

that is, $u_i = (C_i^A)^\mu (C_i^M)^{1-\mu}$ where $\mu \in (0, 1)$ is the constant expenditure of the latter. With free trade in the A-sector, the wage of the immobile worker is equalized, and we normalize it to unity by taking A-sector goods as the numéraire. Consequently, region i 's expenditure on the M-sector goods is given by $e_i = \mu(w_i x_i + l_i)$ where l_i denotes the mass of immobile workers in region i .

In the M-sector, to produce q units, a firm requires $\alpha + \beta q$ units of mobile labor. Profit maximization of firms yields the price of differentiated goods produced in region i and exported to j as $p_{ij} = \frac{\sigma\beta}{\sigma-1} w_i \tau_{ij}$, which in turn determines gravity trade flow from j to i . That is, when X_{ij} denotes the price of M-sector goods produced in region i and sold in region j , $X_{ij} = m_{ij} e_j$ where the share $m_{ij} \in (0, 1)$ is defined by (D.6) with $\phi_{ij} \equiv \tau_{ij}^{1-\sigma}$. The proximity matrix is thus $[\phi_{ij}] = [\tau_{ij}^{1-\sigma}]$.

Given \mathbf{x} , we determine the market wage $\mathbf{w} \equiv (w_i)_{i \in \mathcal{N}}$ by the M-sector product market-clearing, zero-profit, and mobile labor market-clearing conditions. These conditions are summarized by the trade balance $w_i x_i = \sum_{j \in \mathcal{N}} X_{ij}$, or (D.5) with $e(x_i, w_i) = \mu(w_i x_i + l_i)$. By adding up (D.5) for the Krugman model, we see $\sum_{i \in \mathcal{N}} w_i x_i = \frac{\mu}{1-\mu} L$, which constrains the total income of mobile workers at any configuration \mathbf{x} . The existence and uniqueness of the solution for (D.5) follow from standard arguments (e.g., [Facchinei and Pang, 2007](#)). Given the solution $\mathbf{w}(\mathbf{x})$ of (D.5), we have the indirect utility of mobile workers, which is given by $v_i = \Delta_i^{\frac{\mu}{\sigma-1}} w_i$, where $\Delta_i \equiv \sum_{k \in \mathcal{N}} x_k w_k^{1-\sigma} d_{ki}$.

To satisfy Assumption S, let $l_i = l \equiv \frac{L}{N}$ for all $i \in \mathcal{N}$. We have

$$\nabla \log \mathbf{v}(\bar{\mathbf{x}}) = \frac{\mu}{\sigma-1} \mathbf{M}^\top \text{diag}[\mathbf{x}]^{-1} - \mu \mathbf{M}^\top \text{diag}[\mathbf{w}]^{-1} \mathbf{W}_x + \text{diag}[\mathbf{w}]^{-1} \mathbf{W}_x \quad (\text{D.14})$$

$$= \frac{1}{\bar{x}} \frac{\mu}{\sigma-1} \mathbf{D} + \frac{1}{\bar{w}} (\mathbf{I} - \mu \mathbf{D}) \mathbf{W}_x, \quad (\text{D.15})$$

where (D.4) and (D.8) give \mathbf{W}_x . By plugging $\delta = \frac{\mu(\bar{w}\bar{x}+l)}{\bar{w}\bar{x}} = 1$ and $\epsilon_x = \epsilon_w = \mu$ to (D.8),

$$\mathbf{W}_x = \frac{\bar{w}}{\bar{x}} (\sigma \mathbf{I} - \mu \mathbf{D} - (\sigma-1) \mathbf{D}^2)^{-1} (\mu \mathbf{D} - \mathbf{D}^2). \quad (\text{D.16})$$

Then, (D.15) and (D.16) imply

$$\mathbf{V} = \bar{x} \nabla \log \mathbf{v}(\bar{\mathbf{x}}) = \frac{\mu}{\sigma-1} \mathbf{D} + (\mathbf{I} - \mu \mathbf{D}) (\sigma \mathbf{I} - \mu \mathbf{D} - (\sigma-1) \mathbf{D}^2)^{-1} (\mu \mathbf{D} - \mathbf{D}^2), \quad (\text{D.17})$$

or equivalently, $\mathbf{V} = G(\mathbf{D})$ where

$$G(\chi) = \underbrace{\frac{\mu}{\sigma-1} \chi}_{(a)} + \underbrace{(1 - \mu \chi)}_{(b)} \underbrace{\left(\frac{1}{\sigma} \right) \frac{\mu \chi - \chi^2}{1 - \frac{\mu}{\sigma} \chi - \frac{\sigma-1}{\sigma} \chi^2}}_{(c)}. \quad (\text{D.18})$$

From (D.18) we have $\mathbf{V} = G^b(\mathbf{D})^{-1}G^\sharp(\mathbf{D})$, where we define

$$G^\sharp(\chi) \equiv \mu \left(\frac{1}{\sigma-1} + \frac{1}{\sigma} \right) \chi - \left(\frac{\mu^2}{\sigma-1} + \frac{1}{\sigma} \right) \chi^2, \quad (\text{D.19})$$

$$G^b(\chi) \equiv 1 - \frac{\mu}{\sigma} \chi - \frac{\sigma-1}{\sigma} \chi^2. \quad (\text{D.20})$$

Remark D.1. Using the Krugman model as an example, we discuss how economic forces in a model are embedded in G and G^\sharp . We recall that positive (negative) terms in G represent agglomeration (dispersion) forces. In (D.18), (a) corresponds to the elasticity of price index with respect to agents' spatial distribution \mathbf{x} , (b) to the elasticity of payoff with respect to nominal wage \mathbf{w} , (c) to the elasticity of wage with respect to agents' spatial distribution. Here, (a) and the second term in (b) corresponds to the so-called cost-of-living effect through price index; (a) is positive, i.e., it is an agglomeration force, as the price index in a region becomes lower when more agents (firms) locate geographically close regions; the second term in (b) (i.e., $-\mu\chi$) is negative because higher wage in a region implies higher goods prices in its nearby regions. Also, (b) as a whole is positive, meaning that the payoff of a region is increasing in wages even with the negative effect through price index. The last component (c) includes both positive and negative terms; in its numerator, the first term ($\mu\chi$) is demand linkage where firms' profits rise when they are close to regions with high total income, and the second term ($-\chi^2$) is the market-crowding effect due to competition between firms. The sign of (c) is χ -dependent; for example, it is negative when χ is high (ϕ is low) and positive otherwise. The denominator of (c) represents the general equilibrium effects through the so-called short-run equilibrium condition under given \mathbf{x} , i.e., (D.5). As G^\sharp is obtained by combining these components and collecting terms according to the order of χ , these economic forces affect both the first- and second-order coefficients of G^\sharp . Concretely, in (D.19), $\frac{\mu}{\sigma-1}\chi$ comes from (a), $\frac{\mu}{\sigma}\chi$ comes from (b) \times (c), $-\frac{1}{\sigma}\chi^2$ comes from (b) \times (c), and $-\frac{\mu^2}{\sigma-1}\chi^2 = -\left(\frac{\mu^2}{\sigma} + \frac{\mu^2}{\sigma(\sigma-1)}\right)\chi^2$ comes from all three components while its leading term $-\frac{\mu^2}{\sigma}\chi^2$ comes from (b) \times (c). Thus, by considering G^\sharp for a model, one can examine the net effect of *all* economic forces in the model at once, and the net effect is decomposed according to its spatial scale (i.e., the order of χ). ■

Remark D.2. In Figure C.1, we set $\mu = 0.5$, $\sigma = 10$, and $L = 8$. ■

Remark D.3. To obtain G^\sharp for $\mathbf{l} = (l_i)_{i \in \mathcal{N}}$, we evaluate $\mathbf{V}_l = -\tilde{\mathbf{V}}_w \mathbf{S}_w^{-1} \mathbf{S}_l$ as $\mathbf{A} = \frac{l}{\bar{v}} \mathbf{V}_l$. From Example D.3, $\mathbf{S}_l = -\mu \mathbf{D}$. Also, $\tilde{\mathbf{V}}_w = \bar{v} \frac{\partial}{\partial \mathbf{w}} \log \mathbf{v}(\bar{\mathbf{x}}) = \frac{\bar{v}}{\bar{w}} (\mathbf{I} - \mu \mathbf{D})$ and $\tilde{\mathbf{V}}_l = \mathbf{0}$. Thus,

$$G^\sharp(\chi) = c \frac{\chi(1-\mu\chi)}{G^b(\chi)} > 0 \quad (\text{D.21})$$

where $c = \frac{l}{\bar{w}} \frac{\mu}{\sigma} = \frac{1-\mu}{\sigma} \bar{x} > 0$. It then follows that

$$\delta(\chi) = -\frac{\bar{x}}{\bar{a}} \frac{G^\sharp(\chi)}{G(\chi)} = -\frac{c\bar{x}}{\bar{a}} \frac{\chi(1-\mu\chi)}{G^\sharp(\chi)}. \quad (\text{D.22})$$

Straightforward algebra verifies that $\delta'(\chi) < 0$ if $G^\sharp(\chi) > 0$. ■

D.2.2 Helpman (1998) and Redding and Sturm (2008) model

Helpman (1998) removed the A-sector in the Krugman model and assumed that all workers are mobile. Instead of the A-sector, the model introduces the housing (abbreviated as H) sector. Each region i is endowed with a fixed stock a_i of housing. Workers' preference is Cobb–Douglas of M-sector CES aggregate

C_i^M and H-sector goods C_i^H , $u_i = (C_i^M)^\mu (C_i^H)^\gamma$, where $\mu \in (0, 1)$ is the expenditure share of the former and $\gamma = 1 - \mu \in (0, 1)$ is that for the latter. There are two variants for assumptions on how housing stocks are owned: *public landownership* (abbreviated as PL) and *local landownership* (LL). The original formulation by Helpman (1998) supposes housing stocks are equally owned by all workers (i.e., PL). The income of a worker in region i is the sum of the wage and an equal dividend $r > 0$ of rental revenue *over the economy*. However, Ottaviano et al. (2002), Murata and Thisse (2005), and Redding and Sturm (2008) assumed that housing stocks are locally owned (i.e., LL). The income of a worker in region i is the sum of the wage and an equal dividend of rental revenue *in each region*. In fact, the model by Redding and Sturm (2008) is the LL version of the Helpman model.

Regarding the market equilibrium conditions, the only difference from the Krugman model is regional expenditure e_i on M-sector goods in each region:

$$[\text{PL}] \quad e_i = \mu (w_i + r) x_i, \quad (\text{D.23})$$

$$[\text{LL}] \quad e_i = w_i x_i. \quad (\text{D.24})$$

Also, the market wage is given as the solution for (D.5). For the PL case, we set $r = 1$ for normalization. For the LL case, $w(\mathbf{x})$ is uniquely given up to normalization. The indirect utility function is, with $\Delta_i \equiv \sum_{j \in \mathcal{N}} x_j w_j^{1-\sigma} \phi_{ji}$ and $r > 0$,

$$[\text{PL}] \quad v_i = \left(\frac{x_i}{a_i} \right)^{-\gamma} (w_i + r)^\mu \Delta_i^{\frac{\mu}{\sigma-1}}, \quad (\text{D.25})$$

$$[\text{LL}] \quad v_i = \left(\frac{x_i}{a_i} \right)^{-\gamma} w_i^\mu \Delta_i^{\frac{\mu}{\sigma-1}}. \quad (\text{D.26})$$

Let $a_i = 1$ to satisfy Assumption S. We compute that

$$\mathbf{V} = \bar{x} \left(\frac{\mu}{\sigma-1} \mathbf{M}^\top \text{diag}[\mathbf{x}]^{-1} + \hat{\mathbf{V}}_w \mathbf{W}_x - \gamma \text{diag}[\mathbf{x}]^{-1} \right), \quad (\text{D.27})$$

$$\text{where } [\text{PL}] \quad \hat{\mathbf{V}}_w \equiv \mu \left(\text{diag}[\mathbf{w} + r\mathbf{1}]^{-1} - \mathbf{M}^\top \text{diag}[\mathbf{w}]^{-1} \right), \quad (\text{D.28})$$

$$[\text{LL}] \quad \hat{\mathbf{V}}_w \equiv \mu \left(\mathbf{I} - \mathbf{M}^\top \right) \text{diag}[\mathbf{w}]^{-1}, \quad (\text{D.29})$$

and \mathbf{M} is defined by (D.6). For the PL case, we obtain $\mathbf{V} = G(\mathbf{D})$ with

$$G(\chi) = -\gamma + \frac{\mu}{\sigma-1} \chi + \frac{\mu(\mu-\chi)\chi(1-\chi)}{\sigma-\mu\chi-(\sigma-1)\chi^2} \quad (\text{D.30})$$

where we compute \mathbf{W}_x from (D.7) with $\zeta = \frac{\mu(\bar{w}+1)}{\bar{w}}$, $\epsilon_x = \frac{\bar{w}+1}{\bar{w}}$, $\epsilon_w = \mu$; we note that $\frac{\bar{w}}{\bar{w}+1} = \mu$ under our normalization. Thus, for the PL case, we can choose G^\sharp and G^\flat that satisfy $\mathbf{V} = G^\flat(\mathbf{D})^{-1} G^\sharp(\mathbf{D})$ as follows:

$$G^\sharp(\chi) \equiv -\gamma + \left(\frac{\mu}{\sigma-1} + \frac{\mu(\mu+\gamma)}{\sigma} \right) \chi - \left(\frac{\mu^2}{\sigma-1} + \frac{\mu+\gamma}{\sigma} - \gamma \right) \chi^2, \quad (\text{D.31})$$

$$G^\flat(\chi) \equiv 1 - \frac{\mu}{\sigma} \chi - \frac{\sigma-1}{\sigma} \chi^2 \quad (\text{D.32})$$

where we recall $\mu + \gamma = 1$.

Remark D.4. As in the Krugman model (Remark D.1), one can identify the correspondence between the coefficients in G (D.31) and those in G^\sharp (D.30). For example, local dispersion force $-\gamma$ in (D.30)

affects not only constant term in $G^\sharp(\cdot)$ but also the first- and the second-order terms of χ . Other forces can be understood similarly to the Krugman model (Remark D.1). ■

For the LL case, \mathbf{W}_x is given in Example D.1 and we obtain

$$G(\chi) = -\gamma + \frac{\mu}{\sigma-1}\chi + \frac{\mu(1-\chi)\chi}{\sigma+(\sigma-1)\chi}. \quad (\text{D.33})$$

We can choose G^\sharp and G^b as follows:

$$G^\sharp(\chi) \equiv -\gamma + \left(\frac{\mu}{\sigma-1} + \frac{\mu+\gamma}{\sigma} - \gamma \right) \chi, \quad (\text{D.34})$$

$$G^b(\chi) \equiv 1 + \frac{\sigma-1}{\sigma}\chi. \quad (\text{D.35})$$

Remark D.5. Definition 2 (and Table 1) classifies canonical models based on the spatial scale of the “effective” dispersion forces. The Helpman model with public landownership (D.31) has global dispersion forces because $c_2 < 0$ under Assumption E. However, unlike the Krugman model, the global dispersion forces in the Helpman model are not “effective” in the sense that, under any admissible values of μ and σ , this force does not stabilize the uniform distribution for any level of transport costs. If we drop the local dispersion force $c_0 < 0$ from G^\sharp , we have $c_1\chi + c_2\chi^2 > 0$ for all χ and \bar{x} is always unstable. Thus, the only dispersion force in the Helpman model that can stabilize \bar{x} is its local dispersion force. ■

Remark D.6. Equilibrium is unique when $\gamma\sigma = (1-\mu)\sigma > 1$ (Redding and Sturm, 2008). For both PL and LL, it implies that $G^\sharp(\chi) < 0$ for all $\chi \in (0, 1)$. ■

Remark D.7. The regional model in §3 of Redding and Rossi-Hansberg (2017) is a variant of the Helpman model with LL, in which variable input of mobile labor depends on region i (i.e., productivity differs across regions). The cost function of firms in region i is $C_i(q) = w_i(\alpha + \beta_i q)$. The market equilibrium condition for this case is, with $a_i \equiv \beta_i^{1-\sigma} > 0$, given by

$$s_i(\mathbf{x}, \mathbf{w}) = w_i x_i - \sum_{j \in \mathcal{N}} \frac{x_i a_i w_i^{1-\sigma} \phi_{ij}}{\sum_{k \in \mathcal{N}} x_k a_k w_k^{1-\sigma} \phi_{kj}} w_j x_j = 0. \quad (\text{D.36})$$

The payoff function is given by (D.29) with $\Delta_i = \sum_{k \in \mathcal{N}} x_k a_k w_k^{1-\sigma} \phi_{ki}$.

From Example D.2, $\mathbf{S}_a = -\frac{\bar{w}\bar{x}}{a}(\mathbf{I} - \mathbf{D})(\mathbf{I} + \mathbf{D})$ as $\bar{e} = \bar{w}\bar{x}$. Also, we have $\tilde{\mathbf{V}}_w = \frac{\bar{v}}{\bar{w}}\mu(\mathbf{I} - \mathbf{D})$, $\tilde{\mathbf{V}}_a = \frac{\bar{v}}{a}\frac{\mu}{\sigma-1}\mathbf{D}$, and $\mathbf{S}_w = \sigma\bar{x}G^b(\mathbf{D})$. As $\mathbf{V}_a = \tilde{\mathbf{V}}_a - \tilde{\mathbf{V}}_w\mathbf{S}_w^{-1}\mathbf{S}_a$ and $\mathbf{A} = \frac{\bar{a}}{\bar{v}}\mathbf{V}_a = G^\sharp(\mathbf{D})$, we compute

$$G^\sharp(\chi) = c \frac{(\sigma-1) + \sigma\chi}{G^b(\chi)} > 0 \quad (\text{D.37})$$

where $c \equiv \frac{\bar{v}}{a}\frac{\mu}{\sigma} > 0$. This in turn implies

$$\delta(\chi) = -\frac{\bar{x}}{a} \frac{G^\sharp(\chi)}{G(\chi)} = -\frac{c\bar{x}}{a} \frac{(\sigma-1) + \sigma\chi}{G^\sharp(\chi)} \quad (\text{D.38})$$

where $G^\sharp(\chi)$ is that for the LL case (D.35). We have $\delta'(\chi) > 0$ for all χ whenever $(1-\mu)\sigma > 1$. ■

D.2.3 Pflüger and Südekum (2008) model

The Pflüger–Südekum model builds on Pflüger (2004) and introduces the housing sector (again denoted by H). In this model, a quasi-linear upper-tier utility is assumed: $u_i = C_i^A + \mu \log C_i^M + \gamma \log C_i^H$. The

production cost for a firm in $i \in \mathcal{N}$ is $\alpha w_i + \beta q$. Then, \mathbf{w} is given as follows:

$$w_i = \frac{\mu}{\sigma} \sum_{j \in \mathcal{N}} \frac{\phi_{ij}}{\sum_{k \in \mathcal{N}} \phi_{kj} x_k} (x_j + l_j). \quad (\text{D.39})$$

The indirect utility of a mobile worker in region i is

$$v_i(\mathbf{x}) = \frac{\mu}{\sigma - 1} \ln[\Delta_i] - \gamma \ln \frac{x_i + l_i}{a_i} + w_i, \quad (\text{D.40})$$

where $\Delta_i = \sum_{j \in \mathcal{N}} \phi_{ji} x_j$, and l_i and a_i denote the mass of immobile workers and amount of housing stock in region i , respectively. The nominal wage in region i is given by (D.39). Let $l_i = l$ and $a_i = a$ for all i to meet Assumption S. Then, we see that $\mathbf{V} = \frac{1}{v} G^\#(\mathbf{D})$ with

$$G^\#(\chi) = -\frac{\gamma}{1+L} + \mu \left(\frac{1}{\sigma-1} + \frac{1}{\sigma} \right) \chi - \frac{\mu}{\sigma} (1+L) \chi^2. \quad (\text{D.41})$$

Remark D.8. In Figures C.3A and C.3B, $\mu = 0.4$, $\sigma = 2.5$, $L = 4$, $\gamma = 0.5$, and $a_i = 1$. ■

D.2.4 Allen and Arkolakis (2014) (AA) model

The AA model is a perfectly competitive [Armington \(1969\)](#)-based framework with positive and negative local externalities. We consider a discrete-space version of the model and abstract away all exogenous differences across regions. In the model, productivity of a location is proportional to x_i^α with $\alpha > 0$, representing positive externalities. The market equilibrium condition is

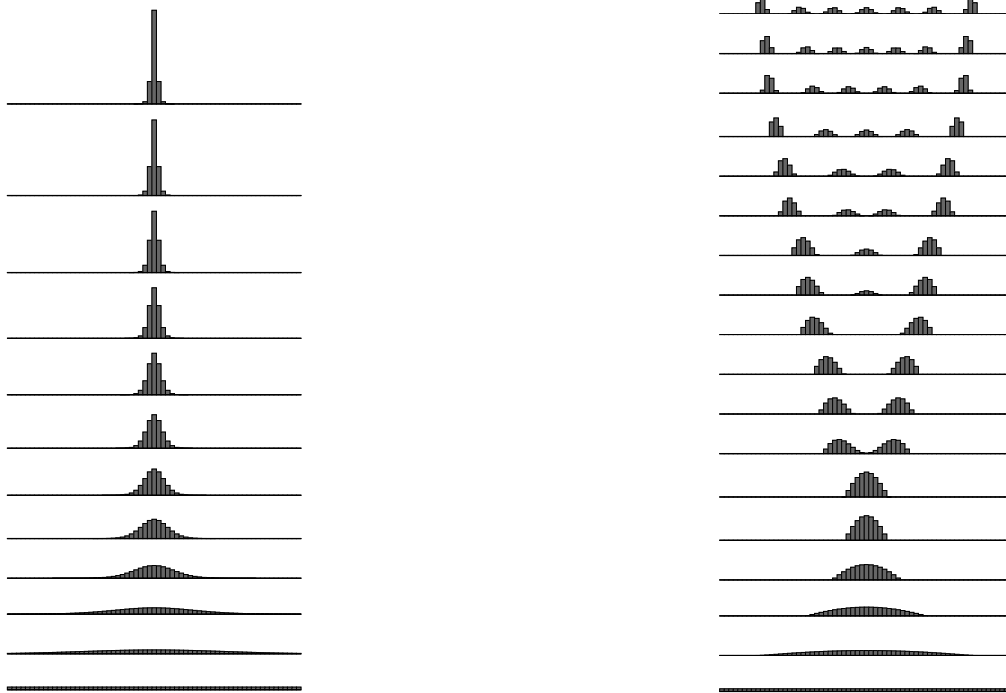
$$s_i(\mathbf{x}, \mathbf{w}) = w_i x_i - \sum_{j \in \mathcal{N}} \frac{w_i^{1-\sigma} x_i^{\alpha(\sigma-1)} \phi_{ij}}{\sum_{k \in \mathcal{N}} w_k^{1-\sigma} x_k^{\alpha(\sigma-1)} \phi_{kj}} w_j x_j = 0. \quad (\text{D.42})$$

With market wage \mathbf{w} , we have $v_i(\mathbf{x}) = x_i^\beta w_i \Delta_i^{\frac{1}{\sigma-1}}$ with $\Delta_i \equiv \sum_{k \in \mathcal{N}} w_k^{1-\sigma} x_k^{\alpha(\sigma-1)} \phi_{ki}$; x_i^β ($\beta < 0$) represents negative externalities from congestion. We have $\mathbf{V} = G^b(\mathbf{D})^{-1} G^\#(\mathbf{D})$ with

$$G^\#(\chi) = -\left(\alpha + \beta - \frac{1+\alpha}{\sigma} \right) + \left(\alpha + \beta + \frac{1-\beta}{\sigma} \right) \chi, \quad (\text{D.43})$$

$$G^b(\chi) = (\sigma + (\sigma - 1)\chi) (1 - \chi). \quad (\text{D.44})$$

Remark D.9. In Figure C.2, we set $(\alpha, \beta, \sigma) = (0.5, -0.3, 6)$. ■



(A) The Helpman model (Class II)

(B) The Pflüger-Südekum model (Class III)

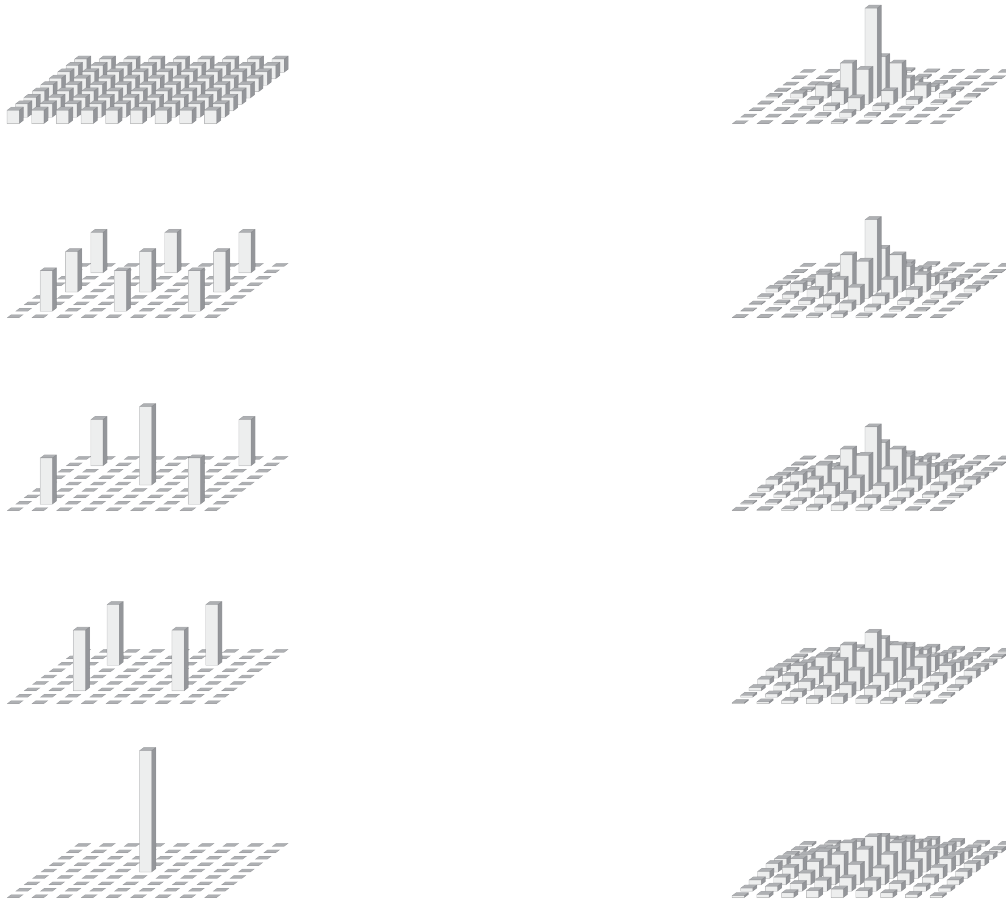
Figure E.1: Stable spatial patterns for Classes II and III in a line segment (number of regions $N = 65$). All regions share the same local parameters. The transport cost between every consecutive pair of regions is uniform. The level of transport cost monotonically decreases from top to bottom. For an extensive discussion on the behavior of a Class I model in a line segment, see Ikeda et al. (2017b).

E Geographical advantages

The implications of **Proposition 1** qualitatively generalize to different geographical setups such as one-dimensional line segment, two-dimensional spaces with and without boundaries. In particular, the spatial distribution of agents become polycentric in Class I models, whereas it becomes monocentric in Class II models, even when we relax Assumption RE.

The simplest way to introduce geographical asymmetry into our one-dimensional setup is to consider a bounded line segment, which is a standard spatial setting in urban economic theory. Ikeda et al. (2017b) considered a Class I model (Forslid and Ottaviano, 2003) in a line segment. The study showed that multiple agglomerations emerge as in the racetrack economy and demonstrated that the evolution of spatial structure in a line segment approximately follows the “period doubling” behavior discussed in Section C.1. For Class II and III, Figure E.1 reports examples of endogenous agglomeration patterns in the Helpman and Pflüger-Südekum models. For both models, qualitative properties of the spatial patterns are consistent with those discussed in Appendix C.

The real-world geography is two-dimensional. The two-dimensional counterpart of the racetrack economy is bounded lattices with periodic boundary conditions (i.e., flat torus), for which a basic theory of spatial agglomeration is provided in Ikeda and Murota (2014). For Class I models, they typically produce multiple disjointed agglomerations and period-doubling behavior as observed in the racetrack setup studied in this paper (see, e.g., Ikeda et al., 2012a, 2014, 2017a, 2018). As concrete examples, Figure E.2 shows endogenous equilibrium spatial patterns over a bounded square economy with $9 \times 9 = 81$ regions in the course of increasing ϕ for the Krugman and Allen-Arkolakis models. The parameters are



(A) The Krugman model (Class I)

(B) The Allen–Arkolakis model (Class II)

Figure E.2: Stable spatial patterns in a square economy ($N = 9^2 = 81$).

the same as Figure C.1 and Figure C.2. The Krugman model (Class I) engenders multiple disjointed agglomerations. When ϕ increases, the number of agglomerations gradually decreases while the spacing between them enlarges. For the AA model (Class II), in contrast, the spatial pattern is initially unimodal. As ϕ increases, it gradually flattens to exhibit suburbanization. All these behaviors are qualitatively consistent with **Proposition 1** and examples in Appendix C, suggesting the robustness of qualitative implications of our theoretical developments.

The implications of **Proposition 1** seem to extend to different assumptions on transport technology that are not formally covered by Assumption RE. For example, *linear* transport costs are often assumed in the literature (e.g., Mossay and Picard, 2011; Picard and Tabuchi, 2013; Blanchet et al., 2016). Mossay and Picard (2011) considered a variant of the Beckmann model (Class II) and showed that the only possible equilibrium is a unimodal distribution in a continuous line segment. Blanchet et al. (2016) considered a general Class II model over a continuous one- or two-dimensional space; they showed that the equilibrium spatial pattern for the Beckmann model is unique and given by a regular concave paraboloid, i.e., a unimodal pattern. Picard and Tabuchi (2013) also considered a Class II general equilibrium model in a two-dimensional space and showed that spatial distribution becomes unimodal. The numerical results of Anas and Kim (1996) and Anas et al. (1998) in line segments bear a close resemblance to, respectively, agglomeration behaviors of Class I and II models, although they assume endogenous transport costs between locations.

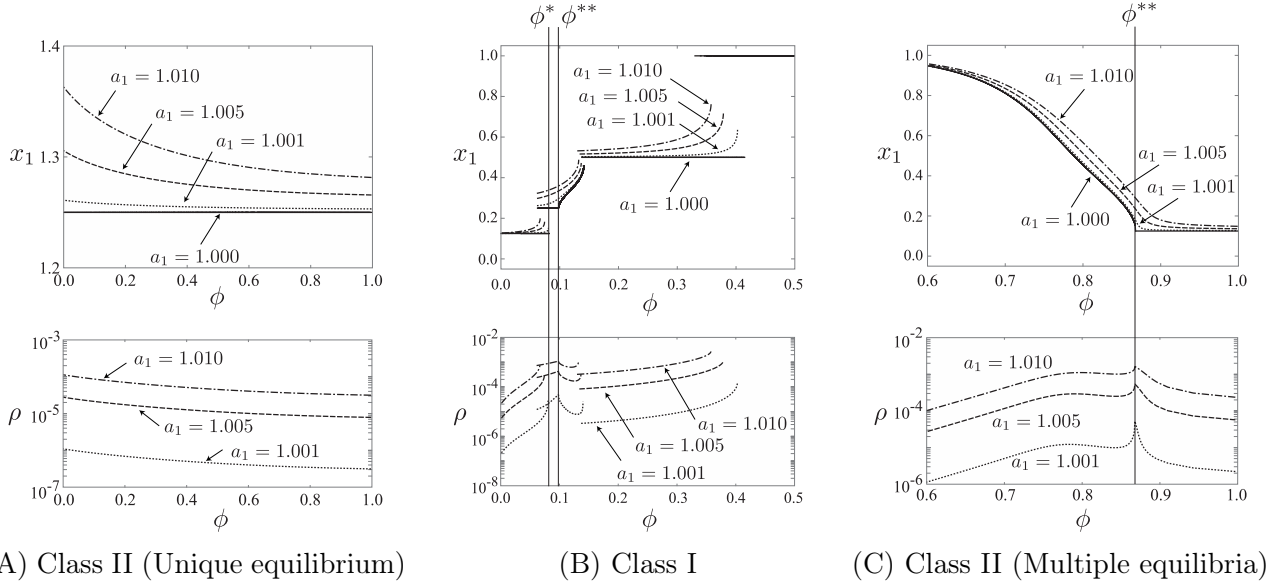


Figure F.1: Population share of the advantageous region 1 and covariance ρ

F Local advantages

F.1 The racetrack economy with an advantageous region

This section provides numerical examples for **Proposition 2** for the $N = 8$ case. As in Example A.4, we multiply the payoff in region 1 by $a_1 \geq 1$, whereas we let $a_i = 1$ for all $i \neq 1$. We consider the Krugman and Allen–Arkolakis (AA) models and basic model parameters to be the same as Figure C.1 and Figure C.2 except that region 1 has an exogenous advantage.

Figure F.1A reports the evolutionary paths of x_1 for the AA model (Class II) under the uniqueness of the equilibrium. The curves depict region 1's population share, x_1 , at stable equilibria against ϕ . Four incremental settings $a_1 \in \{1.000, 1.001, 1.005, 1.010\}$ are considered, including the baseline case with no location-fixed advantage ($a_1 = 1.000$). We have $\delta'(\chi) > 0$ for all $\chi \in (0, 1)$ and see that $x_1 - \bar{x} > 0$ when $a_1 > 1$ and $x_1 - \bar{x}$ increases as a_1 increases, which are intuitive. Additionally, $x_1 - \bar{x}$ decreases as ϕ increases. We confirm that $\rho(\phi) > 0$ and $\rho'(\phi) < 0$ for all ϕ .

Similarly, Figure F.1B and Figure F.1C consider, respectively, the Krugman and AA models under a multiplicity of equilibria. Unlike the AA model, the Krugman model admits multiple equilibria for some ϕ for *any* pair of the structural parameters (μ, σ) . **Proposition 2** correctly predicts the sign of $\rho'(\phi)$ for the range of ϕ such that \bar{x} is stable when $a_1 = 1$; we have $\rho'(\phi) > 0$ when $\phi \in (0, \phi^*)$ for the Km model, whereas $\rho'(\phi) < 0$ when $\phi \in (\phi^{**}, 1)$ for the AA model.

Although **Proposition 2** does not cover the ranges where \bar{x} is unstable, it tends to predict the general tendency of the evolution of ρ . In Figure F.1B, in particular, $\rho'(\phi) > 0$ holds true except for the transitional phase after ϕ^{**} .

In Figure F.1B, the definition of ρ is modified for spatial patterns with unpopulated regions. For the range $\phi \in (\phi^*, \phi^{**})$, ρ is evaluated with respect to the four-centric pattern $(2\bar{x}, 0, 2\bar{x}, 0, 2\bar{x}, 0, 2\bar{x}, 0)$:

$$\rho \equiv \sum_{i \in \mathcal{I}(\mathbf{x})} (x_i - 2\bar{x})(a_i - \bar{a}(\mathbf{x})), \quad (\text{F.1})$$

where $\mathcal{I}(\mathbf{x}) = \{i \in \mathcal{I} \mid x_i > 0\}$ is the set of populated regions and $\bar{a}(\mathbf{x}) \equiv \frac{1}{|\mathcal{I}(\mathbf{x})|} \sum_{i \in \mathcal{I}(\mathbf{x})} a_i$. We define ρ

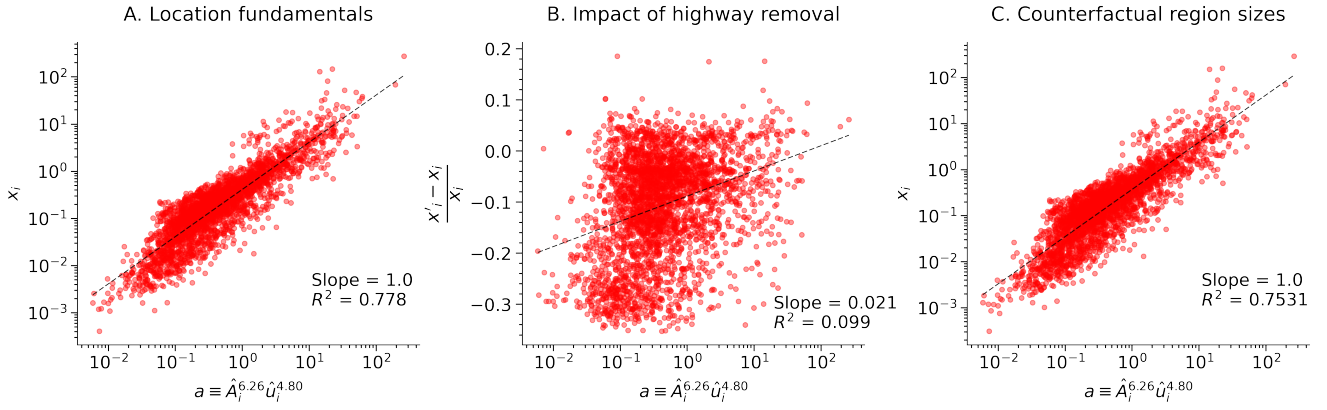


Figure F.2: The counterfactual exercise in [Allen and Arkolakis \(2014\)](#), Figure XVIII.

for two-centric pattern $(4\bar{x}, 0, 0, 0, 4\bar{x}, 0, 0, 0)$ similarly. For the transitional phase after ϕ^{**} we let

$$\rho \equiv \sum_{i \in \mathcal{I}(\mathbf{x})} (x_i - x_i^*)(a_i - \bar{a}(\mathbf{x})), \quad (\text{F.2})$$

where x_i^* corresponds to the stable solution for the symmetric case ($a_1 = 1$). We have $\rho'(\phi) > 0$ for the four- and two-centric patterns. This is natural because these patterns may be regarded as the uniform distribution on the four- and two-region cases, respectively.

For Figure F.1C, we employ (F.2) as the definition of ρ for the case $\phi \in (0, \phi^{**})$, i.e., we consider the deviation from the baseline equilibrium ($a_1 = 1$). We observe that $\rho'(\phi) < 0$ does not necessarily hold true for $\phi \in (0, \phi^{**})$. For instance, $\rho'(\phi) > 0$ when ϕ is small. Nonetheless, when the hypothesis of **Proposition 2** holds ($\bar{\mathbf{x}}$ is stable in the baseline case), ρ decreases in ϕ .

F.2 Quantitative example

We observe that **Proposition 2** is consistent with a counterfactual experiment presented in [Allen and Arkolakis \(2014\)](#), which suggests the empirical relevance of the discussion in Section 4. Figure F.2A shows the relation between the calibrated local parameters and the observed county population for their counterfactual analysis presented in Figure XVIII (bottom). The observed population x_i is plotted against the aggregated location characteristic $\hat{a}_i \equiv \hat{b}_i^{6.26} \hat{u}_i^{4.80}$ where the exponents are obtained by a logarithmic regression. The unobserved location fundamentals account for 78% of the logarithmic population variations. Figure XVIII in [Allen and Arkolakis \(2014\)](#) considers the removal of the Interstate Highway System, which induces an increase in the level of interregional transport costs. We can confirm $\Delta\rho > 0$ under this counterfactual transport costs change, which is consistent with **Proposition 2** despite the asymmetry of transport costs. Also, Figure F.2B shows the county population growth rates against the local parameter \hat{a}_i in the counterfactual experiment. On average, the model predicts that the counterfactual increase in the transport cost level induces agglomeration towards advantageous regions. This is in line with the basic property of Class II models, as improved transport access in this class of models promotes dispersion of population from existing agglomerations (cf. Figure 7).

In Figure 10, we apply the model to Japan data. As for the underlying geography, we follow [Sugimoto et al. \(2023\)](#) (since [Sugimoto et al. \(2023\)](#) is published in Japanese, details are available upon request). Specifically, we consider $N = 432$ regions based on Urban Employment Areas that are connected by the ground transport network (see Figure 10C or D). The interregional transport cost matrix is assembled also

following Sugimoto et al. (2023), based on the Digital Road Map (DRM), *Kokudo Suchi Joho* provided by MLIT of Japan, and data obtained with NAVITIME API. As for the population data, the 2005 Japanese Census grid population data are aggregated to construct the population distribution over the 432 regions. The location-specific parameters $\{(\hat{A}_i, \hat{u}_i)\}_{i=1}^N$ are then calibrated to realize the observed population data as the spatial equilibrium, assuming $\alpha = 0.1$ and $\beta = -0.3$ so that $\alpha + \beta < 0$. In Figure 10C, we consider 50% decrease of the interregional transport costs. We also note that, in Figure 10, we interpret the local amenity component in (43) as $u_i \times (x_i/\text{Area}_i)^\beta$ instead of $u_i \times x_i^\beta$, where Area_i is the total inhabitable area in region i . This interpretation allows us to remove the effect of Area_i in the local amenity coefficient u_i in the original framework.